EFFECT OF RESIDENTIAL SOLAR PV PENETRATION ON DISTRIBUTION NETWORK PROTECTION SCHEMES

Ilandari Dewa Sandamali Sanchala

(159323K)

Dissertation submitted in partial fulfilment of the requirements for the
Degree Master of Science in Electrical Engineering

Department of Electrical Engineering

University of Moratuwa
Sri Lanka

November 2018

DECLARATION OF THE CANDIDATE & SUPERVISOR

I declare that this is my own work and this dissertation does not incorporate without acknowledgement any material previously submitted for a Degree or Diploma in any other University or institute of higher learning and to the best of my knowledge and belief it does not contain any material previously published or written by another person except where the acknowledgement is made in the text.

Also, I hereby grant to University of Moratuwa the non-exclusive right to reproduce and distribute my dissertation, in whole or in part in print, electronic or other medium. I retain the right to use this content in whole or part in future works (such as articles or books).

Signature: Date:

The above candidate has carried out research for the Masters dissertation under our supervision.

Signature of the supervisor: Date
Dr. K.T.M.U. Hemapala

Signature of the supervisor: Date
Dr. W.A.D.S. Rodrigo

Signature of the supervisor: Date
Dr. L.N.Widanagama Arachchige

Abstract

Electricity generation from solar PV has been increasing due to many reasons including heavy environmental considerations, reduction of burning fossil fuels, fast developments in the solar technology and the industry, consequent reduction in investment costs etc. Especially in Sri Lanka, the government took lot of steps to encourage the consumer end to install roof top Solar PV`s. As an initiation Government revised the tariff system and provided considerable financial support for the consumers to encourage PV generation. Especially, in the urban areas the number of rooftop solar PV connected to the LV distribution system (0.4 kV) has increased. Due to this heavy solar PV penetration, fault current seen by the grid side has been changing. Hence, it is required to analyze the changes in fault current levels and consequent impact on the protection coordination in the medium voltage (MV) distribution system.

The main objective of this research is to assess the impact of increasing solar PV penetration levels on the MV level protection coordination and to propose a methodology for revising the protection settings for proper relay coordination with the increasing solar PV levels.

For the analysis a MV feeder having high penetration of solar PV has been selected and simulated. Modelling of the low voltage (LV, 0.4 kV) distribution system with widely dispersed solar PV integration has been a key challenge in this research. As the protection coordination has been evaluated at the MV side, the total LV distribution system has been simulated as an equivalent system and the solar PV has been modelled as an equivalent voltage source inverter. The equivalent solar PV model has been validated using already verified built-in solar PV model in PSCAD/EMTDC version 4.5.

Initially, performance of the MV level protection coordination has been analyzed in the selected feeder without solar PV being integrated. Then, the performance of the protection system has been analyzed based on the present PV penetration levels and fault current variation for different fault locations considering all probable fault types. Analysis indicated that, with the present PV penetration levels, existing protection settings can still be used, as they effectively maintain the required protection coordination.

After analysing the system behaviour with increasing solar penetration levels, a generalized method has been proposed to evaluate the MV level protection system performance. If the any system relay parameters fail to perform the expected outcome, a technique has been proposed to identify a criterion to review the relay settings.

KEYWORDS: Equivalent system, Medium Voltage level (MV), PV-photovoltaic, Relay parameters.

Acknowledgement

It is with great pleasure that I express gratitude to those who were behind me in completing my research project.

Firstly, I would like to express my sincere gratitude to my supervisor Dr. K.T.M.U Hemapala, Dr W.A.D.S. Rodrigo, Dr. L.N. Widanagama Arachchige for their great insights and perspective with much patience throughout the entire period and their continuous support with immense knowledge motivating me to do this research. Their guidance helped me all the time, from starting of this research, up until the end writing of this dissertation. Thank you very much for giving me the opportunity to work with you all.

In addition, I would like to thank all the Lecturers in the Department of Electrical Engineering and the Post Graduate Studies Division, Faculty of Engineering, who engaged in this MSc course in various ways to educate us and broaden our vision.

My sincere thanks go to my managers and colleagues at Ceylon Electricity Board and Lanka Electricity Company (Private) Limited, who helped me in many ways during this period.

Finally, I am thankful to my family members including my husband, parents and sister who always encouraged and help me to complete this research.

Table of Contents

List of Figures

List of Tables

List of Abbreviations

Abbreviation	Description
PV	Photovoltaic
MV	Medium Voltage
IEC	International Electro technical Commission
IEEE	Institute of Electrical and Electronic Engineers
kWh	Kilo Watt Hour
LECO	Lanka Electricity Company (pvt) Ltd
VSI	Voltage Source Inverter
CSI	Current Source Inverter
FL	Fault Level
OC	over Current
EF	Earth Fault
BCU	Trip Circuit Supervision
WECC	Eastern Electricity Coordination Council

CHAPTER 1

1. INTRODUCTION

The Power System, which supplies electricity to the consumer, basically comprises of three sectors, namely generation, transmission, and distribution. In general, distribution sector of a typical power system comprised with loads only. With the thriving motivation for non conventional renewable power generation concepts, the distributed generation started to be connected to the distribution system. With the addition of the distributed generation, it has become a vital issue to evaluate the level of impact to the existing system parameters. Impacts due to the connected distributed generation can be observed on different aspects of the system such as voltage profile variation, system controlling issues, protection system performance. This research scope limits only to evaluate the impact of heavy solar PV penetration to the MV level protection coordination.

In the first place, when the impact on the MV protection level analyzed due to heavy solar PV penetration, fault current level variation had to recognize. All the electrical equipment in the system has been selected based on the maximum fault level that the equipment had to withstand. Normally this fault level has been calculated considering only the grid side fault current contribution. When the solar PV has been connected to the distribution network, it could operate as a source providing an additional parallel path to system causing equivalent thevenin impedance to be smaller and resulting in higher fault current levels. Based on factors such as solar PV capacity and fault location, fault resistance this fault current level increase can be varied. Henceforth it is important to analyze the fault level increase for typical distribution feeders before determining the level of PV penetration.

Nevertheless, the distribution coordination might also have an impact from variation of the fault current contribution due to heavy solar penetration. The main reason is, in the protection setting preparing process the over current and earth fault TMS values set to achieve adequate coordination margin at the maximum fault current level. If the considered maximum fault current level changed from the actual maximum fault

current, the expected coordination gap will not be able to achieve in relay operation for actual fault. Hence it is required to affirm the performance of the existing MV distribution protection coordination system.

This study is focused on such a critical yet less addressed problem, which has a higher probability to appear in the distribution MV level protection system performance in the future. Figure 1-1 shows the solar PV variation from 1995-2012 globally. [12]

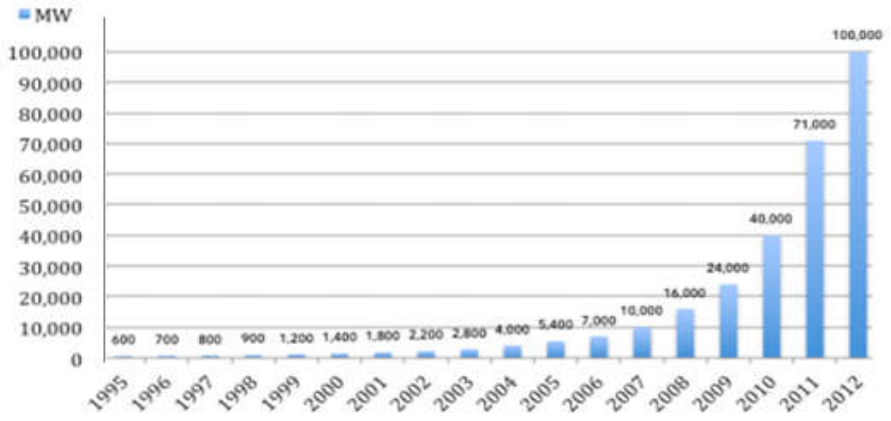

Figure 1-1: Solar PV Global Capacity Increase

1.1. Importance of the Research

Due to different reasons, such as government policy and political pressure, the solar PV penetration level has increased in the distribution system of Sri Lanka in a considerable rate. Consequently, there is an urgent requirement to analyze the impact on the fault level at distribution MV level due to the heavy solar PV penetration. Though the number of connected rooftop solar PV increasing, there has been no attempt to analyze the impact to the fault current level due to the connected roof top solar PV. This research provides basic guidance and suggests a generalized method to analyze the impact from solar PV to the distribution MV level protection coordination for any feeder comprise with the distributed generation. Further it provides basic guideline to represent the widely distributed loads, connected roof top solar PV`s as a lump load and source which is recommended by WECC.

Furthermore suggested generalized method is important to analyze the suitability of the existing protection system with heavy solar PV penetration to distribution system.

1.2.Main Objective of Research

The main objective of this research is to evaluate the impact of increased solar PV penetration level on the performance of an existing MV distribution protection scheme and to propose a generalized protection review process for revising the existing protection relay settings to gain improved density of accommodated solar PV level.

1.3. Research Methodology

Suitable software selecting for the simulation- In order to model the protection scheme, the software shall be capable to simulate transient faults in the electromagnetic time domain. Additionally, the software shall be comprised with adequate features to allow model the equivalent PV sources, simulate asymmetrical and symmetrical faults. Nevertheless, relay time coordination shall also be able to analyze. For the selection, 3 software were used namely MATLAB, ETAP, and PSCAD. Among these software, PSCAD has been selected for the protection coordination for the purpose of stepwise fault analysing capability and the system performance capability to be evaluated in very smaller steps.

Developing Equivalent Solar PV distributed LV Network - two main purposes are expected to be fulfilled by the developed model. The model shall be comprised with pre defined settable, aggregated solar PV active and reactive power reference points. Furthermore, the model shall not be comprised with complex switching, which has less impact on the protection coordination study. Thus, solar PV has been modelled as equivalent voltage source inverter where reference active and reactive power reference can be pre settable.

Identify the suitable method to simulate loads as equivalent components - 0.4kV LV distribution system is comprised with widely spread network in a large geographical area with thousands of consumers connected. So it is not fruitful to model the whole network in the simulation. Hence the 0.4kV network impedance has not been

considered for simulation. Even the MV network is comprised with hundreds of MV/LV transformers that are connected. Hence, for the purpose of simulating the protection coordination in MV network all 0.4kV/11kV transformers have been simulated as equivalent system which is recommended by WECC.

Model the protection equipment with existing settings and verify the operation without PV – For the simulation, few LECO feeders have been selected with heavy solar PV penetration and with known loading and PV capacity levels. Ethul Kotte Primary substation all the relays, CTs, breakers have been modelled using the actual data obtained from the site. Using the developed simulation, faults have been created at different locations using different probable fault loop impedances, arc resistance etc... Fault level variation, relay tripping scheme have been observed. Based on that protection scheme operating level (expected fault clearing time boundaries and fully isolating of the fault) the accuracy of the system operation has been determined.

Determination of the MV level protection scheme Performance with Existing Solar PV-Initially, with the existing loading conditions and connected PV capacities, the fault level change and relay operating time has been observed. Especially it should be mentioned that, in the simulation PV side protection scheme has not been implemented. When the fault occurred, after 200ms (expected maximum fault current injection duration of the solar PV) equivalent VSI side breaker operates and isolates PV from grid. Nevertheless, if the current output from the PV become higher than 1.5 times of rated current, the PV side breaker instantaneously operate to isolate the fault.

Determination of the Impact on the MV level coordination with higher PV penetration level- It is observed that the relay operation has been occurring in an optimum way by fully isolating the fault with proper coordination.

1.4. With Distributed Generation Probable Protection Issues

There are different research papers that have been published, regarding the protection system operating issues and protection system issues with the extensive distributed generation accommodation. Especially, the distributed generation such as Mini Hydro, which are comprised with synchronous generators provide considerable fault

current level which is in 7-8 times of the rated current. So when that type of Mini hydro power plants are connected, special attention is paid for the raise of the fault current level and most of the time they are connected to the dedicated feeders by the utility. But when the distributed non conventional renewable resource considered which are comprised with inverters the fault current contribution is considered to be negligible. It is an accurate fact that the inverter based generators, detect islanding and disconnect from the grid quickly. Further the controllers make sure to limit the maximum fault current contribution from the inverter. The fault current contribution limited because the internal power electronic equipment such as IGBT cannot withstand high fault currents. Hence most of the references (based on the available experimental inverter fault current data) revealed that the fault current contribution from the inverter varied as per inverter type. The maximum short circuit contribution from the inverter can increase up to 2 times of the rated current. The maximum time which taken by the PV inverter controllers to disconnect from the grid in short circuit situation is 200 ms (10 cycles) [16] [17]. This current contribution can be smaller when compared with the grid current with low PV penetration level. But when the PV penetration level increases overall effect on the short circuit level need to be analyzed. On the other hand the total fault current contribution to the fault is not seen by the protective device at the grid.

In general setting calculation process, only the fault current from the grid considers in order achieving satisfactory relay operating coordination. But the fault current from the grid also change due to the parallel path added to the short circuit impedance network due the added PVs. So it is required to validate weather the existing protection settings capable of performing the expected coordination margin when the solar PV added. Further due to the increased fault current contribution, the impact for the switch gear equipment rating need to be revised.

For this research only the MV level coordination problems have been analyzed. But actually LV level protection equipments comprised only with fuses. Fuses which are coordinated as per the fault current level can also be vulnerable to protection coordination issues [5]. When PV`s are connected in the middle of the feeder, upper and downstream coordination can be deviated from the expected discrimination

margin. In some cases, the upper protective device can be operated before the downstream device because only the upper stream protective device can see the fault current contribution from the PV connected in between 2 protective devices.

In typical power system protection philosophy it is expected that the upstream protective device operate as the backup for the downstream device due to the fault current seen by both protective devices is same. But this phenomenon is violated with the PV penetration in the distribution system. For example upstream protective device may not see the fault current and only downstream protective device sees the fault current. If the downstream breaker is not operated, the fault can be sustained and the upstream protective device cannot be operated as the backup. These issues have not been addressed in this research. The reason is mainly in Sri Lanka LV network, fuses are used to isolate sector at an over load situation. Fuses are rarely used for coordination. Thus in my research, I mainly focused on the MV level protective equipment, where the numerical relays are used to obtain protection coordination in isolating faults.

1.5. Over view of Thesis

The dissertation encapsulates the most vital technical details of this study and information on literary analysis of related work and background studies. The preparation and order of the thesis is according to the chronological order of the approach to the project, hence should be referenced in the following order. A summary of content of each chapter has provided.

1. Introduction:

   Introduces the reader to the project and briefly discusses the traits of the initiation of the project. This discusses the background of the project, motivation for selecting the project, objective, methodology and organization of the report.

2. Project Overview:

   This chapter describes the theoretical background of protection relaying, basics of detailed PV modelling, previous research work (what type of network modelled, PV modelling). The results and observation of the previous studies are thoroughly evaluated and comprehensive understanding about related scope is given.

3. Methodology and System Modelling

   This section gives a comprehensive idea about the methodology of the research carried out. Further this chapter contains collected data, selection of suitable software, scenarios to be considered in modelling etc...

   Furthermore, comprehensive modelling of average solar PV equivalent is presented. Additionally the equivalent network modelling is discussed in detail. Obtaining the other related details is also described in this chapter.

4. Results

   This chapter presents the fault current variation and MV level protection coordination for the existing PV penetration level. Then, when the PV penetration level is increased the impact to the fault current level and relay tripping time coordination is observed. Simulation results were analyzed and understood the fault current contribution for different PV penetration levels. As a conclusion a generalized protection scheme has been proposed which can be used to evaluate the impact of the PV penetration on the MV protection coordination.

5. Conclusion:

Summarizes the study indicating how the objectives are achieved and discusses advantages, disadvantages and the future direction for the research.

CHAPTER 2

2. PROJECT OVERVIEW

This chapter provides the basic theory coverage for different aspects of the research. The primary objective of this research is to understand the impact to the MV level protection coordination from the heavy penetration of solar PV. For that I would like to describe the protection coordination methodologies and the main components of the detailed solar PV system.

2.1. Grid Connected PV inverters

The grid tied PV unit is comprised with main components of PV panel, DC-DC boost converter and inverter. PV panel converters the solar energy in to electric energy. The produced DC power is proportional to the solar isolation level and cell temperature. Then DC power is fed to the boost converter which steps up the DC link voltage and feed to the inverter. Inverter controllers make sure that inverter produced alternating power output with respect to the Maximum power point tracking (MPPT) form the PV array output. Inverter IGBT switching pattern is decided to obtain that power output inverter. A brief disruption of each component can be presented as below.

2.1.1.Main components of the detailed model

PV panel is a collection of photovoltaic cells connected in series with parallel strings. Power generate from the PV cell depends upon the cell temperature and irradiation level. If the solar PV panel represents as equivalent model, solar cell can be considered as a diode which converts the solar energy to electrical energy. Due to the solar energy absorption photon moves to the higher energy level and then falls to lower energy levels creating electron hole pairs. This leads to the electricity generation in side photovoltaic cell. There are some losses associated with the process which can be represented by shunt and series resistance of the cells. Hence the equivalent PV cell can be represented by parallel two current flow paths (across diode and shunt resistor) and series resistance path.[9]. Equations can be derived for the

obtained equivalent circuit. Per cell I-V curve can be plotted based on the varying irradiance and module temperature.

When the external environmental conditions vary, controllers of DC-DC converter must make sure to achieve the maximum power point. There are different types of maximum power point tracking algorithms are being used in the practice. One of the mot accepted technique is incremental conductance method(IC). In that method DC link output voltage is determined by giving small increments to voltage and its impact to the power output from PV is observed. If the power output increases when the voltage increases that value consider as the new set point for the DC link voltage. This iterative process is followed until the point where active power output reduces when the set voltage increases. At that time the previous set point is kept as the voltage with respect to the maximum power point. Hil-top method, perturb and observation method are also used for this maximum power point tracking. Based on obtained reference voltage value, using any of the mentioned method, DC/DC converter power electronic device duty cycle can be determined. When the inverter controls considered the firing angle controllers are being determined based on the Phase Locked Loop algorithm voltage vector and set voltage.

The figure 2-1 shows the schematic drawing of the detailed PV modelled using PSCAD/EMTDC software.

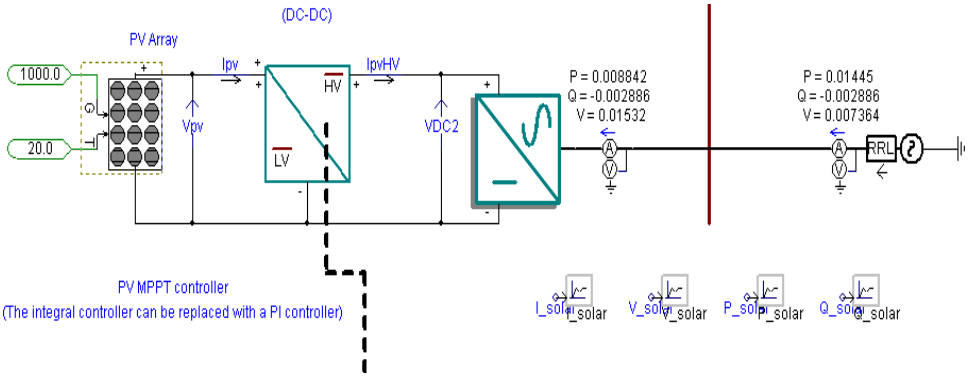

Figure 2-1: Schematic of the Detailed Solar PV Model on PSCAD/EMTDC platform

2.2. Protection System Setting Philosophy

There are different factors need to be considered in setting the power system protection settings.

In order to limit further damage to equipment and restrict the danger to human life, it is required to apply fast electrical protection. Protective devices play vital role in this purpose as they operate to isolate the faulty part of the network by limiting the propagation of the system disturbance.

Power system protection has following five main functions as its level of discipline and functionality shown in the order of priority.

- To ensure safety of personnel
- To safeguard the entire system
- To ensure continuity of supply
- To minimize damage
- To reduce resultant repair cost

To ensure these requirements, it required to detect the fault soon, localize and isolate rapidly. Power system protection should have following requirements, in order to satisfy above functions [5].

1. Reliability – to operate in a pre-set manner when an electrical fault is detected
2. Selectivity / Discrimination – to detect carefully and safely isolate only the faulty section
3. Stability / Security – to leave all healthy circuits intact and undisturbed and to ensure stability of supply.
4. Sensitivity – to detect even the smallest values of fault current or system abnormalities and operate correctly as per pre-set settings
5. Speed – to operate speedily when it is required, thereby minimizing harm and ensuring safety to personnel

In this research the main focus is on the MV level protection coordination issues. As per the IEEE standards MV level is from 600V to 35kV. Sri Lankan system comprised with 33kV and 11kV distribution voltage levels. 220kV and 132kV levels are used as transmission voltages and 0.4kV is used as the LV network. 33kV voltage

level is used by the CEB up to a considerable percentage all over the country. 11kV level is only used by the LECO and CEB (only urban areas). In the research the selected case studies are also comprised with 11kV distribution system as most of the rooftop solar PV connected to the grid from the urban areas.

2.3. Protection Schemes used at MV level

The MV level distribution feeders mainly comprise with 2 protection functions. Over current (OC) protection and Earth fault (EF) protection. Additionally to these protections, the generator feeders comprise with Directional over current and directional earth fault function. Additionally to these functions the relays are comprised with Trip circuit supervision (74) and lockout (86) function as separate Bay controller function is not provided at 33kV level.

When power system protection is considered, special attention can be paid to the CTs which convert the primary current in to secondary current and feed to trip relays for protection calculation. At 33kV level the CT selection for distribution feeders are decided base on the feeder type. If the conductor type is Racoon the CT ratio can be selected as 200/1, if the conductor type is Lynx CT ratio can be selected as 400/1. Switch gear equipment such as breaker can be selected based on the maximum short circuit current for that particular place. Normally breakers can be selected with capability of withstanding short circuit current capacity of 25kVA for time duration of 1 s. Hence with the solar PV penetration level increases, the short circuit fault current level increase need to identify. Short circuit current increase shall be within breaker withstanding capability.

Most of MV level feeder protection is effectuate by the numerical type relays. But for some feeders still the electromechanical and static type relays are also used. Numerical relays from different manufactures have being connected to system such as ABB (REF 650, REF 542+), Siemens (7J680), and Micom (P122, P144), and WAMP etc...Protection setting philosophy, for more complex protection functions such as distance, differential, need to be adjusted based on the manufacture. But as

MV level only comprises with over current and earth fault function, the setting philosophy is independent from the manufacture.

2.4.Grading of Over current and Earth Fault Relays.

The main requirement of setting philosophy is to provide accurate discrimination and selectivity. It is expected that when a fault occurs in power network, the protection relay closest to the fault should operate and isolate the healthy network undisturbed. This phenomenon is called grading. The grading of relays can be achieved by using of following methods.

- Current grading
- Time grading
- Current and time grading

2.4.1. Discrimination by Time

In this method, an appropriate time interval is set between each of the relays by controlling the CBs in a power system to ensure that the breaker nearest to the fault opens first. The lowest time setting is given to the down most protective equipment. The operating time increases when the equipment situated up stream of network. The main disadvantage of this method is the longest fault clearance time near the source.

2.4.1. Discrimination by current

Based on the fault location, fault current varies due to the equivalent thevenin impedance seen by the system change is different based on fault location. Fault level near to the source is higher. Hence Current setting of upstream equipment can keep a higher value and setting of the downstream equipment can keep a lower value. The main disadvantage of this method is difficulty of achieving considerable time margin between two upstream and downstream relays if the feeder length is relatively small. In this method to achieve considerable clearing time margin the conductor impedance between two points should be comprised with considerable length. As a solution “discrimination using both time and Current” method is used.

2.4.2. Discrimination Using both Current and Time.

In this method the curve is decided based on both time and operating current. In this characteristic, the time of operation is inversely proportional to the fault current level and actual characteristic is a function of both “time” and “current” settings. There are different curve types which are used in over current and earth fault protection when the inverse time characteristics are used.

IEC Standard Inverse Characteristic

$$t(s) = \frac{0.14 \times T_d}{M^{0.02} - 1} \qquad (2.1)$$

$$T_d = Time\ Index$$

$$M = \frac{Fault\ Current(A)}{I\ pick\ Up(A)}$$

This operating time characteristic operates inversely proportional to the current and hence when the fault current higher the relay operating time become progressively reduced. IDMT curves are used by many countries as standard practice of many countries. Figure 2-2 shows the set of curves which are discriminated using both time and current.

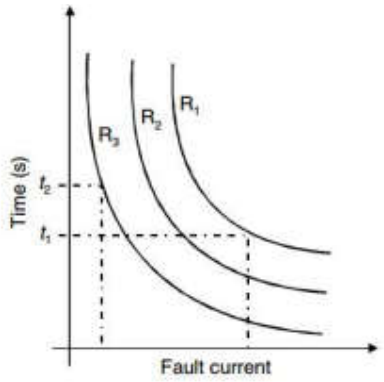

Figure 2-2: IDMT Relay Characteristic for Over Current and Earth fault Protection

If the curve is IEC Very Inverse time curves

$$t(s) = \frac{13.5 \times T_d}{M^1 - 1} \qquad (2.2)$$

If the curve is IEC Extremely Inverse time curves

$$t(s) = \frac{80 \times T_d}{M^2 - 1} \qquad (2.3)$$

Define Time Relay

This relay operates when the current reaches to the predefined setting value. The operating parameter is only current magnitude. In this relay current setting and tripping time delay has to set. The current setting will be kept based on the fault level and the tripping time will be less than 0.1s. As shown in the figure 2-3 , for a particular feeder section relay shall be operated with a fixed pre defined time delay for any fault current reading, when the fault current more than the set current value.

Instantaneous Relay Characteristic

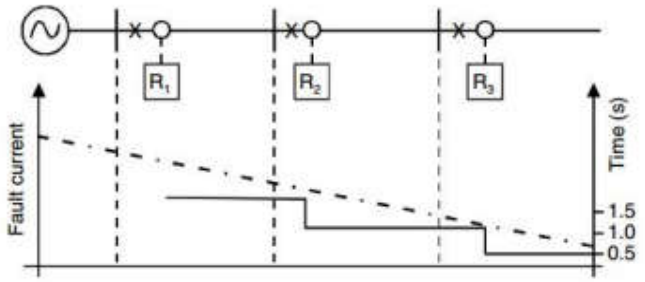

Figure 2-3: Definite Time Relay Characteristic

These curves are used to obtain the required discrimination of relay operation of the MV level. Both Normal inverse curve and Define time curves are used in distribution level.

2.5. Statement of Problem

With heavy rooftop solar penetration in Sri Lanka LV system many protection and controlling issues can be merged in the system. Before the PV penetration level increase arbitrary by allowing more solar PV customers to be connected, the system impact due to that need to be analyzed using simulations. There are many aspects to be considered in evaluating the level of rooftop solar PV accommodating.

In this research I have mainly focused on the protection coordination issues that may be occurred due to the fault level variation with connected solar PV. As research out come a generalized method has suggested which can be use to evaluate the impact

from different solar PV connected to the LV network and if any violation occur how to propose new protection scheme.

2.6. Objectives of the Study

The main objective of this research is to identify the impact on the MV level protection coordination and fault current variation with heavy solar PV penetration level in the LV distribution system.

In order to achieve above main objective, suitable methods are to be identified in order to represent the widely dispersed LV distribution loads and PV connected as equivalent at the MV level. To represent the equivalent impact from the solar PV, generic model developed and the model has been validated with the detailed model.

Based on the existing penetration level, the protection system coordination is evaluated. The impact on fault current and consequently, the protection system performance is analysed under the high solar penetration scenario.

Finally a generalized method is being suggested to evaluate the impact from heavy solar PV penetration level and anew protection philosophy is being proposed.

CHAPTER 3

3. METHODOLOGY AND SYSTEM MODELING

For the research several feeders have been selected which are having considerable solar PV penetration. Hence 11kV distribution feeders have been selected form the LECO network as there the connected solar capacity known for each 11/0.4kV transformer. Five feeders were selected from the Ehul Kotte 11/33kV primary substation for the study. Total 0.4kV LV network loads and solar PV`s were connected as equivalent lump components according to the recommendations from WECC. The entire 11kV network simulated as equivalent collector system as shown in the figure 3-1.

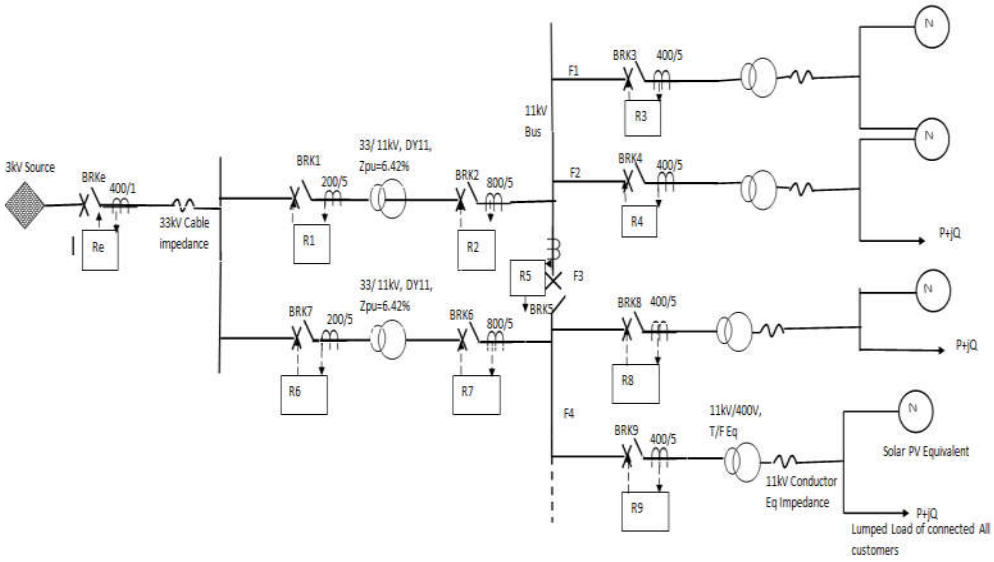

Figure 3-1: Overall Schematic Diagram for Simulation

All the MV level existing relay protection functions have simulated using PSCAD/EMTDC software. The variation of the fault current level and relay operating time analyzed for different types of faults at different fault locations with different fault resistances.

3.1.Component Modelling for the Simulation

3.1.1. Average Solar PV Modelling

In the LV distribution 0.4kV level rooftop solar PV have spread extensively though out the network with smaller capacities. Thus it is impossible to model each and every small capacity PV`s to examine effect on the MV level protection coordination. On the other hand, since this study is about fault study, complex switching and controllers are not required to be modelled. WECC recommends that average generic PV model can be used for the fault study simulation to observe the fault current contribution from a solar PV [1][2] [3].

In order to observe the protection system performance at electromagnetic transient level, PSCAD/EMTDC software has been selected. In "User Guide for PV Dynamic model Simulation Written on PSCAD Platform" indicated the method of modelling solar PV as average current source inverter [18].

In order to represent solar PV as average model there are 2 possibilities theoretical concepts for modelling.

- Current source inverter
- Voltage source inverter

Developing the Mathematical Model for CSI in PSCAD platform

In order to develop current source inverter, active and reactive power per unit values is required to be derived. The measured Active power at the PV, divides from power base in order to obtain pu value. Figure 3-2 illustrates the method of active and reactive power per unit value deriving method.[18]

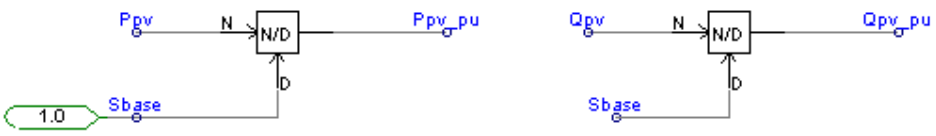

Figure 3-2: PSCAD Model to obtain Measured Active and Reactive Power in PU Base

In order to obtain Current base, apparent power base is divided by square root 3 and obtain line to line voltage. Figure 3-3 describes the method to derive base current to be multiplied by the per unit phase currents to get the actual current phase values to be injected at the CSI.

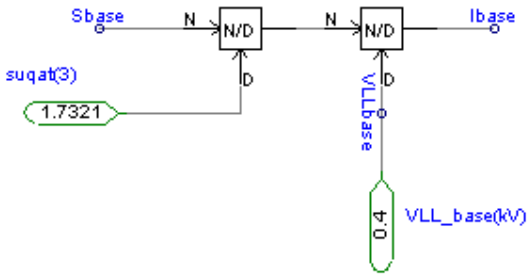

Figure 3-3: Obtain I_base value in simulation

Based on the active and reactive power difference between measured and reference, direct current component and quadratic current components are derived. Figure 3-4 describes the method to derive direct and quadrate current values using the difference of the measured and reference P and Q values of solar PV. The added PI controller and real pole component smooth out the signal and maintain the output signal in the desired range.

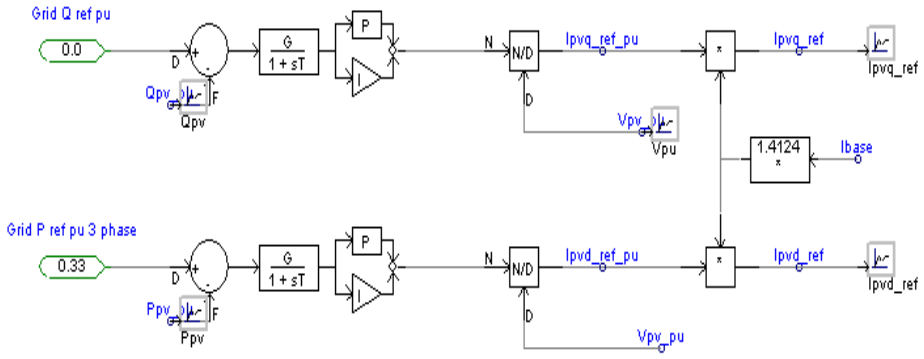

Figure 3-4: Deriving Direct and Quadrature Axis Current Components for CSI

Figure 3-5 describe the PSCAD, DQ to ABC transformation block can be used to obtain 3 phase current waveforms to be injected at the current source inverter.

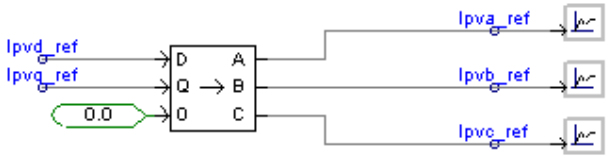

Figure 3-5: Deriving Phase current Components for the CSI

Figure 3-6 shows how the Phase locked Loop block can be utilize to synchronize the CSI current output with the grid frequency.

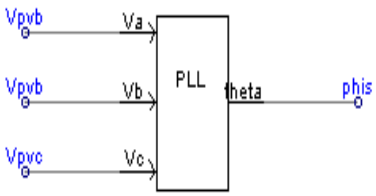

Figure 3-6: Deriving Phase Locked Loop Angle

Figure 3-7 shows the internal configuration settings to be used at the Phase locked loop component.

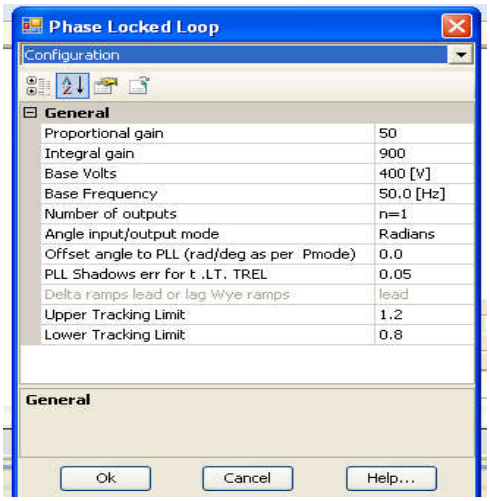

Figure 3-7: Parameter Setting For PLL Block

CSI does not provide, the desired output if the Vpv_pu measured voltage directly taken to derive, direct and quadrature currents because initially the measured voltage is zero and output moves to infinity with zero voltage. Hence, as given in the figure 3-8, if the initially the derived per unit voltage value is zero the PV output cannot stable in the simulation. Thus, initially during 50ms time per unit voltage output is maintained at fixed value of 1 per unit using the algorithm given in figure 3-8.

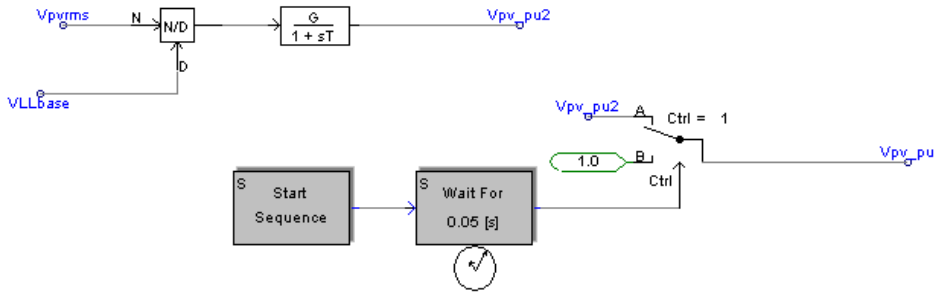

Figure 3-8: Maintain Constant voltage for stabilizing the CSI output

Figure 3-9 illustrates the complete model for simulation of CSI which has been used to create faults at different locations and measured fault current.

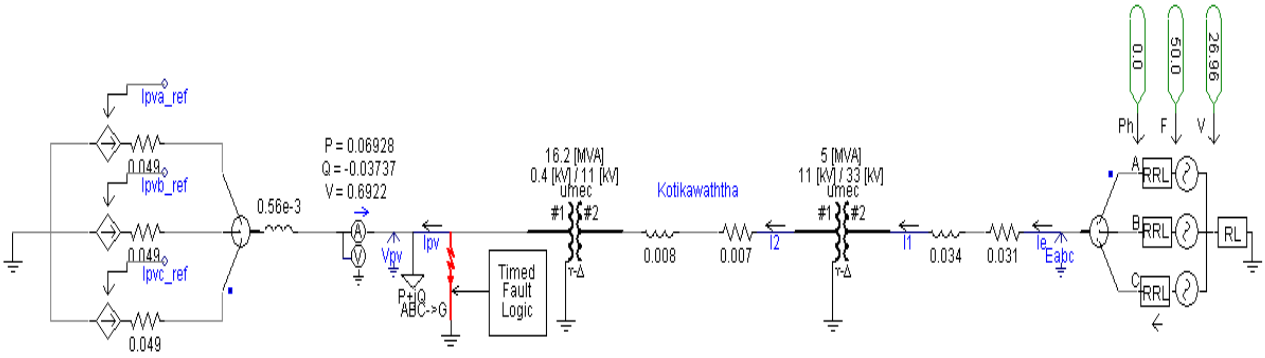

Mathematical Model for Average Voltage Source Inverter

Figure 3-10 shows the relevant schematic Diagram

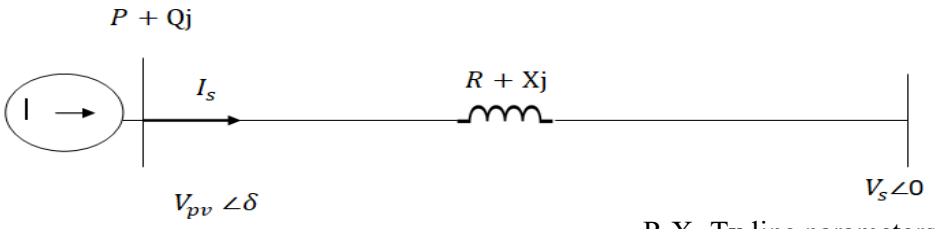

Figure 3-10: Representation of Equivalent PV source injects Is current and P (Active Power) and Q (Reactive Power)

As the solar PV equivalent has connected to the 11kV feeder, the solution for the power flow equation can be obtained by assuming all generalized conditions to solve power flow for transmission network.

From Load flow Equation

$$P_i + jQ_i = V_i \sum_j \left(V_j Y_{ij}\right)^* \quad (3.1)$$

$$S = V_i I_s^* \quad (3.2)$$

$$P + jQ = V_i I_s^* \quad (3.3)$$

$$P + jQ = \frac{V_{pv}\angle\delta (V_{pv}\angle\delta - V_s\angle 0)^*}{(R+jX)^*} \quad (3.4)$$

$$P + jQ = \frac{V_{pv}(\cos(\delta)+jSin(\delta))[V_{pv}(\cos(\delta)-jSin(\delta))-V_s]}{R-jX} \quad (3.5)$$

$$P + jQ = \frac{{V_{pv}}^2 - V_{pv}V_s\cos(\delta) - jV_sV_{pv}Sin(\delta)}{R-jX} \quad (3.6)$$

$$P + jQ = \frac{\left({V_{pv}}^2 - V_{pv}V_s\cos(\delta) - jV_sV_{pv}Sin(\delta)\right)[(R+jX)]}{(R-jX)(R+jX)} \quad (3.7)$$

$$P + jQ = \frac{\left(V_{pv}{}^2 - V_{pv} V_s \cos(\delta) - jV_s V_{pv} Sin(\delta)\right)[(R+jX)]}{R^2+X^2} \tag{3.8}$$

$$P + jQ = \frac{(V_{pv}{}^2 - V_{pv} V_s \cos(\delta))R - V_s V_{pv} Sin(\delta) X) + j(X\left(V_{pv}{}^2 - V_{pv} V_s \cos(\delta)\right) - RV_s V_{pv} Sin(\delta))}{R^2+X^2} \tag{3.9}$$

$$P = \frac{(V_{pv}{}^2 - V_{pv} V_s \cos(\delta))R - V_s V_{pv} Sin(\delta) X)}{R^2+X^2} \tag{3.10}$$

$$Q = \frac{X\left(V_{pv}{}^2 - V_{pv} V_s \cos(\delta)\right) - RV_s V_{pv} Sin(\delta)}{R^2+X^2} \tag{3.11}$$

Assume $\delta \approx 0$ and node voltage closer to 1pu. Thus, V pv, Vs and X will be constants allowing the active power flow to vary proportional to the angle difference of the solar source.

$$P + \Delta P = \frac{(V_{pv}{}^2 - V_{pv} V_s \cos(\delta + \Delta\delta))R - V_s V_{pv} Sin(\delta + \Delta\delta) X)}{R^2+X^2} \tag{3.11}$$

$$P + \Delta P = \frac{(V_{pv}{}^2 R - RV_{pv} V_s(\cos(\delta)\cos(\Delta\delta) - \sin(\delta)\sin(\Delta\delta)) - \mathrm{X}V_s V_{pv}(\sin(\delta)\cos(\Delta\delta) + \cos(\delta)\sin(\Delta\delta))}{R^2+X^2} \tag{3.12}$$

As $\Delta\delta \approx 0$

$\cos(\Delta\delta) = 1$

$$\Delta P = \frac{-V_{pv} V_s R \sin(\delta)\sin(\Delta\delta) - V_{pv} V_s X \cos(\delta)\sin(\Delta\delta)}{R^2+X^2} \tag{3.13}$$

As $\delta \approx 0$ and $\Delta\delta \approx 0$

$$\Delta P = \frac{-XV_{pv}V_s(\Delta\delta)}{R^2+X^2} \quad (3.14)$$

As V_{pv}, V_s and X kept constant.

$$(P_{ref} - P_{pv,measured}) \propto \Delta\delta \quad (3.15)$$

$$Q = \frac{X(V_{pv}{}^2 - V_{pv}V_s\cos(\delta)) - RV_sV_{pv}Sin(\delta)}{R^2+X^2} \quad (3.16)$$

Assuming $\delta \sim 0$ and node voltage closer to 1pu.δ,Vs, X kept constant to increase the reactive power flow by increasing the voltage magnitude

$$Q + \Delta Q = \frac{(X(V_{pv}+\Delta V_{pv})^2 - (V_{pv}+\Delta V_{pv})V_s\cos(\delta) - RV_s(V_{pv}+V_{pv})Sin(\delta))}{R^2+X^2} \quad (3.17)$$

$$\Delta Q = \frac{X(\Delta V_{pv})^2 + 2XV_{pv}\Delta V_{pv} - X(\Delta V_{pv})V_s\cos(\delta) + RV_{pv}V_s\sin(\delta)}{R^2+X^2} \quad (3.18)$$

As $\Delta V_{pv} \approx 0$ and δ≈0

$$\Delta Q = \frac{2XV_{pv}\Delta V_{pv} - X\Delta V_{pv}V_s}{R^2+X^2} \quad (3.19)$$

$$\Delta Q = \frac{\Delta V_{pv}X(2V_{pv} - V_s)}{R^2+X^2} \quad (3.20)$$

As Vpv and Vs constant,

$$(Q_{ref} - Q_{pv,measured}) \propto \Delta V_{pv} \quad (3.21)$$

ΔP and ΔQ can be compensation by injecting corresponding voltage reference waveforms as shown below.

$$(P_{ref} - P_{pv,measured}) \propto \Delta\delta \quad (3.22)$$

$$(Q_{ref} - Q_{pv,measured}) \propto \Delta V_{pv} \tag{3.23}$$

$$Vpv_{a-ref} \approx \Delta V_{pv} \sin(\delta + \Theta) \tag{3.24}$$

$$Vpv_{b-ref} \approx \Delta V_{pv} \sin(\delta + \Theta - \frac{2\pi}{3}) \tag{3.25}$$

$$Vpv_{c-ref} \approx \Delta V_{pv} \sin(\delta + \Theta + \frac{2\pi}{3}) \tag{3.26}$$

Θ-PLL angle to synchronize with reference frame

As per the given mathematical model, by using the active power difference between the measured and reference, voltage waveform phase angle can be derived. Similarly by using the reactive power difference between reactive power differences between measured and reference, voltage waveform magnitude can be derived.

3.1.1.1. Mathematical Model for Average Voltage Source Inverter Implementing PSCAD/EMTDC software

Figure 3-11 shows the method to get per unit quantities of active power and reactive power of the measured value. The peak value of the voltage also can be derived using V_{LL} dividing by $\sqrt{3}$ and multiplying by$\sqrt{2}$ as given in figure 3-11.

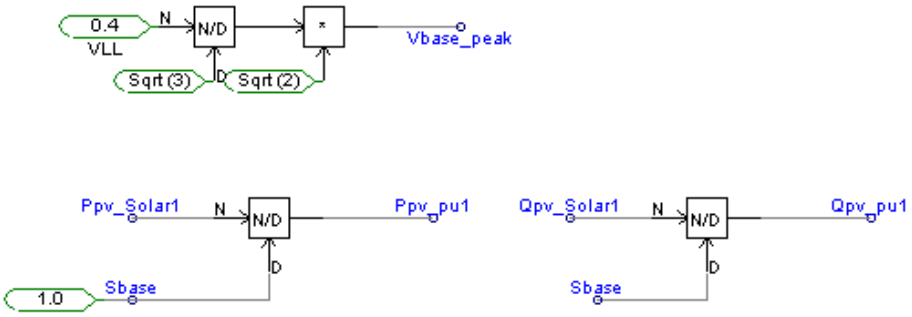

Figure 3-11: Deriving Measured PV Active and Reactive Power Reading Pu Values

As per derived mathematical model as per equation 3-24,3-25,3-26 , using active and reactive power pu difference between measured and reference values, voltage waveform magnitude and angle can derived. Figure 3-12 diagram shows the method to derive VSI voltage waveform magnitude and angle.

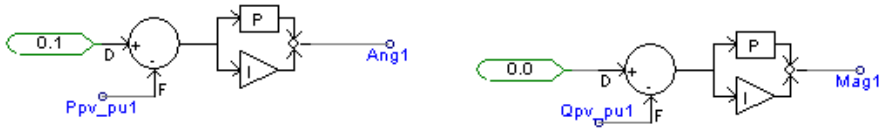

Figure 3-12: Deriving VSI Voltage Waveform Angle and Magnitude

Figure 3-13 illustrates the method to incorporate the phase locked loop angle in order to align the output waveform with the grid reference frequency.

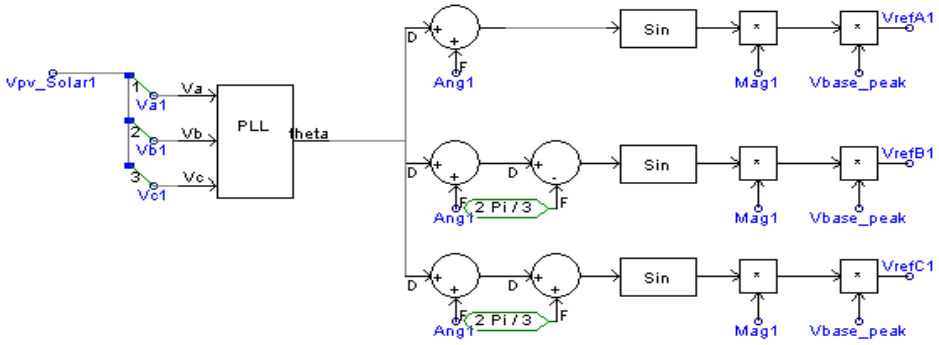

Figure 3-13: Driving Voltage Source Inverter Phase voltage values

Obtaining Average Voltage Source Inverter Using Voltage Direct and Quadrature Voltages in PSCAD/EMTDC software

By using the same mathematical model, the average voltage source inverter can be derived. The Active power difference between the measured and reference value, direct voltage axis reference can be obtained. Quadrature axis voltage reference can be obtained using the reactive power difference of measured at PV output and

reference given. Figure 3-14 illustrates the simulation component used to derive direct and quadrature voltage values.

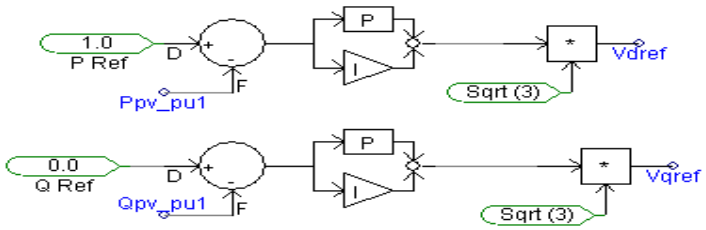

Figure 3-14: Modeling Voltage Source Inverter using Direct and Quadratic Voltage values.

Phase locked loop angle method has been used to align the PV output waveform frequency with the grid frequency.

Using the derived direct and quadratic axis voltage waveforms phase ABC voltage waveforms can be obtained by multiplying by Peak voltage value. Figure 3-15 shows how to obtain voltage phase reference values.

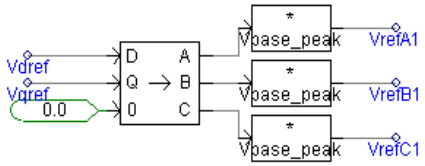

Figure 3-15: Deriving Phase Voltages Using Direct and Quadratic Voltage Values.

The reason for Selecting Average Voltage Source Inverter to simulate the equivalent PV in PSCAD/EMTDC.

All the above derived methods can be used to simulate equivalent average solar PV theoretically. But it has to select which is best to simulate the fault current behaviour while providing the worse case fault current contribution.

The fault current contribution varies rapidly based on the inverter controller response. In conventional system, the fault current contribution can be drived from stedy state voltage value and equivalent Thevinin`s impedance. But for inverter based models fault current contribution is depend upon the inverter controller algorithem. The

inverter can be seperated to 2 main catagories based on,the fault current contribution behaviour during transient .[9]

- Voltage based scheme- The converter try to maintain balance AC voltage at inverter terminals. To regulete the active and reactive power output of the PV, controller develop the inverter volateg constant with respect to terminals.
- Current based scheme-Try to regulate the current output. There are two controler loops. Inner loop controls the power output.

As per the reference [9] the PV with voltage controller fault current contribution is higher value. Current controller fault current contribution is relatively low. In order to observe the given phenomena each model developed in PSCAD/EMTDC platform and identified the fault current contribution for LG fault.

First the fault current contribution from each model obtained as table 3-1. The fault current increase has shown as a percentage of rated current.

Table 3–1: Comparison of Fault current contribution of Each Model

Power Out(MW) Per Phase	CSI % Fault current contribution from rated current	VSI DQ Model % Fault current contribution from rated current	VSI PQ_Model % Fault current contribution from rated current
0.33	22.52%	142.62%	71.17%
0.5	25.30%	92.09%	22.99%
0.75	26.41%	60.60%	25.78%
1	30.12%	46.34%	31.28%
1.35	28.43%	35.44%	23.63%

Normal solar PV, current output is more sensitive to solar isolation level, at steady state condition it is not desirable to consider the constant current output as in average current source inverter controller. It is more appropriate to consider constant voltage is being maintained at the PV common coupling point, by the inverter controllers. Further many references revels that, though fault current contribution varies as per the

inverter type, fault current contribution limits to 2 times maximum. So it is desirable to represent solar PV as voltage source inverter model.

Validating the Model Developed as Average Voltage Source Inverter in PSCAD/EMTDC.

In the developed model for the solar PV, active and reactive power output of the PV can be set using the active and reactive power reference points. When the active and reactive power reference point set to a particular value, the active power, current, voltage, reactive power variation of the solar PV can be obtain as the graphs 3-16.

When P ref = 0.1 pu

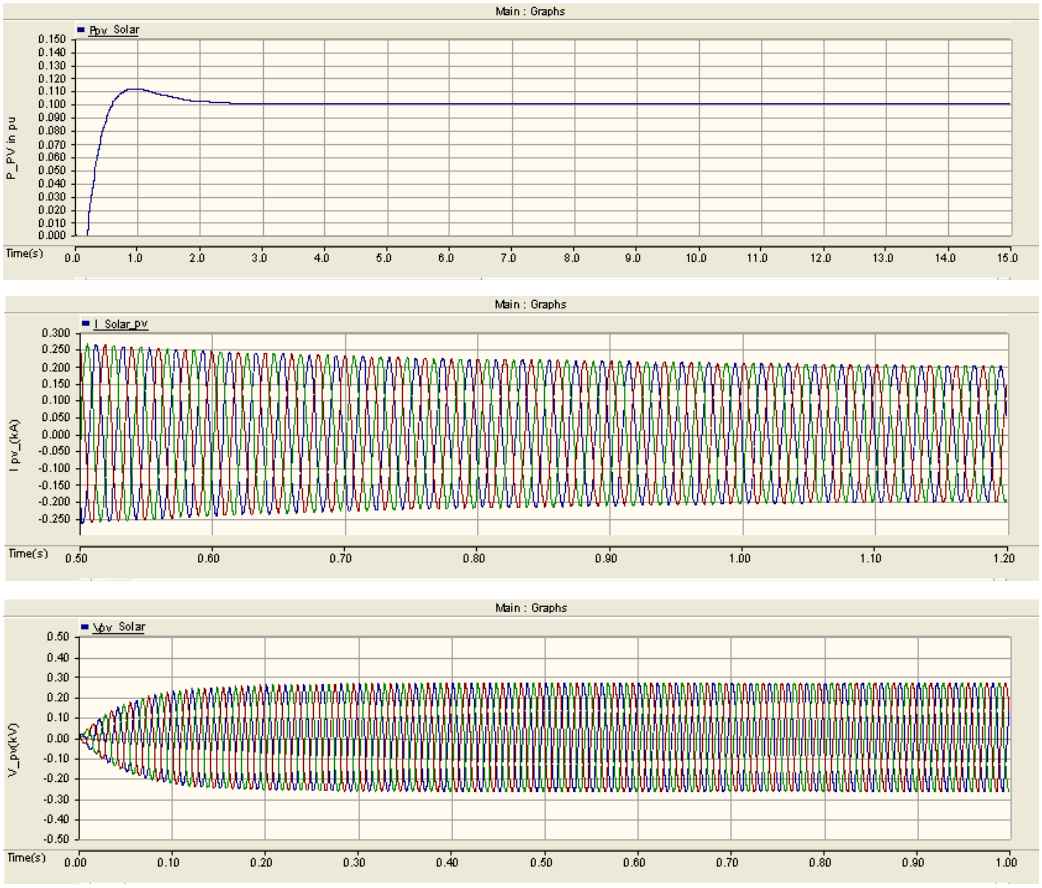

Figure 3-16: Solar VSI Active power, voltage and Current output waveforms at Steady State when the reference set point at 0.1 pu

When P ref = 0.5 pu

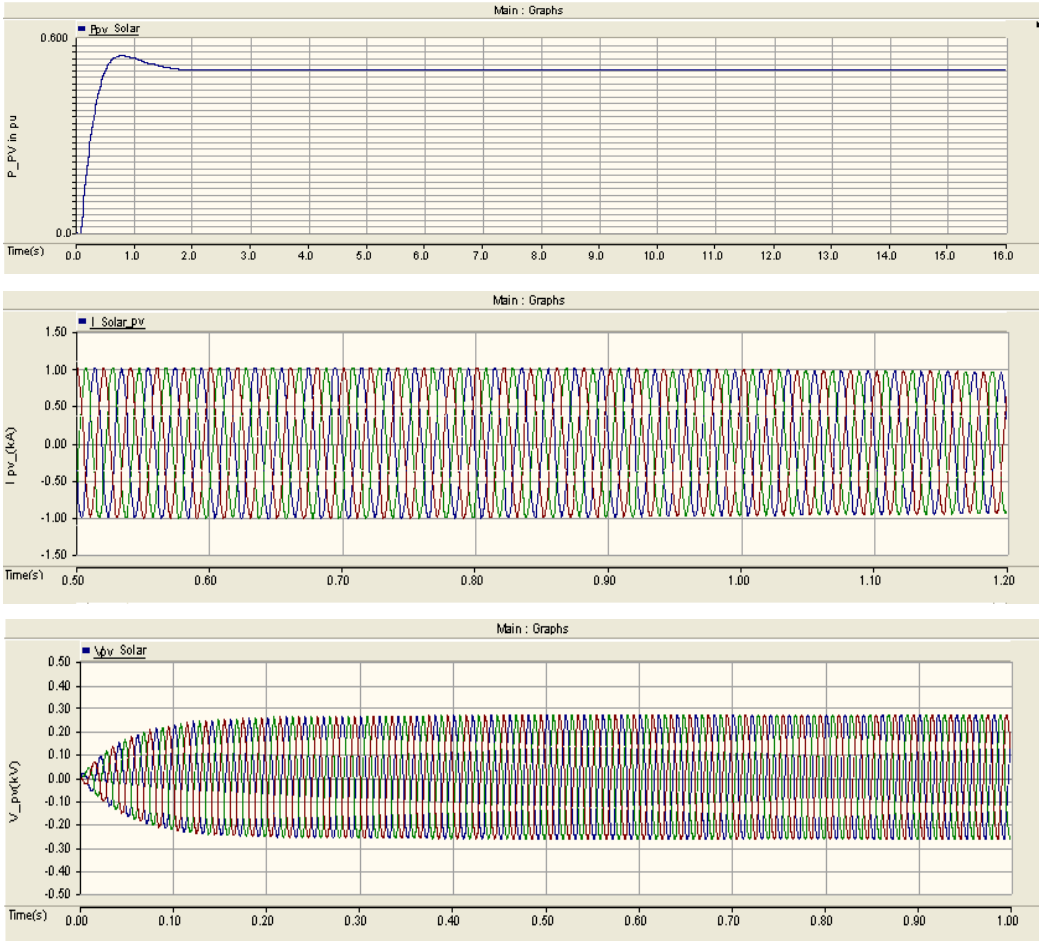

Figure 3-17: Solar VSI Active power, Voltage and Current output waveforms at Steady State when the reference set point at 0.5pu

When P ref = 1 pu

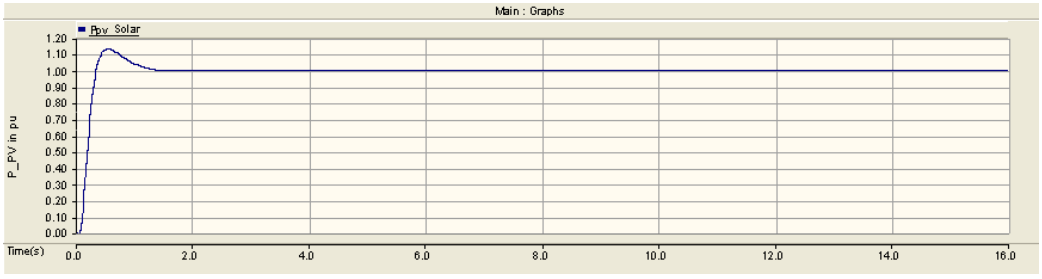

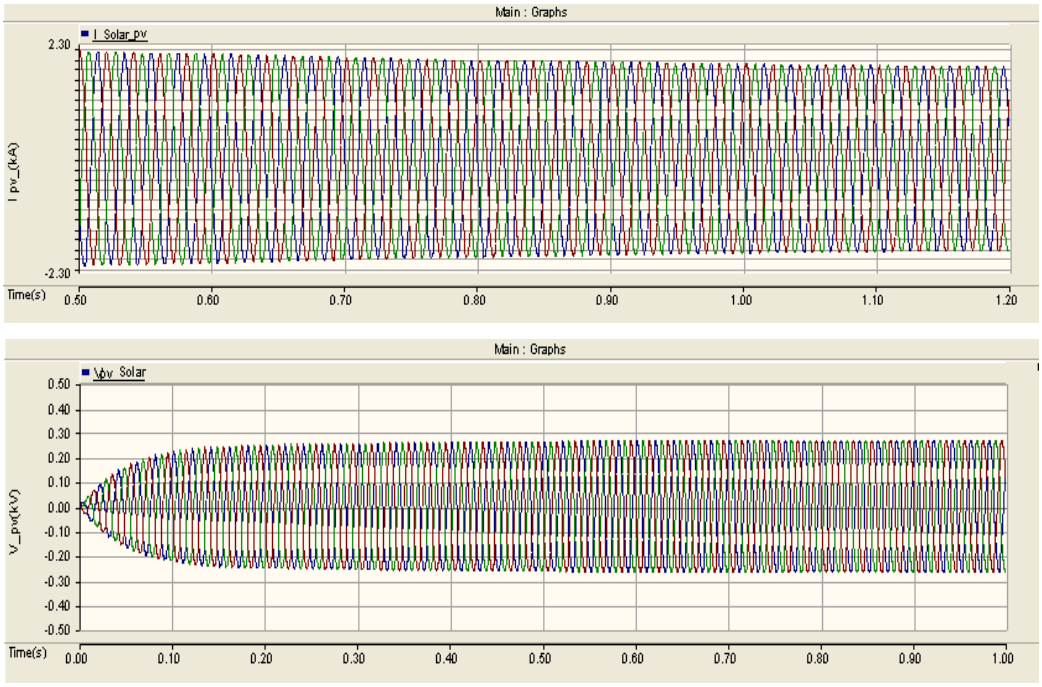

Figure 3-18: Solar VSI Active power, Voltage and Current output waveforms at Steady State when the reference set point at 1 pu

As per the figure 3-17 and 3-18 it can be concluded that the developed model provide the expected power output at desired current and voltage output level. So the model performs accurately for the different steady state power levels.

Validating the Model Developed as Average Voltage Source Inverter using Validated PSCAD/EMTDC Detailed Model.

The developed average VSI is required to be validated of the correct performance at both steady state and dynamic conditions separately. First steady state scenario can be considered. Figure 3-19 shows the comparison of the active power variation for 0.25 pu of both average and detailed solar PV inverter models.

Active Power output variation (when the reference 0.25 pu)

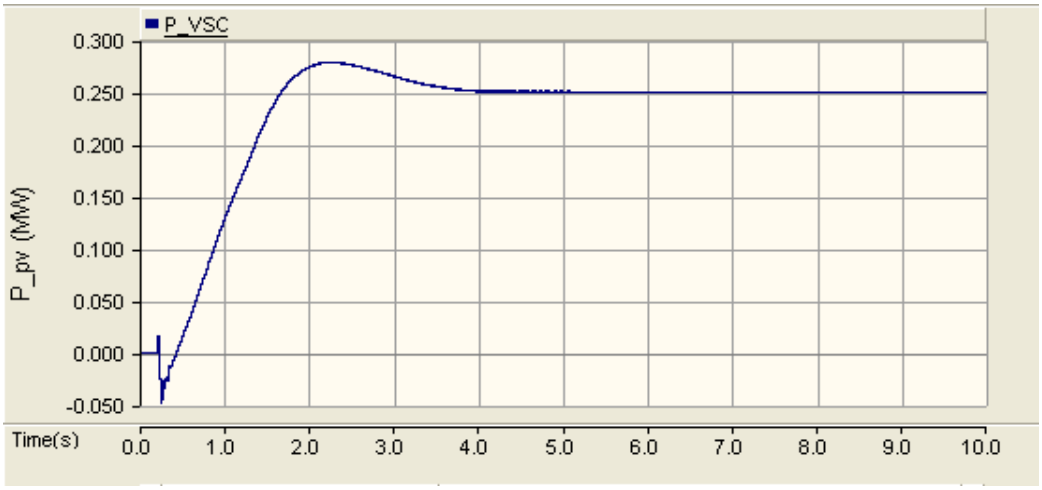

Figure 3-19: Output Active Power Variation of the Detailed Solar PV Model at 0.25referance Point

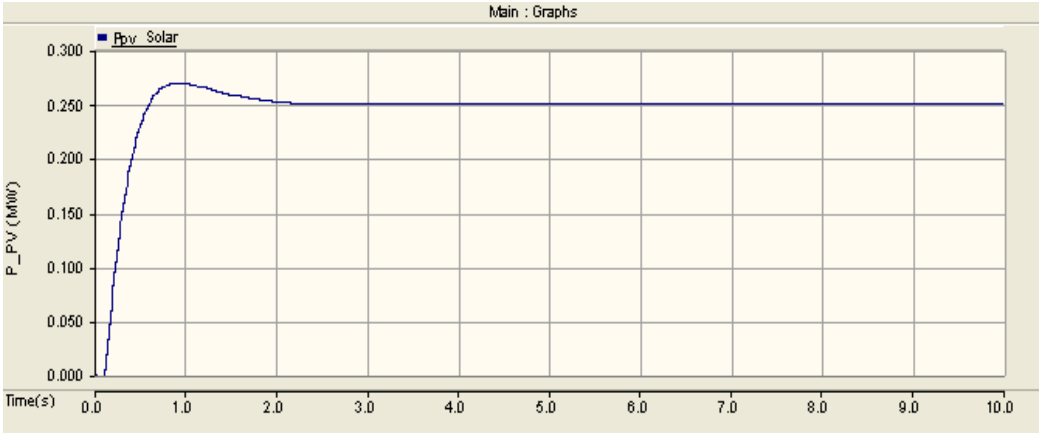

Figure 3-20: Output Active Power Variation of the Average model at 0.25pu reference point

When the figures 3-19 and 3-20 observed, it can be seen that the both models stable at the 0.25pu power output. Hence it can be safely assumed that the average model give the same active power output at steady state condition.

Current output variation (when the reference 0.25 pu)

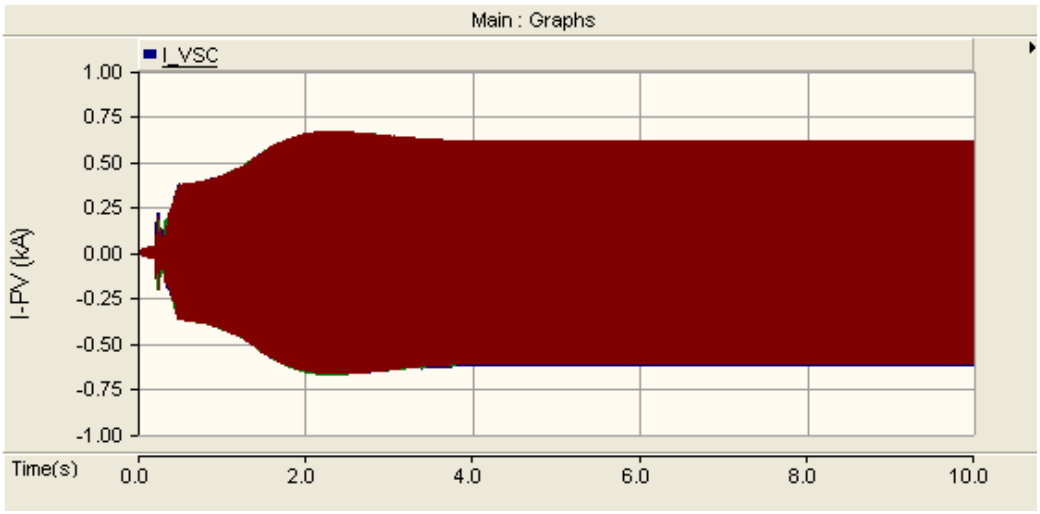

Figure 3-21: Output Current Variation of the Detailed Solar PV Model at 0.25pu reference

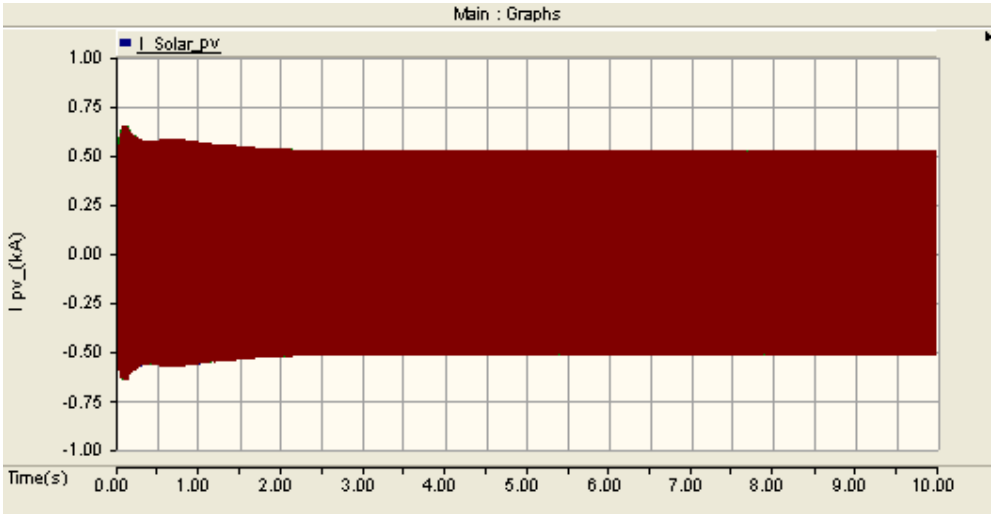

Figure 3-22: Output Current Variation of the Average model at 0.25pu P_reference point

When the current output variation considered (as given in the figure 3-21 and 3-22), it can be observed that the average VSI model and detailed model behave in the same manner.

Voltage output variation (when the reference 0.25 pu)

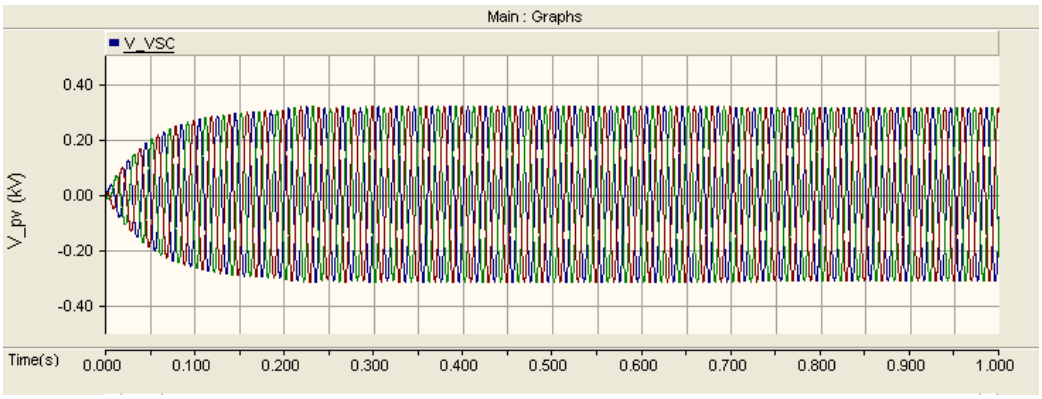

Figure 3-23: Output Voltage Variation of the Detailed Solar PV Model at 0.25pu P_reference point

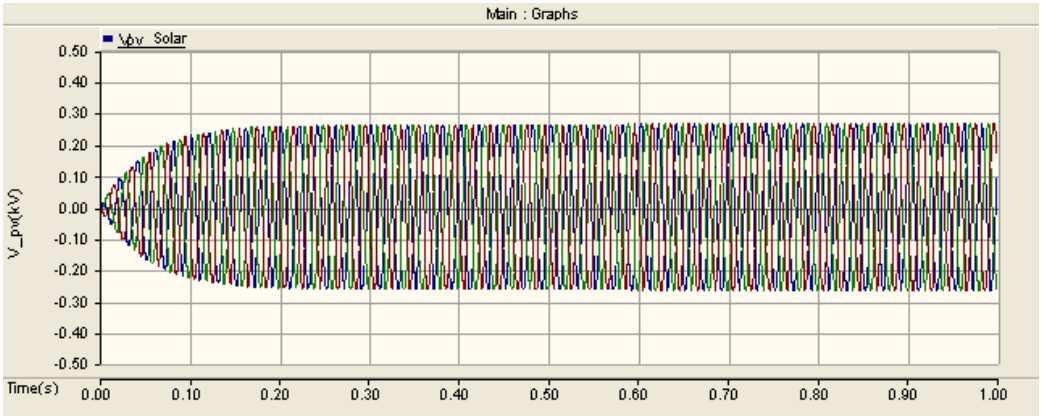

Figure 3-24: Output Voltage Variation of the Average model at 0.25pu P_reference point

As per the figure 3-23 and 3-24, it can be observed that both average and detailed model voltage output provide the expected line to line voltage output.

Reactive Power output variation (when the reference 0.0 pu)

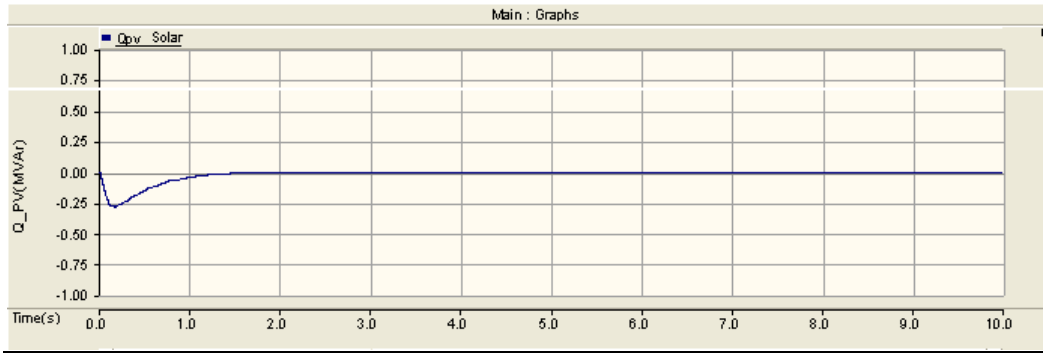

Figure 3-25: Output Reactive Power Variation of the Detailed Solar PV Model at 0.25pu P_reference point

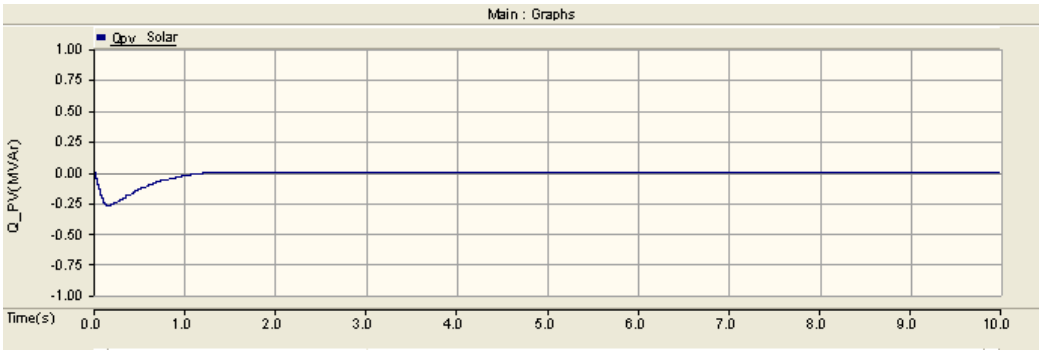

Figure 3-26: Output Reactive Power Variation of the Average model at 0.25pu P_reference point

Developed average solar PV model, performance need to be seperately identified under dynamic condition. This is one of the main component of this reserch. Here for different type of faults, when fault resistance is 0.1 **Ω**, fault current contribution variation is monitored. The graphs has provided in figure 3-23.

Active Power output variation for LG fault (when the reference 0.25 pu)

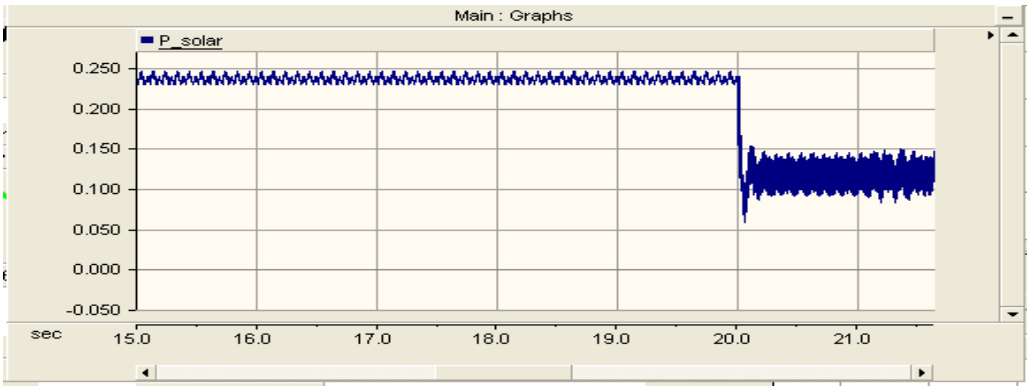

Figure 3-27: Output Active Power Variation for LG faults, of the Detailed Solar PV Model at 0.25pu Reference

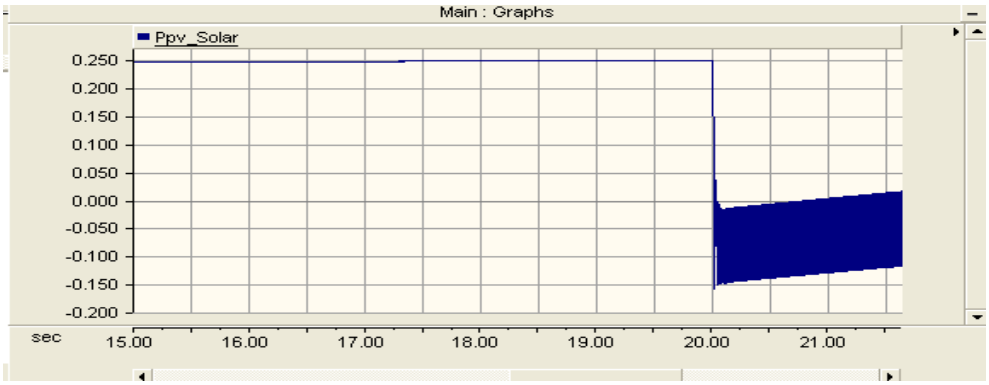

Figure 3-28: Output Active Power Variation for LG faults, of the Average Solar PV Model at 0.25pu Reference

When the figure 3-27 and3-28 observed, it can be observed that the active power output varies in the similar way for average and detailed PV with LG fault created near the PV model. During the fault active power contribution reaches to a minimum value.

Current output variation for LG fault (when the reference 0.25 pu)

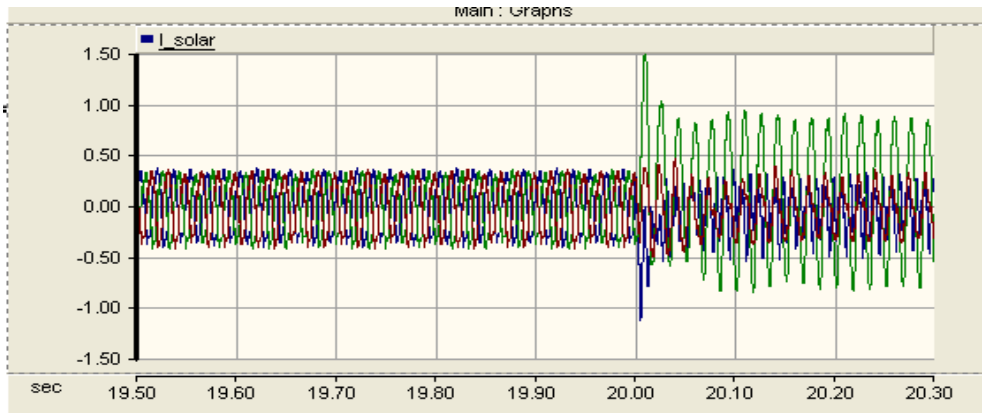

Figure 3-29: Output Current Power Variation for LG faults, of the Detailed Solar PV Model at 0.25pu Reference

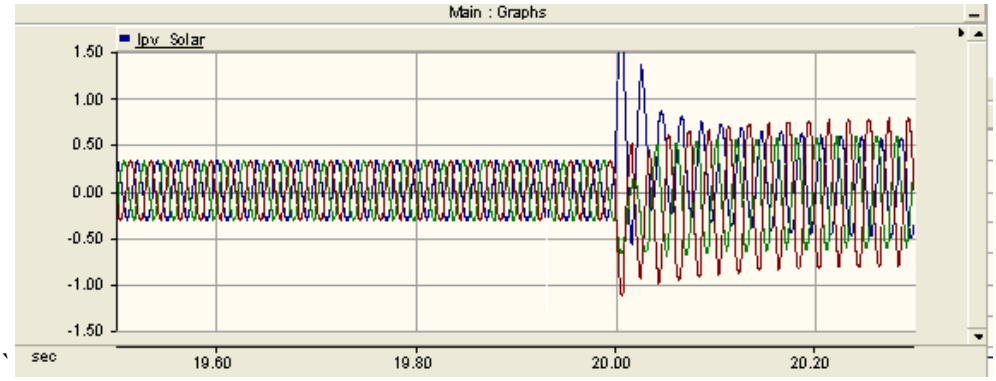

Figure 3-30: Output Current Power Variation for LG faults, of the, Average model at 0.25pu Reference

As per the figure 3-29 and 3-30, it can be seen that the both average and detailed solar PV output current variation for LG fault in the same manner allowing fault current variation in the range of 49% for the faulted phase.

Active Power output variation for LLL fault (when the reference 0.25 pu)

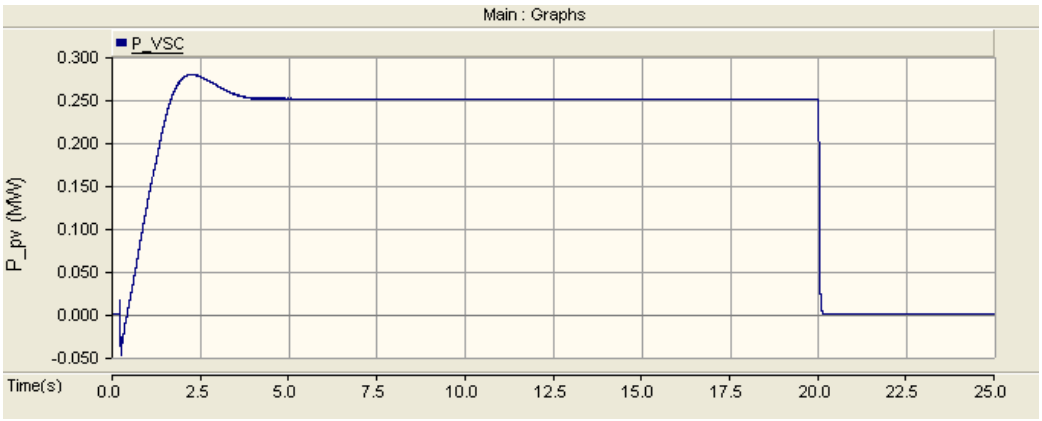

Figure 3-31: Output Active Power Variation for LLL faults, of the Detailed Solar PV Model at 0.25 Reference

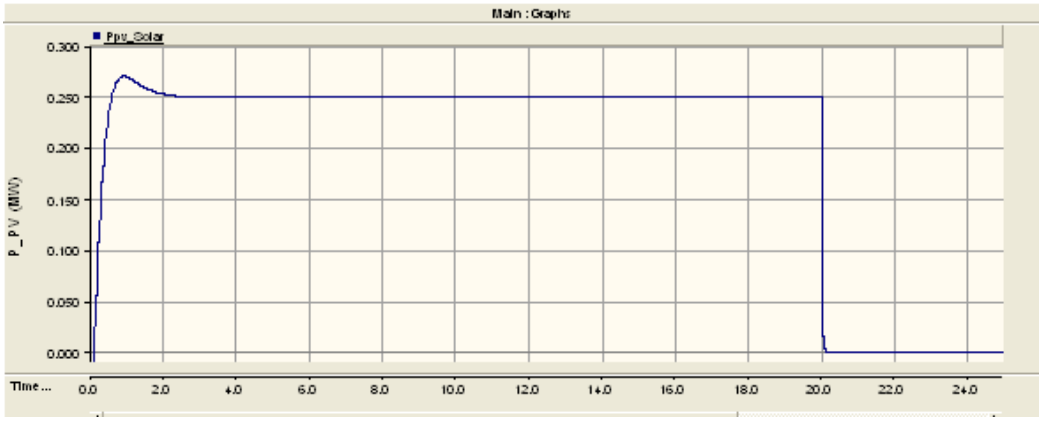

Figure 3-32: Output Active Power Variation for LLL faults, of the Average Solar PV Model at 0.25 Reference

Figure 3-31 and 3-32 illustrate the active power variation of the detailed and average VSI inverter model. During the fault the active power contribution reduces because during the faultly conditon resistive portion of the impedance path reduces with respect to the reactive impedance.

Current output variation for LLL fault (when the reference 0.25 pu)

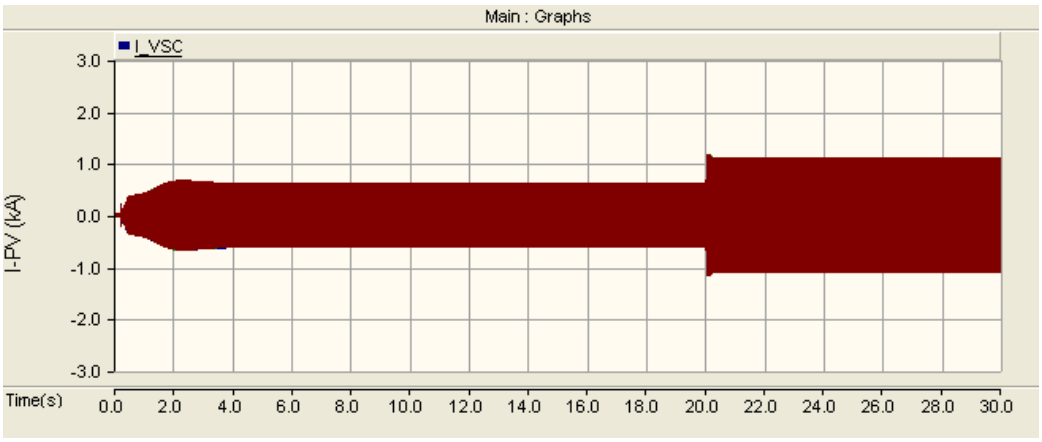

Figure 3-33: Output Current Variation for LLL faults, of the Detailed Solar PV Model at 0.25 Reference

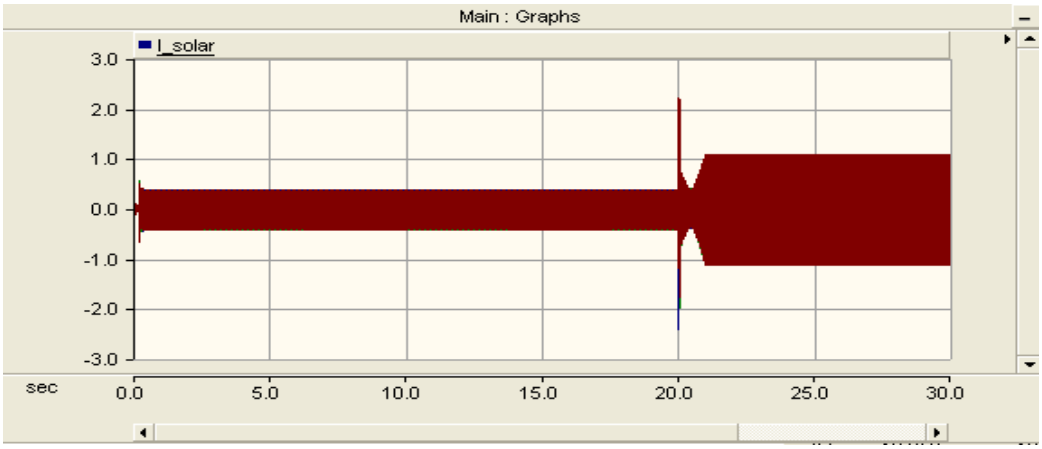

Figure 3-34: Output Current Variation for LLL faults, of the Average model at 0.25 Reference

Figure 3-33 and 3-34 show that the current output variation for a 3 phase fault with the same range of current magnitude during the fault period.

As per the given simulation results, it can be observed that the simulated generic PV module operates in a similar manner as detailed solar PV model during faults in transient domain.

Additionally by reviewing the literature reviews from the experimental data, an idea regarding the solar PV inverter fault current contribution can be obtained. As per reference [6] fault current contribution from solar PV is based on inverter type. Based on the inverter type fault current contribution and contribution duration can be varied. Based on the six types of inverters used for experiment, a generic type of model can be used which can provide fault current up to 50% of rated current during 10 cycles.

In order to identify the short circuit level increase by a set of connected PV systems, arithmetical summation can be taken with the maximum fault current contribution of 120% of the rated current. Though the fault current contribution from the PV is based on the vendor, when the effect from large number of PV is considered, without loss of generality a maximum fault current contribution of 1.2 can be considered. In that contest it has to be assumed that the any DC component injected by the inverter is neglected.

Ref [7] Using IEEE 13 bus network, with connection of solar PV fault current contribution may vary type of the fault and fault location. As a conclusion ,it has been pointed out that the proper analysis need to be carryout in order to identify the impact on the shot circuit level due to heavy solar penetration.

3.2. The selected case studies for simulation and the system modelling using PSCAD.

Ehul kottte Primary substation has been selected for the simulation as that area has a significant solar PV penetration available. In the research, initially protection performance of the existing system has been evaluated without considering the solar PV penetration. Secondly the same system protection performance evaluated considering connected solar PV. Here for the simulation, the protection system performance can be evaluated for different penetration levels.

Figure 3-35 shows the equipment arrangement of the selected substation. The connected 11kV feeders are indicated as F1, F2, F3, and F4.

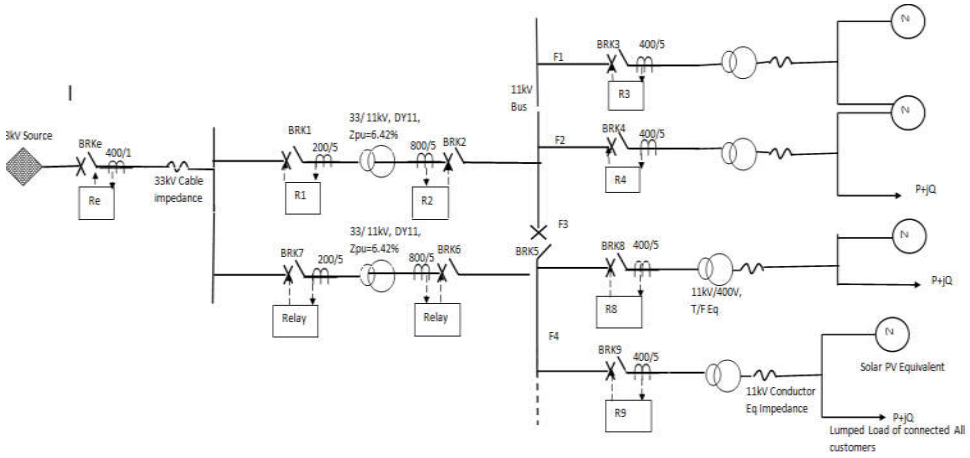

Figure 3-35: Overall Schematic with 11kV distribution Feeders

In this chapter detailed Modelling of each component has been given.

3.2.1 33kV Grid (Upper Network Equivalent)

For the simulation I selected 33kV Sri Japura GSS 33kV feeder. Hence 33kV Sri Jaura Substation is considered as the source. To represent it as a source with finite impedance, the equivalent thevenin impedance is obtained from PSSE simulation obtained from CEB planning branch. These values were the simulation results.

The calculated positive sequence impedance by PSSE=1.3512∟-88.9

The calculated zero sequence impedance by PSSE=1.3512∟-87.8

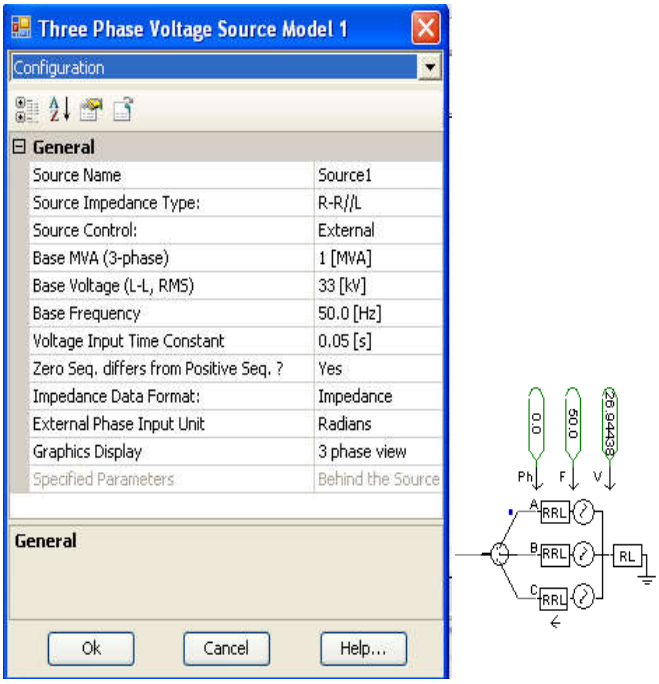

Figure 3-36:33kV Feeder as Source with finite Impedance

To represent the 33kV feeder as the source, three phase voltage source model 01 has been used. This component models 3 phase AC voltage source, with specified source comprised with fixed positive and zero sequence impedance. In this component source power output regulated in a manner that bus voltage, angle and frequency can be kept constant as per set values. So the external controlling inputs are Line to Line voltage, frequency and phase angle. The component configuration can be shown as figure 3-36.

3.2.2. 33kV distribution System Modelling.

Sri Lanka 33kV distribution system is comprised with transmission over head lines and mostly urban areas with underground cables. In the considered situation an underground cable connect Sri Japura GSS and Ethul-Kotte primary. Since this case study comprised with unbalance fault calculation studies, it is required to calculate accurate positive, zero, negative sequence impedance considering actual

characteristics of these distribution system corridors. Both transmission line and underground cable sequence calculation has been described in the section3.2.3.

3.2.3. Modelling Cu 240mm^2 Cable with length of 2.4 km

Table 3-2 shows the parameters used for simulating a cable. Figure 3-37 illustrates how the cable is simulated using the PSCAD/EMTDC software. Further figure 3-37 clearly illustrates the methods to interface the cable using interface for unsymmetrical faults simulation accurately.

Table 3–2:33kV Cable Parameters for Modeling

Parameter	Value
Segment Name	Cable_01
Steady-State Frequency	50 [Hz]
Segment Length	3.2 [km]
Coupling of this segment to others is	disabled

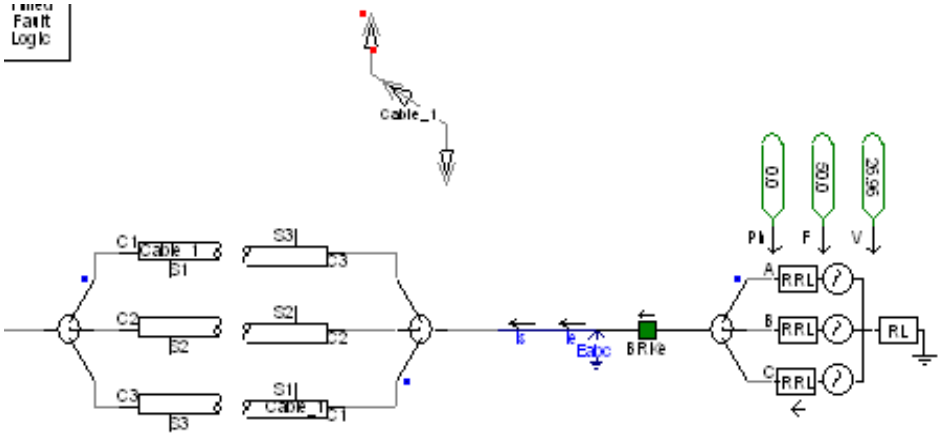

Figure 3-37: Cable Model and Cable Interfacing in PSCSD software

- Defining the cable parameters

Soil Resistivity can be varied from location to location. It is a nominal practice that the utility try to maintain the soil resistance less than 10 **Ω** near towers. But exact soil

resistivity data not available. Hence it has considered that the soil resistivity to be 100 **Ω**.

- Coaxial Cable Cross Section

Table 3–3: Coaxial Cable Data for Simulation

Parameter	Setting Value
Placement in relation to ground plane	Underground
Depth below ground surface	1.0[m]
Horizontal translation from centre	0.0[m]
Layer Configuration	C1/I1
Layer thickness is specified as	Radial from center
Ideal Cross –Bonding(Transposition)	Disabled

Core Conductor Data

Resistivity	0.246[**Ω**m]
Relative Permeability	1.0
Geometry	
Inner radius	0.0(As this is a solid core)
Outer radius	0.0011175[m]-From data sheet

- 1 st Insulation and Semi-Conductor Layer Data

Semi Conductor Layers	Are absent
Electrical Propeties	
Relative Permittivity	3.9(default value)
Relative Permeability	1.0
GEometry	
Outer radius	0.01275 [m]

Other phase conductors have same data except the Horizontal translation from centre. Figure 3-38 shows the method to simulate the underground cable parameters.

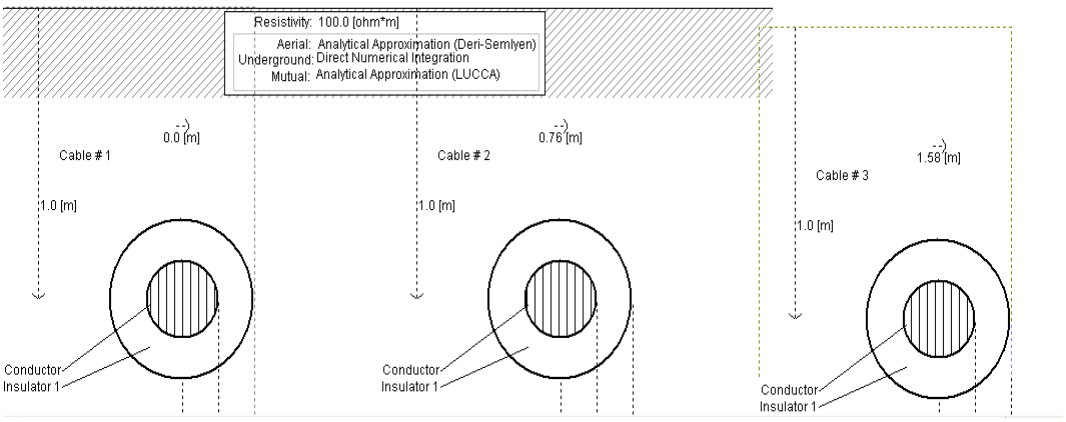

Figure 3-38: Underground cable Configuration

In the PSCAD, cable interface have to be used when cable connecting to the system. As given in the figure the cable interface parameters for the simulation is given as show in the table 3-4.

- **Cable Interface configuration**

Table 3–4: Cable Interfacing Configuration

Configuration	Parameter Value
Cable Name	Cable_1
Number of coaxial cables	3
Encompassing pipe conductor is	Not present
Coaxial Cable 01	Conductor/sheath
Coaxial Cable 02	Conductor/sheath
Coaxial Cable 03	Conductor/sheath

If the 33kV distribution comprised with over head line in order to calculate the sequence components for fault analysis,

- The transmission line parameters

Table 3–5: Parameters for Simulating Transmission Line

Configuration	Parameter Value
Segment Name	T Line
Steady –State frequency	50[Hz]
Segment Length	3.2[km]
Number of conductors	3
Termination Style	Direct Connection
Coupling of this segment to others is	Disabled.

- Finding the Sequence parameters of particular transmission corridor.

For a transmission line corridor with single three phase conductors the parameters can be found considering flat tower configuration,

- **3 conductor Flat Tower configuration**

Table 3–6: Parameters to simulate Tower Configuration

Ideal transposition of the circuit is	Enabled
Shunt Conductance	1.0 e-11[**Ω**/m]
Tower Name	3L1
Relative x-position of the tower centre	0.0[m]
Height of all conductors	15.0 [m]
Horizontal spacing between conductors	7.5 [m]
Height of ground wires over lowest condu	10.0 [m]
Spacing between ground wires	5[m]
Conductor data	
Conductor Style	Solid core
Name	Racoon
Outer Radius	0.02024 [m]-from data sheet
DC Resistance(entire conductor)	0.03206[**Ω**/km]
Relative Permeability	1.0
Sag(all conductors0	10 [m]

Ground wire Data

Table 3–7: Ground Wire Configuration Data

Total number of ground wires is	2
Ground wires are	identical
Ground wire elimination is	enabled
Outer radius	0.0055245 [m]-Data Sheet
DC resistance	2.8645 [**Ω**/km]
Relative Permeability	1.0
Sag(all ground wires)	10 [m]

So using those parameters the simulation can be obtained as figure 3-31.

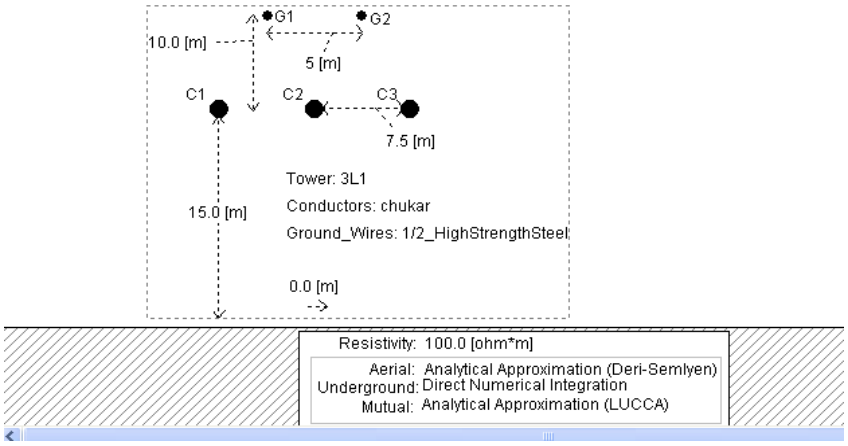

Figure 3-39: Physical Cross section of the simulated tower in Distribution Corridor

In this simulation the obtained cable parameters have been compared with the simulation Synergy software used by the distribution division. The difference between the calculated and practically utilizing value were smaller. So sequence impedance parameters for Cu 240mm2 underground cable was,

$$Z_0 = 0.0318 + 0.03723i$$

$$Z_1 = 0.03192 + 0.03419i$$

3.2.4. 33/11kV Transformers

Figure 3-40 shows the actual name plate data represented in the PSCAD/EMTDC model.

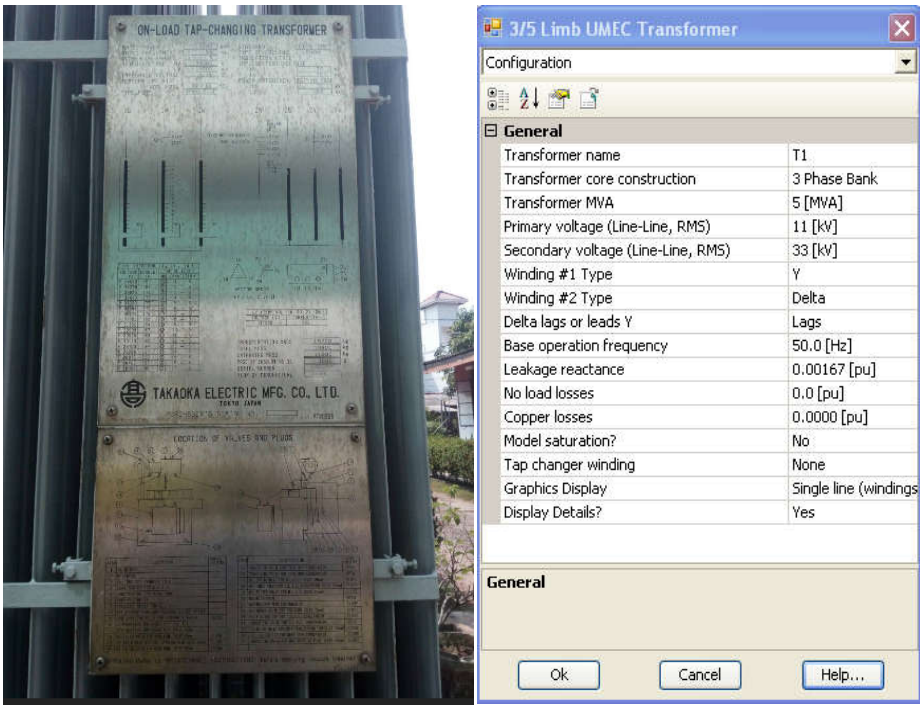

Figure 3-40:11/33kV Transformer Name Plate Data and Parameters for Simulation

According to the name plate data in order to simulate the transformer PSCSD 3/5 Limp UMEC model has been used. Here the option for core saturation has not been utilized. Only the ideal transformer characteristics have been used, neglecting magnetizing branch. As the unavailability of data such as leakage reactance, core geometry, yoke, winding limb dimensions standard values have been used. The equivalent Impedance from the name plate data obtained as 8.35%. This value can be represented in per unit value which calculated using the equation 3.23.

$$11\_33kVEq\_Impedance = \frac{Zgiven}{Zbase_{new}} \times Zbase_{now} = \frac{0.0835}{Zbase_{new}} \times Zbase_{now} \quad (3.23)$$

$$11\_33kVEq\_Impedance\ = 0.00167\ pu$$

3.2.5. 33/11kV 11kV Network Equivalent Network

11kV Feeder network is spread in large geographical area comprised with lot of transformers and loads connected with different configurations (some parts underground, some parts overheads). Part of the considered 11kV feeder geographical map has shown in the figure 3-41.

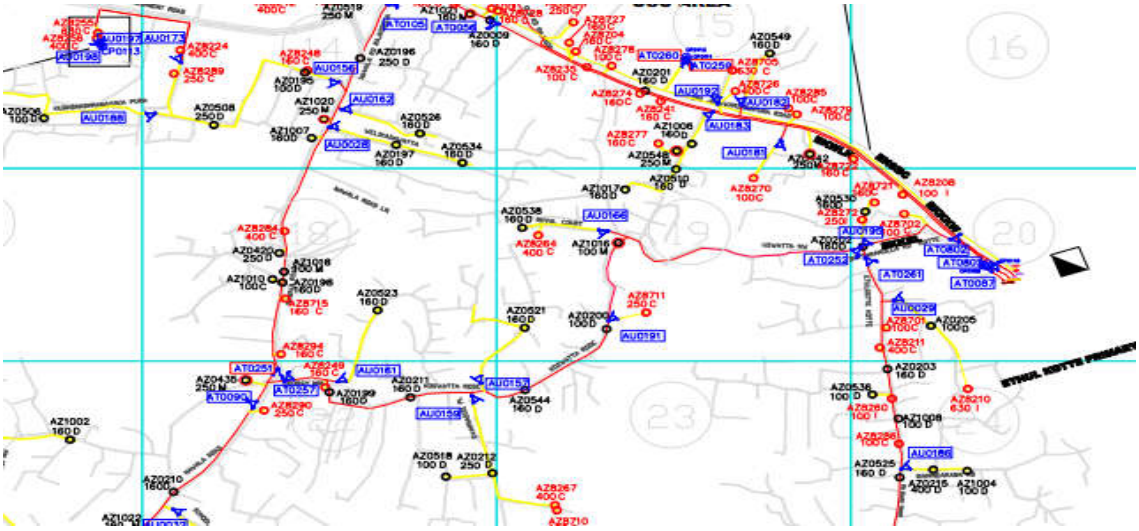

Figure 3-41: Part of the Map of 11kV Network Used for Simulation

It is difficult to model the entire collector system in a widely distributed network. So WECC has recommended obtaining an equivalent collector system. [2][3]

$$Equivalent\ Impedance(Z_{eq}) = R_{eq} + jX_{eq} = \frac{\sum_{i=1}^{I} Z_i n_i^2}{N^2}$$

N- Number of transformers connected. (3.24)

Using the network topology of the system equivalent impedance has calculated considering no of transformers connected to a particular length of a line. The total number of rooftop solar PV connected is considered as lump generation. The table developed to calculate 11kV Collector system equivalent impedance for Kotikawaththa Feeder has shown figure 3-42.

Conductor Type	Fro	To	T/F I	No of	X(ohm/l	R(ohm/l	n	L(ki	Rn	Xn2
11kV UG A143(3*70mm2 AL)	A	B	AZ0173	1	0.00025	0.1576	4	0.2	0.5043	0.0008
			AZ0175	2						
			AZ0177	1						
11kV UG A143(3*70mm2 AL)	B	C	AZ0178	2	0.00025	0.1576	6	0.2	1.1347	0.0018
	C	D	AZ0185	3						
			AZ0191	2	0.00025	0.1576	11	0.2	3.8139	0.00605
11kV UG A143(3*70mm2 AL)	D	E	AZ0192	4	0.00025	0.1576	15	0.2	7.092	0.01125
11kV UG A143(3*70mm2 AL)	E	F	AZ0193		0.00025	0.1576	15	0.2	7.092	0.01125
11kV UG A143(3*70mm2 AL)	G	H	AZ0193	6	0.00025	0.1576	21	0.2	13.9	0.02205
11kV UG A143(3*70mm2 AL)	H	I	AZ0201	12	0.00025	0.1576	33	0.1	17.163	0.027225
11kV UG A143(3*70mm2 AL)	I	J	AZ0353	3						
			AZ0400	1	0.00025	0.1576	37	0.1	21.575	0.034225
11kV UG A143(3*70mm2 AL)	J	K	AZ0401	2	0.00025	0.1576	39	0.1	23.971	0.038025
11kV UG A143(3*70mm2 AL)	K	L	AZ0402	11	0.00025	0.1576	50	0.2	78.8	0.125
11kV UG A143(3*70mm2 AL)	L	M	AZ0403	3	0.00025	0.1576	53	0.2	88.54	0.14045
11kV UG A143(3*70mm2 AL)	M	O	AZ0404	5						
			AZ0405	2	0.00025	0.1576	60	0.2	113.47	0.18
11kV UG A143(3*70mm2 AL)	O	P	AZ0408	4						
			AZ0409	3	0.00025	0.1576	67	0.2	141.49	0.22445
11kV UG A143(3*70mm2 AL)	P	Q	AZ0410	2						
			AZ0411	5						
			AZ0444	5	0.00025	0.1576	79	0.2	196.72	0.31205
11kV UG A143(3*70mm2 AL)	Q	R	AZ0465	3						
			AZ0468	1						
			AZ0549	2						
			AZ0803	4						
			AZ0804	5						
			AZ0806	2	0.00025	0.1576	96	0.2	290.49	0.4608
11kV UG A143(3*70mm2 AL)	R	S	AZ0807	2						
			AZ0810	5						
			AZ0812	2						
			AZ0819	4						
			AZ0829	2						
			AZ1013	2						
			AZ8504	1	0.00025	0.1576	114	0.2	409.63	0.6498
						R eq	0.032		X eq	0.00005

Figure 3-42: Table Used to obtain the equivalent impedance of the MV feeder

In the similar manner equivalent impedance can be obtained for other feeders. The equivalent impedance calculation for each feeder can be given as table 3-8.

Table 3–8: Equivalent 11kV feeder Impedance Table

Feeder Name	Feeder Number	11kV Equivalent Impedance
Kotikawatha	F1	0.00765+0.00894i **Ω**
Welikada	F2	0.00821+0.00857i **Ω**
Kalubowila	F3	0.00902+0.00798i **Ω**
Parliment	F4	0.0076394+0.00026 **Ω**
Baththramulla	F5	0.00865+0.00783i **Ω**

3.2.6. 11/0.4kV Transformers Represent as Equivalent Lumped transformer.

MV/LV transformers are widely spread all over the distribution network. As well as the MV cables MV/LV transformers can be represented by equivalent model according to the recommendation by WECC.

$$Z_{Teq} = \frac{Z_T}{N} \qquad (3.25)$$

$$Z_T - Pu\ impedence\ of\ transformer$$

$$MVA_{Teq} = N \times MVA_T \qquad (3.26)$$

$$N - no\ of\ transformers\ represented\ in\ eqivalant$$

$$MVA_T - Transformer\ MVA.$$

Sri Lankan 11, 33kV Distribution system comprised with transformers of different capacity levels as per the customers and system requirements. When the 11kV LECO feeders considered it is comprised with different capacity levels 50, 100, 160, 250 kVA mostly. To calculate equivalent transformer to represent the system the impedance calculated in the similar manner the equivalent impedance calculated for 11kV feeder.

Z pu % of 160kVA T/F=4.5%

Z pu % of 100kVA T/F=4.19%

The equivalent transformer impedance calculated has shown in the given table 3-7.

Table 3-7: Equivalent MV/LV Transformer Impedance

Feeder Name	Feeder Number	0.4/11kV T/F Equivalent
Kotikawatha	F1	2.017543860E-04i
Welikada	F2	1.393939394E-04i
Kalubowila	F3	7.467532468E-05i
Parliament	F4	1.523178808E-04i
Baththramulla	F5	1.031390135E-04i

- Equivalent Impedance for 0.4kV Solar PV average model

In typical detailed model equivalent, there is no separate impedance represent. But when it represents as average equivalent model separate impedance should be there. The actual value for this can be obtained from experimental data, by obtaining the inverter fault current contribution for the three phase fault. That impedance need to be divided from the number of PV connected because they all operating as parallel paths to feed the fault current.

3.2.7. 11/0.4kV 33kV and 11kV levels Existing Relays and Protection Schemes

In this substation MV level protection has provided using over current and earth fault protection. The relay comprised in numerical relay type with the manufacturers such as ABB, Siemens.

In this research basically covers the medium voltage level protection scheme performance. First simulated system evaluated for different type of faults with different solar PV penetration levels. Initially without considering any PV penetration the existing protection scheme performance has been evaluated for different type of faults at different fault impedances. Figure3-43 shows the existing relay type at each location and their existing setting.

Existing over current setting scheme has shown in figure 3-43.

Location	CT Ratio	Relay Type	Plug Setting2	Curve Type	TMS
33kV Out Going Feeder Relay	400/1	REF 542 Plus	1(400A)	Normal Inverse	0.1
			4(1600A)	DT	60ms
33/11kV T/F HV side Relay	200/5	CDG	5(200A)	Normal Inverse	0.05
33/11kV T/F LV side Relay	800/5	CDG	3.75(600A)	Normal Inverse	0.15
11kV Bus Coupler	600/5	CDG	5(600A)	Normal Inverse	0.075
11kV Out Going Feeder	400/5	7SJ622	3.75(300A)	Normal Inverse	0.15
			12.5(1000)	DT	10ms
11kV Out Going Recloser(Only some Feeders)	400/5	Noja	3.75(300A)	Normal Inverse	0.05

Figure 3-43: Existing Over Current Scheme-Relay Setting Parameters

The figure 3-44, describes how the tripping time changes as per the measured fault current level.

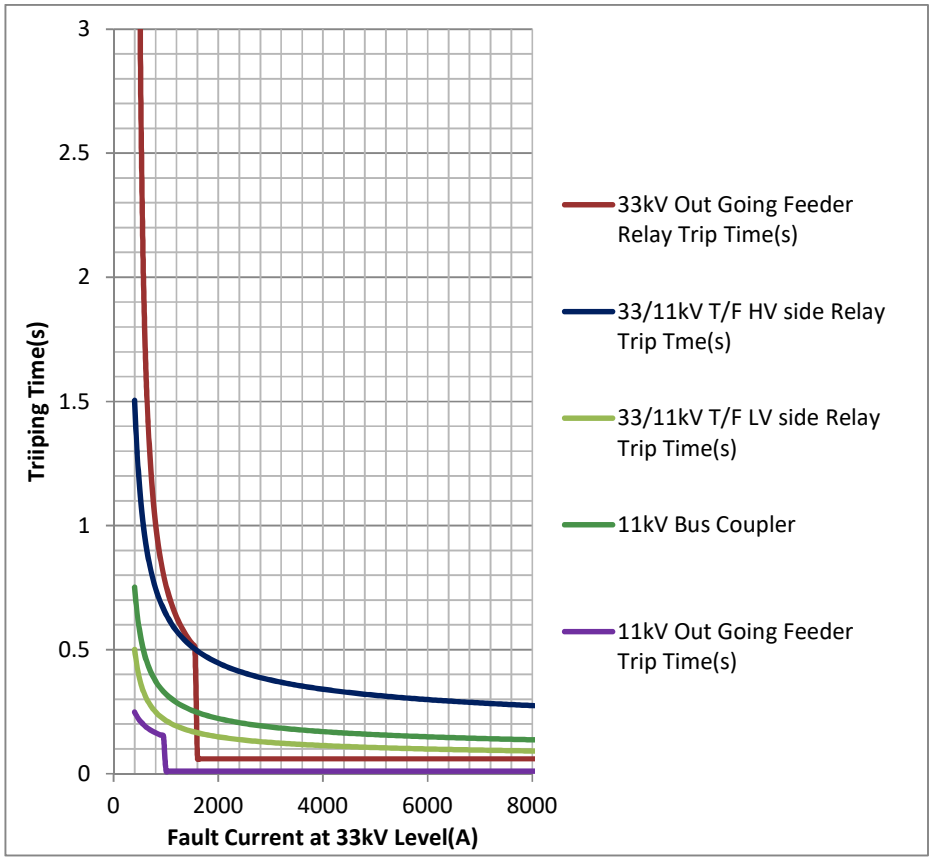

Figure 3-44: Existing Over Current Characteristic

When the figure 3-45 observed, it is obvious that up to 1600A fault current the existing protection coordination is operating accurately with sufficient coordination margin. If the fault current is less than 1600A for an over current fault, the relay is accurately operating. So in order to verify the existing protection coordination with the heavy solar PV penetration, it has to be observed the fault current variation level with added PV generation.

Existing Earth Fault setting scheme has shown in figure 3-45.

Location	CT Ratio	Relay Type	Plug Setting	Curve Type	TMS
33kV Out Going Feeder Relay	400/1	REF 542 Plus	0.1(40A)	Normal Inverse	0.1
			0.4(160)	DT	40ms
33/11kV T/F LV side Relay	800/5	CDG	1(160A)	Normal Inverse	0.2
11kV Out Going Feeder	400/5	7SJ622	0.5(40A)	Normal Inverse	0.25
			4(320A)	DT	10ms

Figure 3-45: Existing Earth Fault Current Scheme-Relay Setting Parameters

When the unbalanced current measured by each relay considers, the tripping time variation in earth fault relays can be given as in figure 3-46.

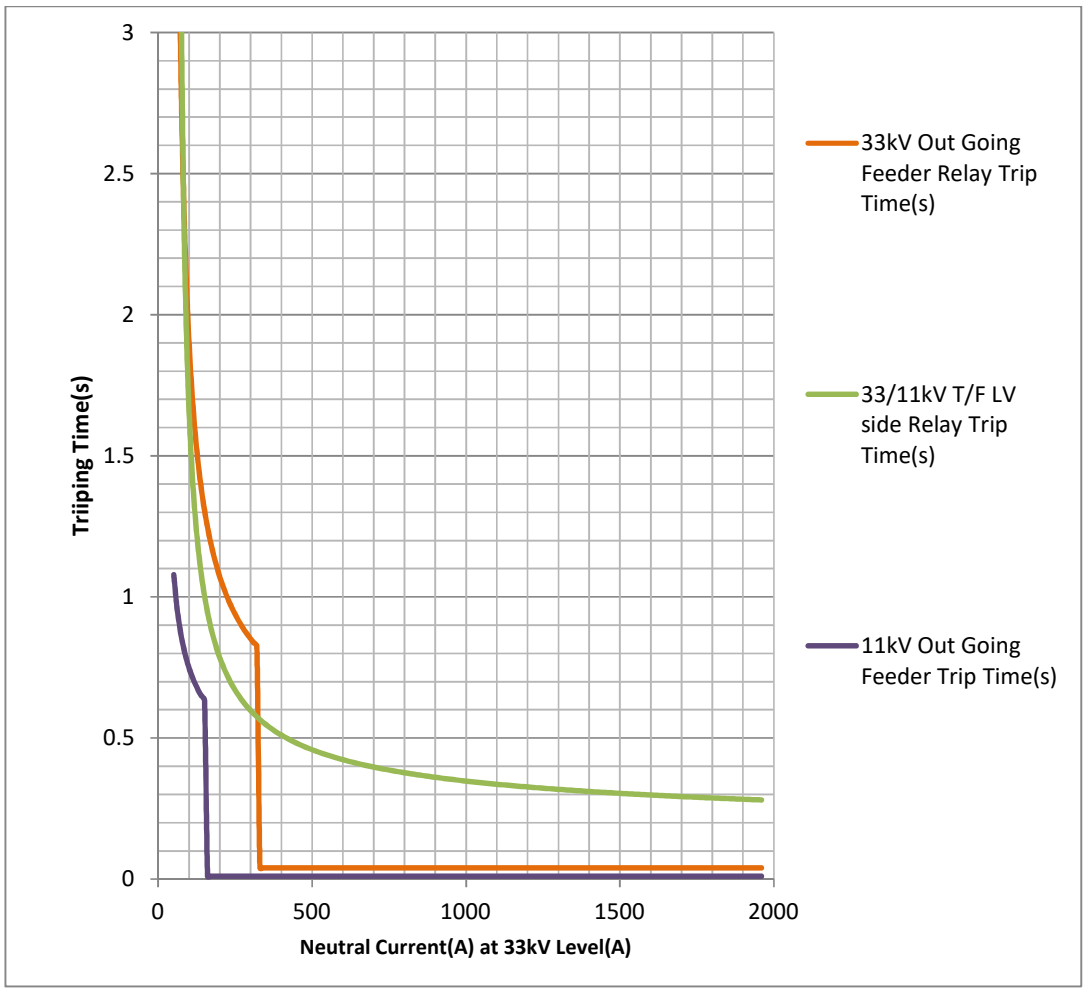

Figure 3-46: Existing Earth Fault Current Characteristic

As per the figure 3-46, it can be observed that the appropriate coordination is available up to the unbalance neutral current of 320A. In order to verify the accurate performance of existing E/F protection coordination, it has to be checked that the unbalance current level increases more than 320A due to added solar PV generation. If the maximum unbalance current less than 320 even after added PV penetration, it can be concluded that the existing earth fault protection scheme operates accurately even with the solar PV penetration to the LV system.

3.2.8. Evaluate the Existing System Coordination for different Fault locations when solar PV Penetration neglected.

The given figure 3-47 shows the fault locations for different type of faults.

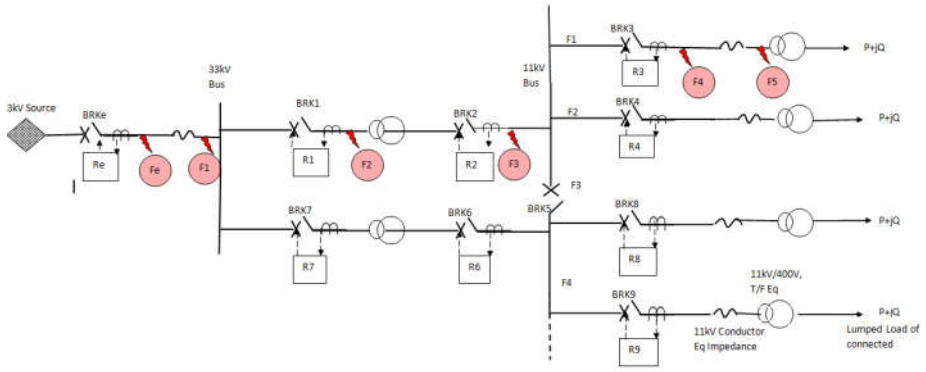

Figure 3-47: Schematic of the Selected Configuration Indicated with Fault Locations

For simulation, existing PV active power and reactive power contribution identified. As the solar PV impact for MV protection coordination is considered, the scenario are selected under the assumption that the solar PV loading higher day peak time. The table 3-9 shows the consumer equivalent loading and equivalent solar PV capacity, consider for the existing protection coordination valuation.

Table 3–9: Equivalent Solar PV and Customer Loading for Existing System simulation

Feeder Number	Rated P Total at 11kV Level	Solar MW
F1	0.51	0.38
F2	0.98	0.73
F3	1.82	1.36
F4	1.09	0.82
F5	0.94	0.70

- ***Over current and Earth fault Relay Simulation in PSCAD.***

When over current relays are considered both IDMT and DT protection functions available. (Protection function detailed described in 2.4.2 section).In order to develop IDMT function the maximum current can be used as the input to the relay. To obtain 51 IDMT protection function standard over current relay can be used as shown in figure 3-48.

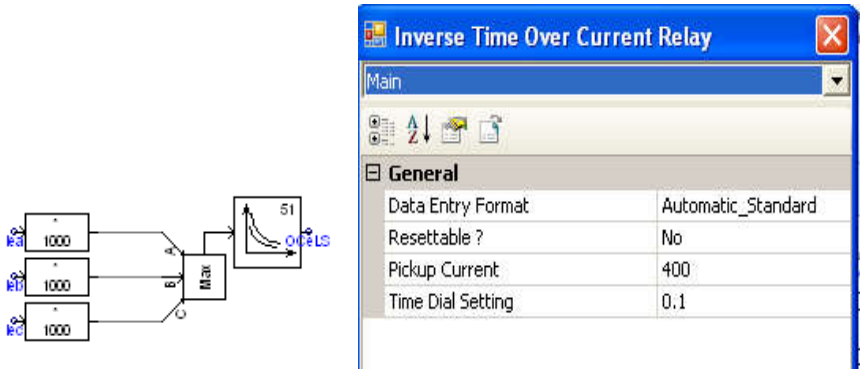

Figure 3-48: Over Current Relay Parameters to simulate in PSCAD

Same way 50 high set over current function can be obtained using 50 over current function can be simulated as shown figure 3-49.

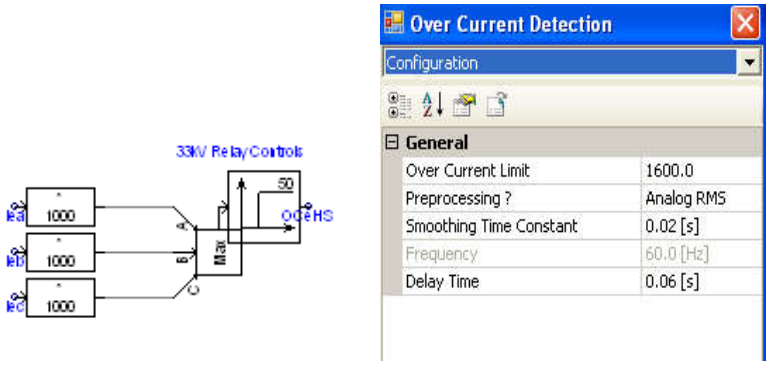

Figure 3-49: Earth Fault Relay Parameters to simulate in PSCAD

In the similar manner earth fault function can be implemented in the PSCAD if the resultant current can be obtained. In normal relays if no neutral CT available, by using phase current relay internally calculate the resultant current and use as the input to the 51N and 50N function.

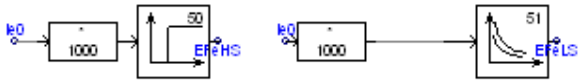

But using the measured current directly and giving to the available relay components expected relay performance cannot be obtained. Especially the existing numerical relays have special furrier transformation algorithms to filter the harmonic currents.

To obtain harmonic filtered phase current and unbalance currents “On-Line Frequency Scanner” component used as shown in figure 3-50.

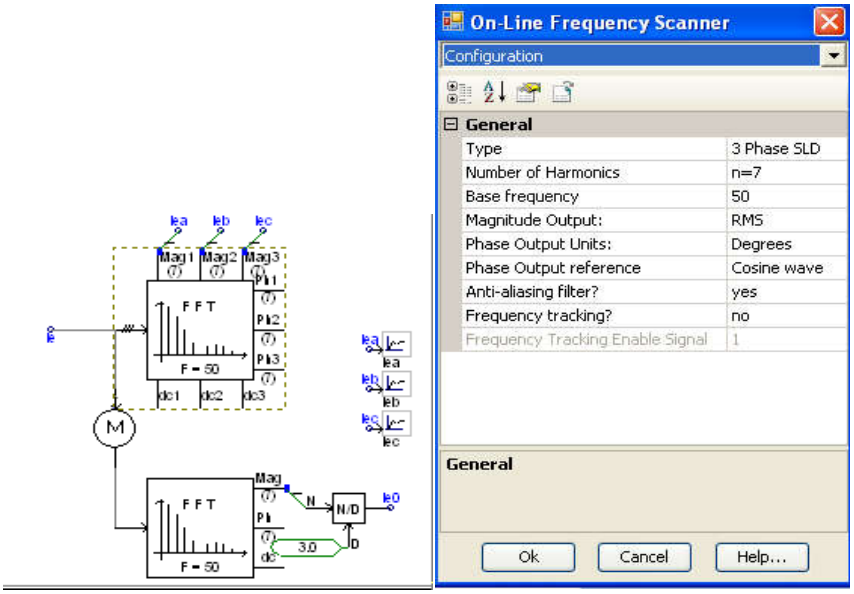

Figure 3-50: Obtaining Harmonic Filtered Phase values similarly as in advanced Numerical Relays

Internal anti Aliasing filter has also enabled, actual numerical relay algorithms comprised with that. To get the accurate zero sequence current, 3I0 need to be divided from 3. The relay output has not given to breaker directly because in actual condition the air insulated breaker take finite time to trip the CB and it has to be remained open until the CB close command issued by the Bay controller unit(as remote CB close) or by mimic panel. To achieve that condition SR latch need to be used as given in the below figure 3-51. In order to give CB close command the Reset push button can be used.

In this simulation in order to simulate the inherent breaker tripping time a delay has added before the CB open. As per the CB manufacturer data sheet inherent time delay has been considered as 60ms. Further in order to keep the CB stable (after the CB tripped it shall remain open until CB close command given. In order to achieve this in the simulation SR latch has used as per the below given figure 3-51.

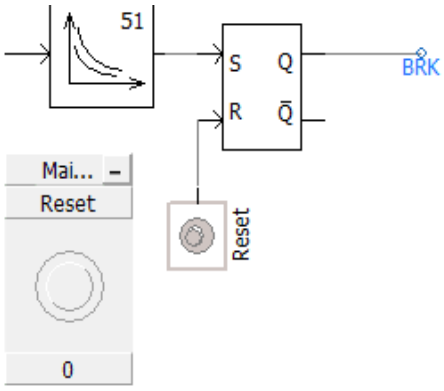

Figure 3-51: SR Latch for Stabilizing the Breaker

When the fault resistance assumed to be 0.1 **Ω**, the primary fault current measured at each CT and the tripping time of each relay were obtained. Initially the correct operation of relays for accurate fault isolation has been identified with the allowable margin of tripping time difference with the expected tripping time with the curve. These expected tripping scheme has been compared with the simulated tripping times. In order to obtain a clear idea about the equivalent solar PV contribution has been separately identified.

CHAPTER 4

4. RESULTS

Initially the existing protection system performance evaluated without solar PV connected. Then at different PV penetration levels the system performance evaluated.

4.1. Analysis of the Protection system performance Expect Theoretically.

In order to isolate the healthy part of the system for a particular fault accurately, particular breakers need to be operated. But each breaker tripping time is mainly based on the fault location and fault type. This chapter describes which protection needs to be operated and which breakers to operate and their tripping times as per the fault type and as per the given settings. Figure 4-1 shows the fault locations and using that it can be easily understand which breakers need to be operated in order to fully isolate the fault.

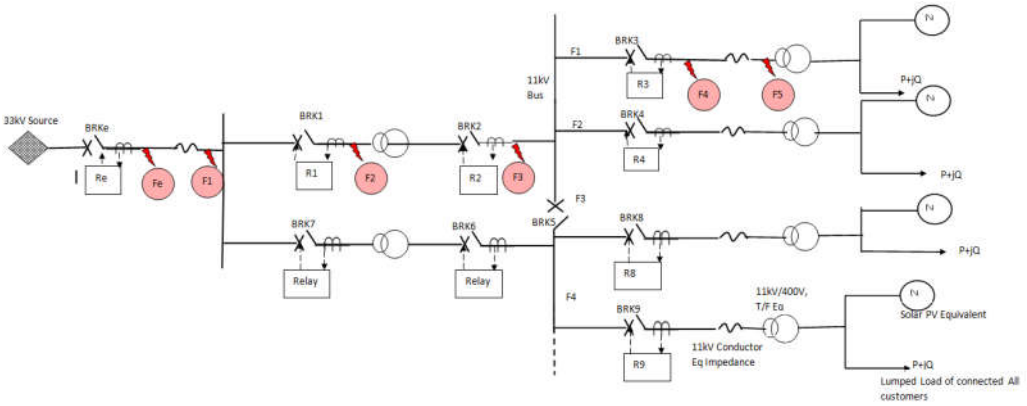

Figure 4-1: Fault Locations in the general schematic of the Model with solar PV

First we can consider a fault at 33kV Bus (at location fe in the figure 4-1). When the fault is just after the 33kV Bus for LG and LLG faults earth fault protection should be operated and fault shall be cleared by the 50N function with 40ms by operating the BRKe. For LL and LLL faults just after the 33kV bus, the fault is cleared by 50 O/C DT function by opening the BRKe.

To clear the faults after the 33kV cable (location f1 as per the figure 4-1), BRKe shall be operated. For LG faults 50N shall be operated with in 40ms. But for LL faults DT-OC (51) shall be operated and clear the faults after 60ms.

The faults occurred in the locations such as location f2 (given in the figure 4-1), can be considered as transformer internal faults. To clear those internal faults normally current differential or restricted earth fault protection functions can be used as the main protection functions. These functions provide instantaneous tripping to both HV and LV breakers in order to isolate the faults immediately. Over current and earth fault function are used as the backup protection for the transformer internal fault protection for the transformers with considerable capacity. But for the 5MVA transformer at the primary GSS only have the over current and earth fault protection even for transformer internal faults. Hence in order to clear the faults after HV side (F2), transformer HV side breaker and LV breaker is operated. Either LV or HV relay tripping issued and inter-trip is issued to the other side instantaneously. For LE fault at HV delta side of the transformer is isolated by the BRK 1 only because the fault current coming though parallel transformer has not an earth path. But as the transformer HV side delta connected side has no earthing transformer earth fault function con not be implemented in the scheme. So for transformer internal LE fault BRK e shall be operated from Sri Japura GSS to isolate the fault. So LE transformer internal fault is cleared by Sri Japura 33kV GIS relay from the 51N (EF-IDMT) function.

But for LL faults at HV delta side , that fault is reflected at the star LV side of the transformer hence both BRK1 and BRK 2 need to be operated to fully isolate the fault. When the HV side is operating for an internal fault it will give direct trip to BRK2 LV side as well to fully isolate the fault and there is no point of LV breaker closing if the transformer has internal fault.

When the fault location f3 (as per the figure 4-1) which occurs after CB LV breaker, for both LG and LL faults initially BRK 02 need to be operated, but to completely isolate the fault BRK 05 bus section breaker should also operate after. For LG faults BRK 01 shall be operated by TFLV-IDMT EF function, then the BRK5 shall be

operated by the IDMT OC function. For the LL faults BEK 01 is operated by TFLV-OC-IDMT and then BRK 05 will be operated by IDMT OC function.

When the fault occurs just after the 11kV feeder breaker (location f4 as per the figure 4-1), BRK 03 operates by EF-DT (50N) function with 10ms delay for LG faults. But for LL faults BRK 03 is operated with delay of 10ms by the OC-DT (50) function. For the faults (location f5 as per the figure 4-1) after 11kV feeder equivalent the relay operates in the same way but may be delayed if the fault current reduces which read by the relay due to added impedance of 11kV conductor.

4.2.Summary of table include Protection system performance as per simulation.

Table 4–1: The Protection Scheme Performance for LG faults at different fault Locations

Fault Location	**AG**					**BG**		
	BRK op.(s)	If(A)	BRK op. (s)	T op. as per curve(s)	Time Dif.(s)	If(A)	BRK op. (s)	Time Dif.(s)
33kV Bus**(fe)**	BRKe	11562	0.13	0.04	**0.09**	11547	0.119	**0.079**
33kV Cable End**(f1)**	BRKe	1289	0.125	0.04	**0.085**	1291	0.128	**0.088**
11/33kV T/F HV side**(f2)**	BRKe	1278	0.119	0.04	**0.079**	1277	0.125	**0.085**
11/33kV T/F LV side**(f3)**	BRK2	2753	0.301	0.226	**0.075**	2745	0.283	**0.057**
	BRK5	2625	0.439	0.345	**0.094**	2747	0.421	**0.076**
11kV Feeder starting point **(f4)**	BRK3	5745	0.072	0.01	**0.062**	5632	0.073	**0.063**
After 11kV Eq. feeder**(f5)**	BRK3	1394	0.081	0.01	**0.071**	1380	0.076	**0.066**

Fault Location	CG				
	BRK op.(s)	If(A)	T op. as per curve(s)	BRK op. (s)	Time Dif.(s)
33kV Bus**(fe)**	BRKe	11531	0.04	0.122	**0.082**
33kV Cable End**(f1)**	BRKe	1279	0.04	0.125	**0.085**
11/33kV T/F HV side**(f2)**	BRKe	1278	0.04	0.123	**0.083**
11/33kV T/F LV side**(f3)**	BRK2	1137	0.226	0.289	**0.063**
	BRK5	2788	0.345	0.432	**0.087**
11kV Feeder starting point **(f4)**	BRK3	5652	0.01	0.071	**0.061**
After 11kV Eqi. feeder**(f5)**	BRK3	1369	0.01	0.075	**0.065**

As shown in the table 4-1 for LG faults earth fault function operate faster than over current function to isolate the fault. Most of the time as the unbalance current exceeds the earth fault high set value, protection operates immediately. As the actual breaker tripping delay has also considered in the simulation the time difference between the expected and actual breaker operating time delay less than 100ms with expected time delay. So it can be concluded that the protection operates accurately for the LG type faults for different fault location with the existing setting system.

For LLG Faults

Table 4–2: Protection Scheme Performance for LLG faults at different fault Locations

Fault Location	ABG					BCG		
	BRK op.(s)	If(A)	BRK op. (s)	T op. curve (s)	Time Dif.(s)	If(A)	BRK op. (s)	Time Dif.(s)
33kV Bus**(fe)**	BRKe	11634	0.114	0.04	**0.074**	11622	0.112	**0.072**
33kV Cable End**(f1)**	BRKe	1295	0.115	0.04	**0.075**	1792	0.122	**0.082**
11/33kV T/F HV side**(f2)**	BRKe	1280	0.123	0.04	**0.083**	1296	0.112	**0.072**
11/33kV T/F LV side**(f3)**	BRK2	3177	0.277	0.206	**0.071**	3175	0.289	**0.083**
	BRK5	2926	0.426	0.328	**0.098**	2996	0.386	**0.058**
11kV Feeder starting point **(f4)**	BRK3	6533	0.074	0.01	**0.064**	6421	0.072	**0.062**
After 11kV Equivalent feeder**(f5)**	BRK3	1322	0.079	0.01	**0.069**	1363	0.082	**0.072**

Fault Location	ACG				
	BRK op.(s)	If(A)	BRK op. (s)	T op. curve(s)	Time Dif.(s)
33kV Bus**(fe)**	BRKe	11697	0.119	0.04	**0.079**
33kV Cable End**(f1)**	BRKe	1286	0.131	0.04	**0.091**
11/33kV T/F HV side**(f2)**	BRKe	1270	0.118	0.04	**0.078**
11/33kV T/F LV side**(f3)**	BRK2	3168	0.288	0.206	**0.082**
	BRK5	3362	0.396	0.328	**0.068**
11kV Feeder starting point **(f4)**	BRK3	6330	0.075	0.01	**0.065**
After 11kV Equivalent feeder**(f5)**	BRK3	1347	0.068	0.01	**0.058**

As shown in the table 4-2, for LLG faults earth fault instantaneous protection operates faster than over current function. Fault current level shall be based on the series positive sequence impedance to parallel impedance of zero and negative sequence equivalent impedance of the network. The unbalance current is proportional to the ratio between negative sequence impedance to summation of parallel of zero and negative sequence impedance and positive sequence impedance. It can be seen that for LLG faults unbalance neutral current exceeds the high set current value and operates with in 100ms. But only for TF internal fault at HV side BRKe operates as TF HV side has no earth fault protection for the HV side.

For LL Faults

Table 4–3: Protection Scheme Performance for LL faults at different fault Locations

Fault Location	AB					BC		
	Breaker op.	If(A)	BRK op. (s)	T op. curve(s)	Time Dif.(s)	If(A)	BRK op. (s)	Time Dif.(s)
33kV Bus**(fe)**	BRKe	11583	0.132	0.06	**0.072**	10134	0.134	**0.074**
33kV Cable End**(f1)**	BRKe	1170	0.7133	0.645	**0.068**	1185	0.7125	**0.068**
11/33kV T/F HV side**(f2)**	BRK1 , BRK 2	1147	0.663	0.583	**0.080**	1146	0.661	**0.078**
11/33kV T/F LV side**(f3)**	BRK2	1252	0.482	0.472	**0.010**	1263	0.497	**0.025**
	BRK5	1165	0.601	0.518	**0.083**	1709	0.572	**0.054**
11kV Feeder starting point **(f4)**	BRK3	3304	0.077	0.01	**0.067**	3323	0.081	**0.071**
After 11kV Eqi. feeder**(f5)**	BRK3	1078	0.089	0.01	**0.079**	1046	0.089	**0.079**

Fault Location	AC				
	Breaker op.	If(A)	BRK op. (s)	T op. curve(s)	Time Dif.(s)
33kV Bus**(fe)**	BRKe	10136	0.119	0.06	**0.059**
33kV Cable End**(f1)**	BRKe	1159	0.725	0.645	**0.08**
11/33kV T/F HV side**(f2)**	BRK1 , BRK 2	1147	0.662	0.583	**0.079**
11/33kV T/F LV side**(f3)**	BRK2	1257	0.497	0.472	**0.025**
	BRK5	1719	0.569	0.518	**0.051**
11kV Feeder starting point **(f4)**	BRK3	3298	0.079	0.01	**0.069**
After 11kV Equivalent feeder**(f5)**	BRK3	1094	0.078	0.01	**0.068**

For LL faults over current highest or over current IDMT function operates based on the fault current level as there is no unbalance current for earth fault to operate. Fault current will be based on the summation of the positive and negative sequence impedances. As per the table 4-3 it can be observed that all the faults are cleared with in 100ms margin with the expected tripping time. Hence it can be claimed that the system operates accurately for the LL faults.

For 3 phase faults (LLL)

Table 4–4: Protection Scheme Performance for LLL faults at different fault Locations

Fault Location	ABC					ABCG		
	Breaker op.	If(A)	BRK op. (s)	T op. curve(s)	Time Dif.(s)	If(A)	BRK op. (s)	Time Dif.(s)
33kV Bus**(fe)**	BRKe	12108	0.126	0.06	**0.066**	11989	0.131	**0.071**
33kV Cable End**(f1)**	BRKe	1283	0.659	0.593	**0.066**	1283	0.662	**0.069**
11/33kV T/F HV side**(f2)**	BRK1 , BRK 2	1286	0.617	0.553	**0.064**	1295	0.617	**0.064**
11/33kV T/F LV side**(f3)**	BRK2	1888	0.37	0.301	**0.069**	1866	0.369	**0.068**
	BRK5	1866	0.554	0.457	**0.097**	1864	0.556	**0.099**
11kV Feeder starting point **(f4)**	BRK3	3805	0.079	0.01	**0.069**	3816	0.077	**0.067**
After 11kV Equivalent feeder**(f5)**	BRK3	1244	0.08	0.01	**0.07**	1279	0.08	**0.07**

When the table4-4, fault summery has been observed, it can be seen that the expected relays has operated to isolate the faults and further the difference between the expected tripping time of the curve and simulated breaker tripping time difference is with 100ms margin. So without loss of generality it can be finalized that the existing protection scheme operates accurately to clear the faults when solar PV generation neglected.

The fault current obtained for a fault loop with very small resistance value (external fault resistance as only 0.1 **Ω**. But the fault resistance at the fault loop impedance can be varied due to various reasons causing different fault current reading from the relays.

In Actual scenario fault current will be vary depend upon the loop resistance of the fault current circulating path. For LL fault that loop impedance will be depend on the arc resistance which can be calculated by using *Warrington formula*

$$R_{arc} = \frac{28\ 68\ 858 \times length\ of\ the\ Arc\ im\ m\ or\ maximum\ phase\ condutor\ spacing\ in\ m}{Minimum\ Expected\ fault\ current\ phase\ to\ phase^{1.4}}$$

(4.1)

Using the formula 4.1 it can be calculated how the fault resistance varies at different fault current level and different arc lengths.

Table 4–5: Arc Resistance Variation Based on the parameters as per Warrington formula

Using Warrington formula	**S1**	**S2**	**S3**
minimum length	1.1	1.1	1.65
Minimum fault current	1500	3000	1000
R arc	1.13	0.43	2.99

Based on the fault type the fault loop impedance varies. For LL faults, loop resistance arc resistance need to be added.

In 33kV overhead distribution feeders earth faults occur more frequently due to indirect lightening. Insulator flashes and the arc propagation to the ground through the steel structure of the tower are most commonly occurring. With earth wires current flows via several parallel towers footing resistance to earth paths. Due to that the resultant earth fault resistance substantially reduced.

Tower footing resistance and earth wire of the distribution line can be approximated by lot of T sections connected in series (ladder network). For the faults which are far away from the substation can be approximated by two parallel “ladder networks”. When the fault occurs across the tower footing resistance the effective fault current flow circuit can be represented by a schematic as indicated below.

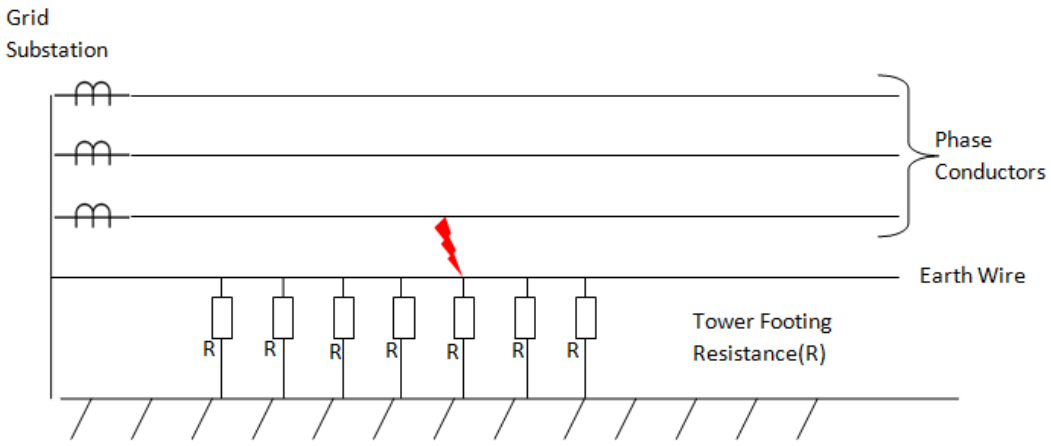

Figure 4-2: Schematic of the Ladder Network

This network can be approximated by the equivalent circuit shown as below diagram.

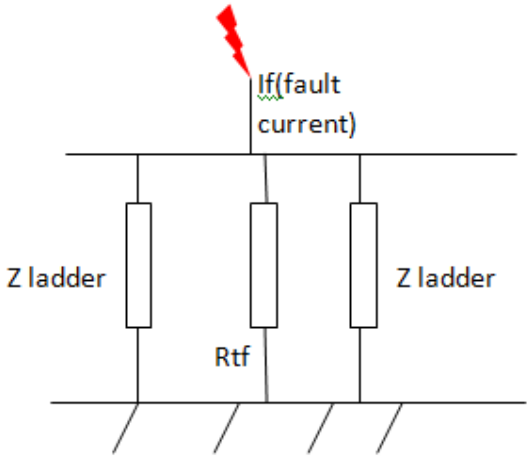

Figure 4-3: Schematic of the Simplified Ladder Network

R_{tf}=Tower footing Resistance)

Z_{ladder}= Impedance of the ladder network of over head lines and resistance of further towers

Z_{ETF}=Effective tower footing resistance

R_{TF} =Average Tower footing resistance

R_{EW}=Resistance of the earth wire in Ohm/km

X_{EW}=Reactance of the earth wire in Ohm/km

Z_{EW}=Impedance of the earth wire

l_{AS}=Average Span between Towers/km

$$Z_{ladder} = \frac{Z_{EW} \times l_{AS}}{2} + \sqrt{\frac{(Z_{EW} \times l_{AS})^2}{4} + R_{TF} \times Z_{EW} \times l_{AS}} \quad (4.2)$$

It has to be assumed that the impedance of the parallel connected ladder is small in comparison to the tower footing resistance, resulting earth fault impedance can be derived from the below equation

$$Z_{ETF} = 0.5 \times \sqrt{R_{TF} \times Z_{EW} \times l_{AS}} \quad (4.3)$$

For earth faults the fault loop impedance is the summation of arc resistance and this effective tower footing resistance. The below table shows how the relay operating time varies based on the fault loop impedance.

Table 4–6: Tripping Time Variation Based on the Fault Loop Impedance variation at different fault Locations

Fault Type	**R f(Ω)**	**Trip time without solar(s)**	**Trip time with solar(s)**
LL-33kV Conductor End	0.01	0.7133	0.72
	0.5	0.715	0.726
	1	0.718	0.729
	3	0.722	0.735
LG-33kV Conductor End	0.01	0.125	0.115
	5	0.121	0.118
	10	0.125	0.12

4.3. With Solar PV penetration System modelling and Verify the Existing Protection system Performance

As described in the chapter 3.2.8 at each of the line end solar PV equivalent VSI model is connected. For the same cases simulation carried out and observed the fault current contribution from the solar PV and relay trip time for each fault type. When the solar PV connected to the system and fault occurred, fault current level at considered location increases due to reduction in the thevenin equivalent impedance seen from the grid side. Solar PV`s also contributes to the fault current, based on the equivalent thevenin impedance seen by the PV side. The effect to the equivalent thevenin impedance with the addition of the solar PV can be verified by the figure 4-4 sequence network diagram. That sequence diagram has connected for LG fault and from that it can be understand that impedances which have impact on the difference in the fault current level.

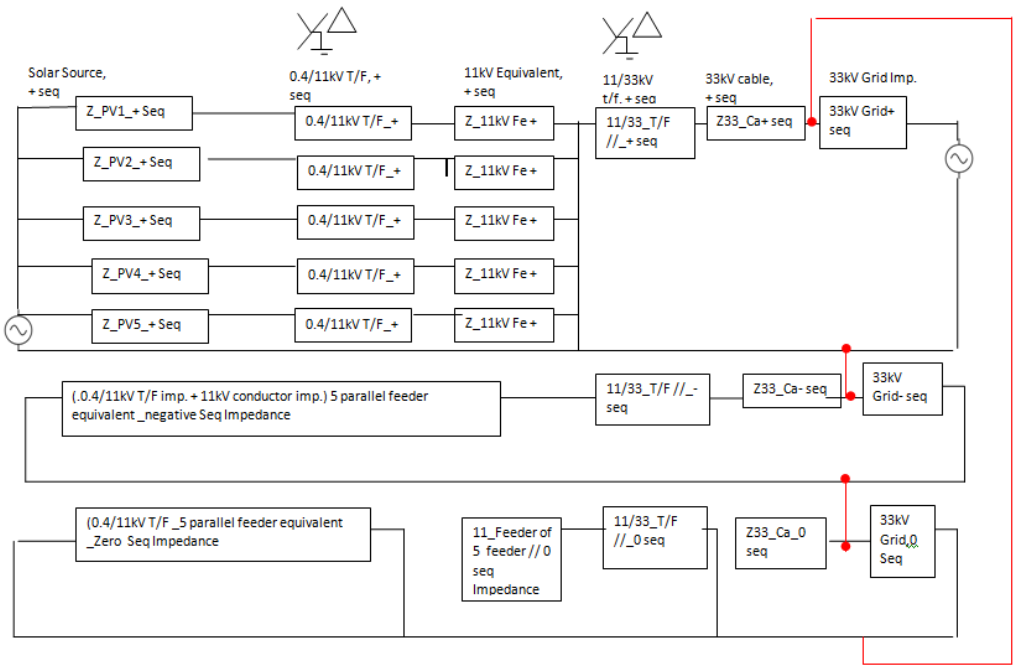

Figure 4-4: Sequence Component Diagram for Unbalanced Fault Analysis

Figure4-4 helps to get a rough idea regarding, how the equivalent thevenin impedance reduces and fault current increases due to added solar PV source path at a considered Bus. From the simulation at each fault location fault current contribution from each solar PV can be identified.

For symmetrical faults, tough the PV connected, fault current contribution from the grid does not change. As well as in homogenous system, as per the super position theorem the fault current contribution from the source is independent from the other source. In homogenous system though more sources get connected fault current contribution from each source does not change. But fault level of the particular faulted bus can increased due the added fault current contribution from the PV contribution.

But if the system is non-homogenous the fault current contribution can vary as per the connected source impedances. Mainly this will be depending upon the connected source sequence impedances. As per the figure 4.5 the positive sequence fault current read from the relay can be considered as I_{f2}. When there is no distributed generator is connected I_{f2} can be taken from the ratio of positive sequence voltage to the source impedance.

$$.I_{f2} = \frac{V_{1f}}{Z2} \qquad (4.4)$$

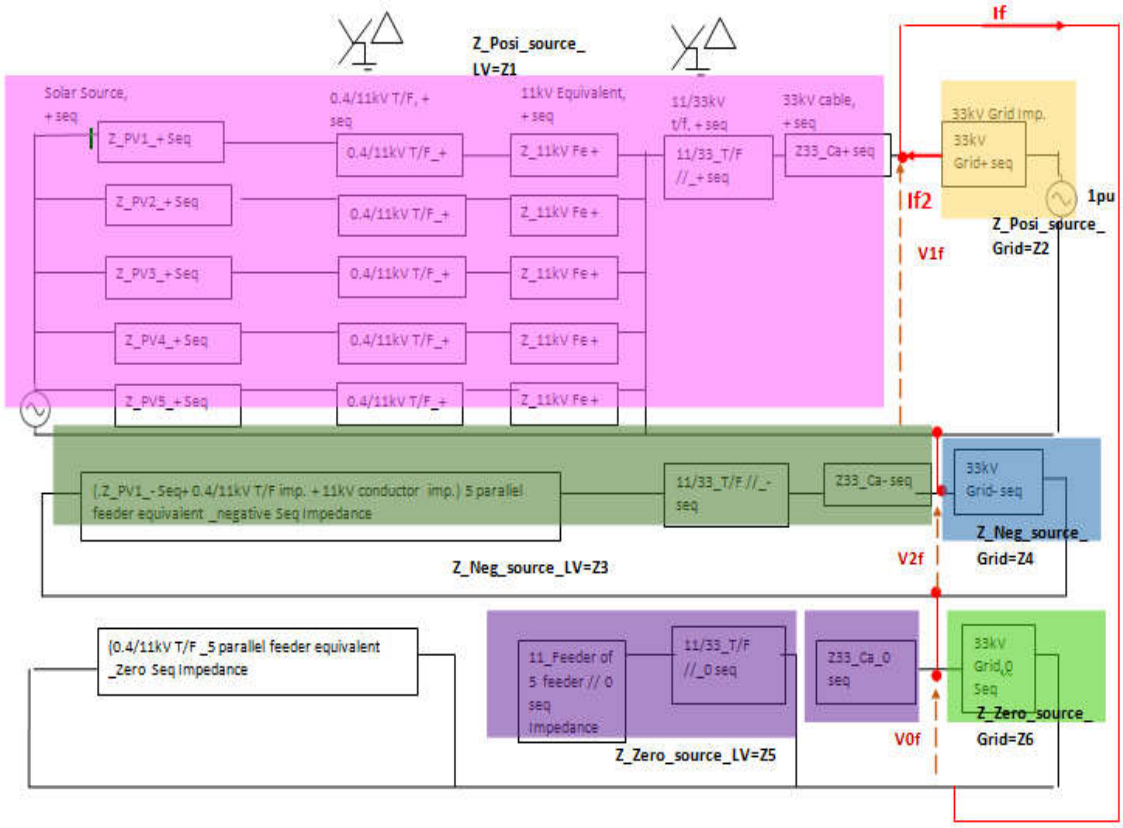

Figure 4-5: Sequence Component Diagram for Unbalanced Fault Analysis with distributed generator connected

First let's consider a case where only positive sequence is added to the LV side (Z1). In that case, V_{1f} reduced, because when other two impedance loop impedance kept constant only positive sequence impedance reduced (now positive sequence impedance proportional to the $\frac{Z_2 Z_1}{Z_2+Z_1}$, obviously the parallel impedance is less than the smaller impedance of Z_2 and Z_1). In that case I_{f2} reduced due to reduction of V_{1f} compared to the, without Distributed Generator case. But the if the distributed generator has negative sequence impedance component (Z_3) , situation gets changed. That scenario V_{2f} gets reduced comparted to the without distributed generator case. Based on the equivalent impedances of the positive and negative loop impedances the

positive and negative sequence voltage distribution can vary. Based on that impedances fault current contribution from the grid side may also change.

Without distributed generator connected fault current contribution from the grid,

$$I_{f\_Relay_{WO}DG(I_{f2})} = \frac{1}{Z_2+Z_4+Z_6} \tag{4.5}$$

After distributed generator connected fault current contribution from the grid.

$$I_{f\_Relay\_WithDG(I_{f2})} = \frac{1}{\frac{Z_2Z_1}{Z_2+Z_1}+\frac{Z_3Z_4}{Z_3+Z_4}+Z_6} \times \frac{Z_1}{Z_2+Z_1} \tag{4.6}$$

As per the equations 4.5 and 4.6, if impedance based fault current analysis adopted, we can observe that the fault current contribution for unbalanced faults can be varied as per the source impedances.

As per the ref.[18] if the sequence components considered, positive sequence of the solar PV source is considerable value compared to the negative sequence impedance and there is no zero sequence value. If the solar PV controllers can fully filter the waveforms it causes to negligible negative sequence impedance. Hence only positive sequence impedance added as parallel to the 33kV source impedance. When a parallel path is added the equivalent positive sequence impedance gets smaller than the smallest impedance connected in parallel. Then the voltage across the positive sequence impedance gets smaller and thus the positive sequence fault current contribution reduced compared with the without solar PV scenario.

But if the solar source has negative sequence impedance value that causes the equivalent negative sequence impedance to reduce and that will reduce the voltage across negative sequence loop. That scenario can lead to increase voltage across positive sequence loop and that can lead to increase the positive sequence fault current contribution increase. If fault impedance presents in the loop, this scenario can further vary due to the added voltage of three times of fault impedance in to fault current. When the fault current increases due to added parallel path the voltage across

the positive sequence loop can be increased compared to without solar scenario and current reading of the relay can be increased.

The table 4-7 shows the fault current contribution from each solar PV and grid fault current contribution for 33kV Cable Start Fault.

Table 4–7: Fault Current Contribution from the grid side and PV side and Relay Trip Times for 33kV Cable Start

Fault Location and Fault Type	**Fault Current From Grid(A)**	**Fault current Level % Increase**	**PV**	**Fault current contribution from solar(A)**	**PV% current increase**	**Breaker Trip Time(S)**	**Trip Time Delay (S)**
LG	1289	0.23	PV 1	9.95	50.1	BRKe	0.001
			PV 2	19.10	50.1	0.662	
			PV 3	35.61	50.6		
			PV 4	21.21	50.2		
			PV 5	18.29	50.3		
				104.17			
LL	1175	0.43	PV 1	10.06	51.7	BRKe	0.0067
			PV 2	19.16	50.6	0.72	
			PV 3	35.66	50.8		
			PV 4	21.37	51.3		
			PV 5	18.35	50.8		
				104.61			
LLG	1391	0.750	PV 1	9.82	48.1	BRKe	-0.067
			PV 2	19.03	49.5	0.105	
			PV 3	35.43	49.8		
			PV 4	20.99	48.7		
			PV 5	18.08	48.6		
				103.36			
LLL	1290	0.55	PV 1	10.21	53.9	BRKe	0.001
			PV 2	18.16	42.7	0.66	
			PV 3	34.42	45.6		
			PV 4	20.61	45.9		
			PV 5	18.50	52.0		
				101.89			
LLLG	1293	0.31	PV 1	10.08	52.1	BRKe	0.001
			PV 2	18.16	42.7	0.66	
			PV 3	33.82	43.0		
			PV 4	20.47	45.0		

			PV 5	18.67	53.4		
				101.20			

The table 4-7 shows the fault current contribution from each solar PV and grid fault current contribution for 33kV Feeder End Point. When the table 4-8 observed it can be seen that the highest PV fault current contribution increase is for the LG type faults. Highest PV fault current contribution is for the highest PV penetrated feeder because there is the minimum equivalent impedance present. But it cannot observe a direct coherence between the fault current contribution percentage increases with PV penetration level. But with the available results as shown in the figure 4-7 it can be concluded that the protection system operates accurately for the 33kV level faults even with PV penetration considered.

Table 4–8: Fault Current Contribution from the grid side and PV side and Relay Trip Times for 33kV Cable End

Fault Location and Fault Type	**Fault Current From Grid(A)**	**Fault current Level % increase**	**PV**	**Fault current contribution from solar(A)**	**PV% current increase**	**Breaker Trip Time(S)**	**Trip Time Delay (S)**
LG	11562	0.87	PV 1	9.37	50.1	BRKe	-0.147
			PV 2	17.99	50.1	0.104	
			PV 3	33.43	50.0		
			PV 4	19.98	50.1		
			PV 5	17.21	49.9		
				97.98			
LL	11583	0.25	PV 1	10.07	5.9	BRKe	-0.001
			PV 2	19.41	6.6	0.72	
			PV 3	36.42	8.3		
			PV 4	21.90	8.5		
			PV 5	18.46	6.8		
				106.27			
LLG	11799	0.55	PV 1	10.01	50.5	BRKe	-0.007
			PV 2	19.14	49.5	0.112	
			PV 3	35.82	176.7		
			PV 4	21.32	49.3		
			PV 5	18.32	51.4		
				104.61			

LLL	12397	0.239	PV 1	9.27	48.3	BRKe	0.02
			PV 2	18.17	51.1	0.13	
			PV 3	33.65	51.4		
			PV 4	20.19	51.6		
			PV 5	17.43	51.8		
				98.72			
LLLG	12046	0.48	PV 1	10.05	49.9	BRKe	-0.003
			PV 2	19.35	51.0	0.128	
			PV 3	36.56	51.9		
			PV 4	21.60	53.2		
			PV 5	18.53	50.6		
				106.08			

As per the table 4-8, the maximum fault current contribution increase can be observed for the LLL faults. Similarly from the PV side highest fault current contribution can be observed for 3 phase faults. Further it can be observed that the breakers has operated in the expected manner accurately even with solar PV penetration.

The table 4-9 shows the fault current contribution from each solar PV and grid fault current contribution for 11/33kV Transformer Internal Fault.

Table 4–9: Fault Current Contribution from the grid side and PV side and Relay Trip Times for 11/33kV Transformer Internal Fault

Fault Location and Fault Type	**Fault Current From Grid(A)**	**current Level increase %**	**PV**	**Fault current contribution from solar(A)**	**PV% current increase**	**Breaker Trip Time(S)**	**Trip Time Delay (S)**
LG	1343	0.509	PV 1	9.67	49.2	BRKe	-0.004
			PV 2	17.28	36.5	0.155	
			PV 3	33.21	36.3		
			PV 4	19.35	38.5		
			PV 5	17.36	29.9		
				96.87			
LL	1145	0.17	PV 1	10.12	56.1	BRK1	0
			PV 2	19.10	50.8	BRK 2	
			PV 3	35.77	46.7	0.663	
			PV 4	21.37	53.0		
			PV 5	19.37	45.0		

				105.73			
LLG	1390	0.859	PV 1	9.84	51.8	BRKe	-0.003
			PV 2	19.02	50.1	0.112	
			PV 3	35.37	45.1		
			PV 4	21.24	52.1		
			PV 5	17.58	31.6		
				103.04			
LLL	1344	0.451	PV 1	10.33	59.3	BRK1	0.003
			PV 2	20.35	60.7	BRK 2	
			PV 3	37.84	55.2	0.62	
			PV 4	22.72	62.7		
			PV 5	19.33	44.7		
				110.57			
LLLG	1342	0.363	PV 1	10.24	57.9	BRK1	0.001
			PV 2	20.38	60.9	BRK2	
			PV 3	36.63	50.3	0.618	
			PV 4	22.74	62.8		
			PV 5	19.37	45.0		
				109.36			

When the table 4-9 observed it can be observed that the PV fault current contribution increase when the connected PV capacity increases. But the grid side fault current contribution reduces when the fault occur away of the 33kV side source. When the protection system performance considered it can be concluded that the system operate accurately with available protection functions for the transformer internal faults and isolates the faults accurately.

The table 4-10 shows the fault current contribution from each solar PV and grid fault current contribution for Transformer LV side outside the transformer after LV breaker.

Table 4–10: Fault Current Contribution from the grid side and PV side and Relay Trip Times for Outside Transformer at LV side

Fault Location and Fault Type	Fault Current From Grid(A)	current Level increase %	PV	Fault current contribution from solar(A)	PV% current increase	Breaker Trip Time(S)	Trip Time Delay (S)
LG	2943	0.679	PV 1	10.48	49.7	BRK2	-0.008
			PV 2	20.63	61.9	0.293	
			PV 3	37.39	50.0		
			PV 4	22.07	47.8		
			PV 5	19.10	57.8		
				109.68			
LL	1663	0.328	PV 1	10.74	53.3	BRKe	-0.107
			PV 2	20.30	59.4	0.373	
			PV 3	37.60	50.9		
			PV 4	22.51	50.7		
			PV 5	19.42	50.4		
				110.57			
LLG	3238	0.192	PV 1	10.33	47.4	BRKe	0.005
			PV 2	20.01	57.1	0.28	
			PV 3	37.15	49.1		
			PV 4	23.05	54.4		
			PV 5	19.42	50.4		
				109.96			
LLL	1995	0.567	PV 1	10.85	54.8	BRKe	-0.001
			PV 2	20.63	51.9	0.369	
			PV 3	37.64	51.0		
			PV 4	22.53	50.9		
			PV 5	19.42	50.4		
				111.07			
LLLG	1880	0.75	PV 1	10.40	48.4	BRKe	-0.005
			PV 2	20.55	51.3	0.364	
			PV 3	37.64	51.0		
			PV 4	22.58	51.2		
			PV 5	19.37	50.0		
				110.53			

Table 4-10 shows that the fault current contribution from the PV increases further when the fault is closer to the PV side. On the other way fault currents contribution from the grid reduces when the fault is far away from the grid side.

The table 4-11 shows the fault current contribution from each solar PV and grid fault current contribution for Transformer LV kV Feeder Starting Point

Table 4–11: Fault Current Contribution from the grid side and PV side and Relay Trip Times for 11kV Starting Point

Fault Location and Fault Type	Fault Current From Grid(A)	current Level increase %	PV	Fault current contribution from solar(A)	PV% current increase	Breaker Trip Time(S)	Trip Time Delay (S)
LG	5862	0.386	PV 1	10.24	45.2	BRK3	0.003
			PV 2	20.02	56.9	0.075	
			PV 3	36.39	47.6		
			PV 4	22.07	46.5		
			PV 5	19.05	51.9		
				107.78			
LL	3383	0.239	PV 1	10.86	54.0	BRK3	-0.005
			PV 2	20.41	59.9	0.072	
			PV 3	37.64	52.7		
			PV 4	22.58	49.9		
			PV 5	20.63	64.4		
				112.12			
LLG	6589	0.86	PV 1	10.57	49.8	BRK5	-0.002
			PV 2	20.68	62.0	0.072	
			PV 3	37.41	51.7		
			PV 4	22.45	49.0		
			PV 5	19.43	54.9		
				110.53			
LLL	3859	0.142	PV 1	10.85	53.8	BRK3	-0.004
			PV 2	20.86	63.4	0.075	
			PV 3	37.52	52.2		
			PV 4	22.51	49.4		
			PV 5	20.34	62.1		
				112.07			
LLLG	3854	0.75	PV 1	10.92	54.8	BRK3	-0.002
			PV 2	20.76	62.7	0.075	
			PV 3	36.91	49.7		
			PV 4	22.40	48.7		
			PV 5	20.38	62.4		
				111.37			

The table 4-12 shows the fault current contribution from each solar PV and grid fault current contribution for Transformer LV kV Feeder Ending Point

Table 4–12: Fault Current Contribution from the grid side, PV side and Relay Trip Times for 11kV Feeder end

Fault Location and Fault Type	Fault Current From Grid(A)	Fault current Level increase %	PV	Fault current contribution from solar(A)	PV% current increase	Breaker Trip Time(S)	Trip Time Delay (S)
LG	1404	0.324	PV 1	10.95	50.2	BRK3	-0.004
			PV 2	20.99	50.3	0.077	
			PV 3	38.85	49.6		
			PV 4	23.33	50.6		
			PV 5	20.91	56.7		
				115.03			
LL	1093	0.139	PV 1	11.05	51.7	BRK3	0
			PV 2	21.15	51.5	0.089	
			PV 3	39.07	50.5		
			PV 4	23.42	51.2		
			PV 5	20.18	51.2		
				114.87			
LLG	1347	0.189	PV 1	10.90	49.6	BRK5	0.001
			PV 2	20.99	50.3	0.08	
			PV 3	38.74	49.2		
			PV 4	23.33	50.6		
			PV 5	20.04	50.1		
				114.00			
LLL	1289	0.362	PV 1	11.13	52.7	BRK3	-0.0001
			PV 2	21.24	52.1	0.0799	
			PV 3	39.83	53.4		
			PV 4	23.47	51.5		
			PV 5	20.30	52.1		
				115.96			
LLLG	1286	0.55	PV 1	11.09	52.2	BRK3	0
			PV 2	21.37	53.0	0.08	
			PV 3	38.48	48.2		
			PV 4	22.61	45.9		
			PV 5	20.40	52.9		
				113.95			

In order to consider the overall effect due to PV contribution to the fault level and relay performance all the given data has been summarized as figure 4-4.

Figure 4-5 includes comparison of the fault currents, relay operating times, PV fault current contribution with and without solar PV scenarios for each fault location.

Fault Location	AG						ABG				
	Breaker op.	Grid IF (A)	PV contr. at 33kV Level	t opera. without solar (s)	t opera. with solar (s)	Diff. in Operating Time(s)	Grid IF (A)	PV contr. at 33kV Level	t opera. without solar (s)	t opera. with solar (s)	Diff. in Operating Time(s)
33kV Bus(fe)	BRKe	11562	99	0.130	0.104	0.026	11634	105	0.114	0.112	0.002
33kV Cable End(f1)	BRKe	1289	104	0.125	0.115	0.010	1295	103	0.115	0.112	0.003
11/33kV T/F HV side(f2)	BRKe	1278	97	0.119	0.115	0.004	1280	103	0.123	0.112	0.011
11/33kV T/F LV side(f3)	BRK2	2753	110	0.301	0.293	0.008	3177	110	0.277	0.280	-0.003
	BRK5	2625		0.439	0.431	0.008	2926		0.426	0.412	0.014
11kV Feeder starting point (f4)	BRK3	5745	108	0.072	0.010	0.062	6533	111	0.074	0.072	0.002
After 11kV Equivalent feeder(f5)	BRK3	1394	115	0.081	0.077	0.004	1322	114	0.079	0.072	0.007

Figure 4-6: Summery of Existing System Performance for LG Faults at different locations

Figure 4-5 summarises the protection system performance for two different ground fault scenarios. Further it can be observed that when the fault is getting closer to the grid side the fault current contribution from the solar PV side reduces and fault current contribution from the grid increases.

It can be observed that the PV contribution at 33kV level is considerably smaller compared to the grid fault current contribution. Hence the relay operating time has not much difference compared to the without solar scenario. Then unearthed faults summery can be observed as given in figure 4-6.

Fault Location	AB						ABC					ABCG				
	Breaker op.	Grid IF (A)	I pv at 33kV	t operate (s)	t opera. With PV (s)	Diff. in Time(s)	Grid IF (A)	I pv at 33kV	t operate (s)	t opera. With PV (s)	Diff. in Time(s)	Grid IF (A)	I pv at 33kV	t operate (s)	t opera. With PV (s)	Diff. in Time(s)
33kV Bus(fe)	BRKe	11583	106	0.132	0.131	0.001	12108	99	0.110	0.060	0.050	11989	106	0.131	0.128	0.003
33kV Cable End(f1)	BRKe	1170	105	0.713	0.720	-0.007	1283	102	0.659	0.660	-0.001	1283	101	0.662	0.660	0.002
11/33kV T/F HV side(f2)	BRK1,BRK2	1147	106	0.663	0.663	0.000	1286	111	0.617	0.553	0.064	1295	109	0.617	0.618	-0.001
11/33kV T/F LV side(f3)	BRK2	1252	111	0.482	0.373	0.109	1888	111	0.370	0.369	0.001	1866	111	0.369	0.364	0.005
	BRK5	1655		0.601	0.512	0.089	1866		0.554	0.554	0.000	1864		0.556	0.552	0.004
11kV Feeder starting point (f4)	BRK3	3304	112	0.077	0.072	0.005	3805	112	0.079	0.075	0.004	3816	111	0.077	0.075	0.002
After 11kV Equivalent feeder(f5)	BRK3	1078	115	0.089	0.089	0.000	1244	116	0.080	0.080	0.000	1279	114	0.080	0.080	0.000

Figure 4-7: Summery of Existing System Performance for Non Earthed Faults at different locations

Observing the given summery table few points can be understood. For all LL,LLL,LLLG relays relay tripping time has not much impact.(only for some cases millisecond range operating time difference). But it can be observed that the maximum fault current increase due to PV addition, appear for the faults near 33kV feeder starting point. When the summery taken as a whole, it can be concluded that MV level protection system operates in the expected manner without much impact for the existing PV penetration level.

4.4.Protection System performance verify for the 80% of PV penetration level.

Form chapter 4.3, it has been observed that the existing protection system can perform in the expected manner without having much impact due to existing PV penetration level. But the severity of impact can be changed based on the intensity of the PV penetration level. To test that, the same simulation needs to perform to a maximum possible PV penetration of the system. Maximum probable PV penetration assumed that 80% of the system capacity. When the system capacity of each component considers the most limited capacity encounters at the 33/11 kV transformer HV side. (Transformer LV side rated current capacity has given as 525A, which gives the total capacity only12 MW for two transformers). Based on the

number of transformers connected for each feeder this total capacity distributed as 80% solar and 20% consumer loads.

Table 4–13: The System Equivalent Loading and PV connected when PV penetration increased.

Feeder Number	Rated P Total at 11kV Level	Solar MW
F1	0.38	0.51
F2	0.73	0.98
F3	1.36	1.82
F4	0.82	1.09
F5	0.70	0.94

4.5. Fault current contribution by solar PV and Grid with higher PV Penetration Level.

The table 4-14 shows the fault current contribution from each solar PV and grid fault current contribution for 33kV Cable Staring Point Fault when the PV penetration level increases up to 80%

Table 4–14: Fault Current Contribution from the grid side and PV side and Relay Trip Times for 33kV Feeder Starting Point

Fault Location and Fault Type	Fault Current From Grid(A)	Fault current % increase	PV	Fault current contribution from solar(A)	PV% current increase	Breaker Trip Time(S)	Trip Time Delay (S)
LG	11984	1.98	PV 1	11.72	45.6	BRKe	-0.018
			PV 2	22.76	47.3	0.103	
			PV 3	42.62	48.8		
			PV 4	24.95	45.4		
			PV 5	22.36	51.5		
				124.41			
LL	10341	2.04	PV 1	12.16	51.1	BRKe	-0.002
			PV 2	23.37	51.2	0.127	
			PV 3	43.26	51.0		
			PV 4	26.36	53.7		
			PV 5	23.33	58.0		
				128.48			
LLG	11987	1.97	PV 1	11.73	45.8	BRKe	-0.012
			PV 2	22.97	48.6	0.105	
			PV 3	42.38	47.9		

			PV 4	25.27	47.3		
			PV 5	21.85	48.0		
				124.21			
LLL	11877	1.97	PV 1	12.27	52.4	BRKe	-0.001
			PV 2	23.33	51.0	0.126	
			PV 3	43.24	51.0		
			PV 4	26.00	51.6		
			PV 5	22.10	49.7		
				126.93			
LLLG	11737	0.77	PV 1	12.21	51.7	BRKe	-0.004
			PV 2	23.37	51.2	0.121	
			PV 3	43.30	51.2		
			PV 4	26.08	52.1		
			PV 5	22.39	51.6		
				127.35			

When the figure 4-14 observed, it can be observed that the equivalent PV fault current contribution has increased from 20%-25% when the PV penetration level increase from 20% to 80%. When the number of connected solar PV is high fault current contribution also increases. Maximum fault current contribution from both PV side and grid side is for a three phase fault. BRKe (33kV GIS breaker) has operated to isolate the fault. Protection operating time has reduced compared without solar scenario, due to the fault current increase with heavy PV penetration. As the faults have been reliably cleared even with higher PV penetration, it can be concluded that the existing system can perform accurately even solar penetration level increases up to 80%.

The given table 4-15 shows the fault current contribution from each solar PV and grid fault current contribution for 33kV Cable End Fault when the PV penetration level increases up to 80%.

Table 4–15: Fault Current Contribution from the grid side and PV side and Relay Trip Times for 33kV End Point

Fault Location and Fault Type	Fault Current From Grid(A)	Fault current % increase	PV	Fault current contribution from solar(A)	PV% current increase	Breaker Trip Time(S)	Trip Time Delay (S)
LG	1292	1.02	PV 1	11.85	23.5	BRKe	-0.023
			PV 2	22.90	46.8	0.104	
			PV 3	43.24	51.0		
			PV 4	25.44	48.0		
			PV 5	21.84	47.3		
				125.27			
LL	1181	1.55	PV 1	11.43	48.7	BRKe	-0.018
			PV 2	22.98	48.7	0.704	
			PV 3	42.68	49.0		
			PV 4	25.77	50.2		
			PV 5	22.21	50.4		
				125.07			
LLG	1294	0.31	PV 1	11.70	45.3	BRKe	-0.002
			PV 2	22.86	47.9	0.113	
			PV 3	42.74	49.2		
			PV 4	26.00	51.6		
			PV 5	22.10	49.7		
				125.39			
LLL	1295	0.31	PV 1	12.15	50.9	BRKe	-0.005
			PV 2	23.26	50.5	0.658	
			PV 3	42.85	49.6		
			PV 4	26.05	51.9		
			PV 5	21.01	42.3		
				125.31			
LLLG	1295	0.62	PV 1	11.96	48.6	BRKe	0
			PV 2	22.98	48.7	0.661	
			PV 3	42.47	48.3		
			PV 4	25.55	49.0		
			PV 5	22.16	50.1		
				125.13			

As per the table 4-15 it can be observed that the fault current contribution has increased within 19% to 26% of the PV fault current contribution compared with the 20% of solar penetration level. Grid side maximum fault current contribution can be

observed for the three phase fault. But the maximum percentage increase can be observed for the LL faults. BRKe (33kV breaker from the HV grid) operate to clear the fault. Though the fault clearing time has reduced there is not any impact to the expected protection performance of the system. Hence it can be concluded that the existing protection system can operate accurately for all type of faults when the fault occurred at end of 33kV feeder with 80% of PV penetration level.

The given table 4-16 shows the fault current contribution from each solar PV and grid fault current contribution for 33/11kV Transformer Internal Fault when the PV penetration level increases up to 80%

Table 4–16: Fault Current Contribution from the grid side and PV side and Relay Trip Times for 11/33kV Transformer Internal Fault

Fault Location and Fault Type	Fault Current From Grid(A)	Fault current % increase	PV	Fault current contribution from solar(A)	PV% current increase	Breaker Trip Time(S)	Trip Time Delay (S)
LG	1288	0.16	PV 1	12.17	51.2	BRKe	-0.001
			PV 2	22.76	47.3	0.107	
			PV 3	42.70	49.1		
			PV 4	25.53	48.8		
			PV 5	22.10	49.7		
				125.26			
LL	1187	1.46	PV 1	11.94	48.3	BRK1 &BRK2	-0.005
			PV 2	22.98	48.7	0.658	
			PV 3	42.93	49.9		
			PV 4	25.88	50.9		
			PV 5	21.12	43.0		
				124.85			
LLG	1373	3.17	PV 1	11.94	48.3	BRKe	-0.008
			PV 2	23.27	50.6	0.107	
			PV 3	41.83	46.0		
			PV 4	25.62	49.4		
			PV 5	21.98	48.9		
				124.64			
LLL	1349	3.17	PV 1	12.18	51.4	BRK1 &BRK2	-0.006
			PV 2	22.98	48.7	0.617	
			PV 3	43.37	51.4		

			PV 4	25.52	48.8		
			PV 5	21.77	47.5		
				125.82			
LLLG	1373	3.94	PV 1	11.85	47.3	BRK1 &BRK2	-0.002
			PV 2	22.61	46.3	0.621	
			PV 3	43.45	51.7		
			PV 4	25.50	48.7		
			PV 5	22.07	49.5		
				125.49			

From the table 4-16 it can be observed that the PV fault current fault contribution has increased only 45%-52% compared with the previous loading current. But the fault current has increased up to 25% compared with the 20% solar PV penetration scenario. Faults comprised with the earth path cleared instantaneously by the 33kV Feeder breaker. But for other type of faults OC function operates because transformer HV side delta has no earth fault protection. For that type of faults HV side BRK1 operates and an inter-trip has sent to the BRK2. Hence it can be concluded that, still the protection system performs in accurate way even with the solar penetration available.

The given table 4-17 shows the fault current contribution from each solar PV and grid fault current contribution for outside 33/11kV Transformer at LV side Fault, when the PV penetration level increases up to 80%

Table 4–17: Fault Current Contribution from the grid side and PV side and Relay Trip Times for outside 11/33kV Transformer LV side Fault

Fault Location and Fault Type	**Fault Current From Grid(A)**	**Fault current % increase**	**PV**	**Fault current contribution from solar(A)**	**PV% current increase**	**Breaker Trip Time(S)**	**Trip Time Delay (S)**
LG	2827	1.80	PV 1	11.95	48.5	BRK2	-0.003
			PV 2	23.28	50.7	0.292	
			PV 3	43.58	52.1		
			PV 4	25.67	49.7	BRK5	-0.002
			PV 5	21.96	48.8	0.379	
				126.45			
LL	1738	2.18	PV 1	12.11	50.5	BRK2	-0.004

			PV 2	23.09	49.4	0.398	
			PV 3	42.44	48.2		
			PV 4	25.90	51.0	BRK5	-0.001
			PV 5	21.88	48.2	0.588	
				125.42			
LLG	3145	0.69	PV 1	11.99	48.9	BRK2	-0.005
			PV 2	22.97	48.6	0.273	
			PV 3	42.76	49.3		
			PV 4	25.82	50.5	BRK5	-0.001
			PV 5	21.92	48.4	0.369	
				125.45			
LLL	1892	0.69	PV 1	12.18	51.4	BRK2	-0.005
			PV 2	23.45	51.8	0.369	
			PV 3	42.62	48.8		
			PV 4	25.75	50.1	BRK5	-0.002
			PV 5	22.07	49.5	0.464	
				126.07			
LLLG	1899	1.17	PV 1	12.22	51.8	BRK2	-0.006
			PV 2	23.47	51.8	0.368	
			PV 3	42.72	49.1		
			PV 4	25.78	50.3	BRK5	-0.005
			PV 5	22.15	50.0	0.461	
				126.33			

Table 4-17 illustrates the fault current contribution from the grid side and PV side for faults externally to the transformer at LV side. It can be observed that the fault level at the grid has increased but less compared with the HV side fault. PV side penetration level has increased compared with the HV side fault. But the relay operating time has no significant impact compared with “no solar PV penetration scenario”.

The scheme has operated in the expected manner. Initially the BRK 02 at LV side operates but the fault is not cleared as the fault current contribution by the parallel transformer across Bus section. After 300ms Bus Section breaker operates from the over current protection isolating the faulty part of the system. Healthy parallel other transformer can continuously provide power to the consumers without interruption.

The given table 4-18 shows the fault current contribution from each solar PV and grid fault current contribution for 11kV Feeder staring Fault, when the PV penetration level increases up to 80%

Table 4–18: Fault Current Contribution from the grid side and PV side and Relay Trip Times for outside 11kV Feeder Starting Point

Fault Location and Fault Type	Fault Current From Grid(A)	Fault current % increase	PV	Fault current contribution from solar(A)	PV% current increase	Breaker Trip Time(S)	Trip Time Delay (S)
LG	5862	3.86	PV 1	12.11	50.5	BRK3	-0.001
			PV 2	23.42	51.5	0.071	
			PV 3	43.65	52.4		
			PV 4	26.21	52.8		
			PV 5	22.33	51.2		
				127.71			
LL	3383	2.39	PV 1	12.38	53.8	BRK3	-0.005
			PV 2	23.79	54.0	0.072	
			PV 3	42.74	49.2		
			PV 4	26.17	52.6		
			PV 5	22.73	53.9		
				127.81			
LLG	6589	1.42	PV 1	12.10	50.3	BRK3	-0.002
			PV 2	23.20	50.1	0.072	
			PV 3	43.01	50.1		
			PV 4	26.24	53.0		
			PV 5	22.24	50.7		
				126.79			
LLL	3859	1.42	PV 1	12.23	52.0	BRK3	-0.004
			PV 2	23.58	52.5	0.075	
			PV 3	43.07	50.4		
			PV 4	26.29	53.3		
			PV 5	22.33	51.2		
				127.49			
LLLG	3854	1.00	PV 1	12.24	52.1	BRK3	-0.002
			PV 2	23.44	51.7	0.075	
			PV 3	42.76	49.3		
			PV 4	26.35	53.6		
			PV 5	22.36	51.5		
				127.16			

When the table 4-18 observed, it can be seen that for all type of faults at 11kV feeder BRK 03 operates and faults are cleared instantaneously by the EF highest function. Hence it can be seen that the fault are isolated in the expected manner with the existing protection system.

Further it can be observed that the percentage increase from the solar PV has increased with higher PV penetration level.

In order to analyze the level of impact to the MV level protection coordination with the 80%solar PV penetration, all the given tables can summarize.

Fault Location	AG						ABG				
	Breaker op.	Grid IF (A)	I pv at 33kV	t operate (s)	t opera. With PV (s)	Diff. in Time(s)	Grid IF (A)	I pv at 33kV	t operate (s)	t opera. With PV (s)	Diff. in Time(s)
33kV Bus(fe)	BRKe	11751	124	0.121	0.103	0.018	11751	124	0.117	0.105	0.012
33kV Cable End(f1)	BRKe	1279	125	0.127	0.104	0.023	1280	125	0.115	0.113	0.002
11/33kV T/F HV side(f2)	BRKe	1286	125	0.108	0.107	0.001	1297	125	0.115	0.107	0.008
11/33kV T/F LV side(f3)	BRK2	2777	126	0.295	0.292	0.003	3145	125	0.278	0.273	0.005
	BRK5	2627		0.381	0.379	0.002	3062		0.37	0.369	0.001
11kV Feeder starting point (f4)	BRK3	5644	128	0.072	0.071	0.001	6533	138	0.074	0.072	0.002
After 11kV Equivalent feeder(f5)	BRK3	1407	143	0.074	0.068	0.006	1336	141	0.0778	0.077	0.0008

Figure 4-8: Summery of Existing System Performance for LG Faults at different locations with Solar PV penetration increased up to 80%

Summery table to analyze the impact on the MV level protection coordination to un earthed type faults when PV penetration level increases up to 80%.

Fault Location	AB						ABC					ABCG				
	Breaker op.	Grid IF (A)	I pv at 33kV	t operate (s)	t opera. With PV (s)	Diff. in Time(s)	Grid IF (A)	I pv at 33kV	t operate (s)	t opera. With PV (s)	Diff. in Time(s)	Grid IF (A)	I pv at 33kV	t operate (s)	t opera. With PV (s)	Diff. in Time(s)
33kV Bus(fe)	BRKe	10134	128	0.129	0.127	0.002	11647	99	0.127	0.126	0.001	11647	127	0.125	0.121	0.004
33kV Cable End(f1)	BRKe	1163	125	0.722	0.704	0.018	1291	102	0.663	0.658	0.005	1291	125	0.663	0.661	0.002
11/33kV T/F HV side(f2)	BRK1	1065	125	0.663	0.658	0.005	1295	126	0.623	0.617	0.006	1296	125	0.623	0.621	0.002
11/33kV T/F LV side(f3)	BRK2	1701	125	0.402	0.398	0.004	1879	126	0.374	0.369	0.005	1877	126	0.374	0.368	0.006
	BRK5	1622		0.591	0.588	0.003	1866		0.466	0.464	0.002	1866		0.466	0.461	0.005
11kV Feeder starting point (f4)	BRK3	3304	143	0.077	0.072	0.005	3805	144	0.079	0.075	0.004	3816	145	0.077	0.075	0.002
After 11kV Equivalent feeder(f5)	BRK3	1116	131	0.076		0.076	1283	144	0.074	0.071	0.003	1284	130	0.083	0.081	0.002

Figure 4-9: Summery of Existing System Performance for non Earthed Faults at different locations with Solar PV penetration increased up to 80%

Using the summery table for all types of fault scenarios', it is perceived that the fault current contribution from the grid has increased. The maximum fault current contribution from the grid side is for the 33kV bus faults. Tough the PV penetration level increase up to 80% still the fault current contribution from the PV remain insignificant to the fault current contribution from the grid. Thus there will be no impact to the switch gear equipment. But the percentage fault current contribution has increased compared to the existing penetration level scenario. But still the relay operating time difference lies within acceptable tolerance range. In most cases the tripping time reduces in millisecond range when compare with the less PV penetration levels.

4.1. With high Resistive Faults, Fault current contribution and Relay discrimination time

When the fault is highly resistive the fault current seen by the protective devices of grid side and PV side may difficult to detect the fault. In that type of scenarios the sensitivity of the earth fault elements are required to reduce. It is very important to identify the most resistive faults that can be occurred in the system using fault analysis data. When the maximum possible fault resistance that would occur in the system is identified, we can estimate the minimum earth fault protection settings to detect the faults. When the figure 4.4 observed with the fault impedance presents the fault current can be obtained as

$$I_{f\_Relay_{WO}DG(I_{f2})} = \frac{1}{Z_2 + Z_4 + Z_6 + 3Z_f} \quad 4.7$$

If the $\boldsymbol{Z_f}$ become larger value the relay might read a less current. For example in this simulation when the fault resistance is 0.01 **Ω** , the grid fault current in the range of 11kA range, but when the fault resistance increased 10**Ω** the fault current reduces to considerably. Hence it is very important to identify the maximum resistance of the fault that can occur in the system.

Using developed simulation lets create faults at different locations while increasing the fault loop resistance, from which we can get an idea about the maximum impedance which can present in the system such that the relay can clear the fault.

Resistance (**Ω**)	Fault Location							
	33kV Feeder Start		33kV Cable End		11kV Feeder starting point		11kV Equivalent feeder **End**	
	If(A)	*t(s)*	*If(A)*	*t(s)*	*If(A)*	*t(s)*	*If(A)*	*t(s)*
1	1263.1	0.20	742.5	0.23	732.6	0.23	661.6	0.24
20	307.0	0.34	290.8	0.35	290.2	0.35	285.1	0.35
40	157.2	0.50	154.8	0.51	154.7	0.51	153.9	0.51
60	105.3	0.72	104.6	0.72	104.5	0.72	104.3	0.72

80	79.1	1.02	78.8	1.03	78.8	1.03	78.7	1.03
100	63.4	1.51	63.2	1.52	63.2	1.52	63.1	1.53
120	52.8	2.51	52.7	2.53	52.7	2.53	52.7	2.53
140	45.3	5.62	45.2	5.69	45.2	5.69	45.2	5.71

Figure 4-10: Summery of Existing System Performance for when the loop resistance varying

As per the table we can understand that until the fault loop impedance increases up to 120**Ω** the system can protection system can perform in the expected manner. If the probable fault-loop impedance could be higher than that value the settings need to make more sensitive.

4.2. Research Out come- Study Methodology of the impact from PV for any distribution feeder

A generalized method can be used evaluate the MV level protection coordination and propose new settings if the mis-coordination or relay malfunctions that can occur with heavy solar penetration level.

In that generalized method it has clearly indicated the data to be collected, method to carry out the research. After developing an accurate simulation for the existing feeder, it has to be evaluated weather the scheme operates accurately for the different fault types. If the protection system is not operating accurately new setting parameters need to be identified as per the used philosophy by the utility. In the flow chart the generalized methodology of the CEB has been given for 33kV feeders.

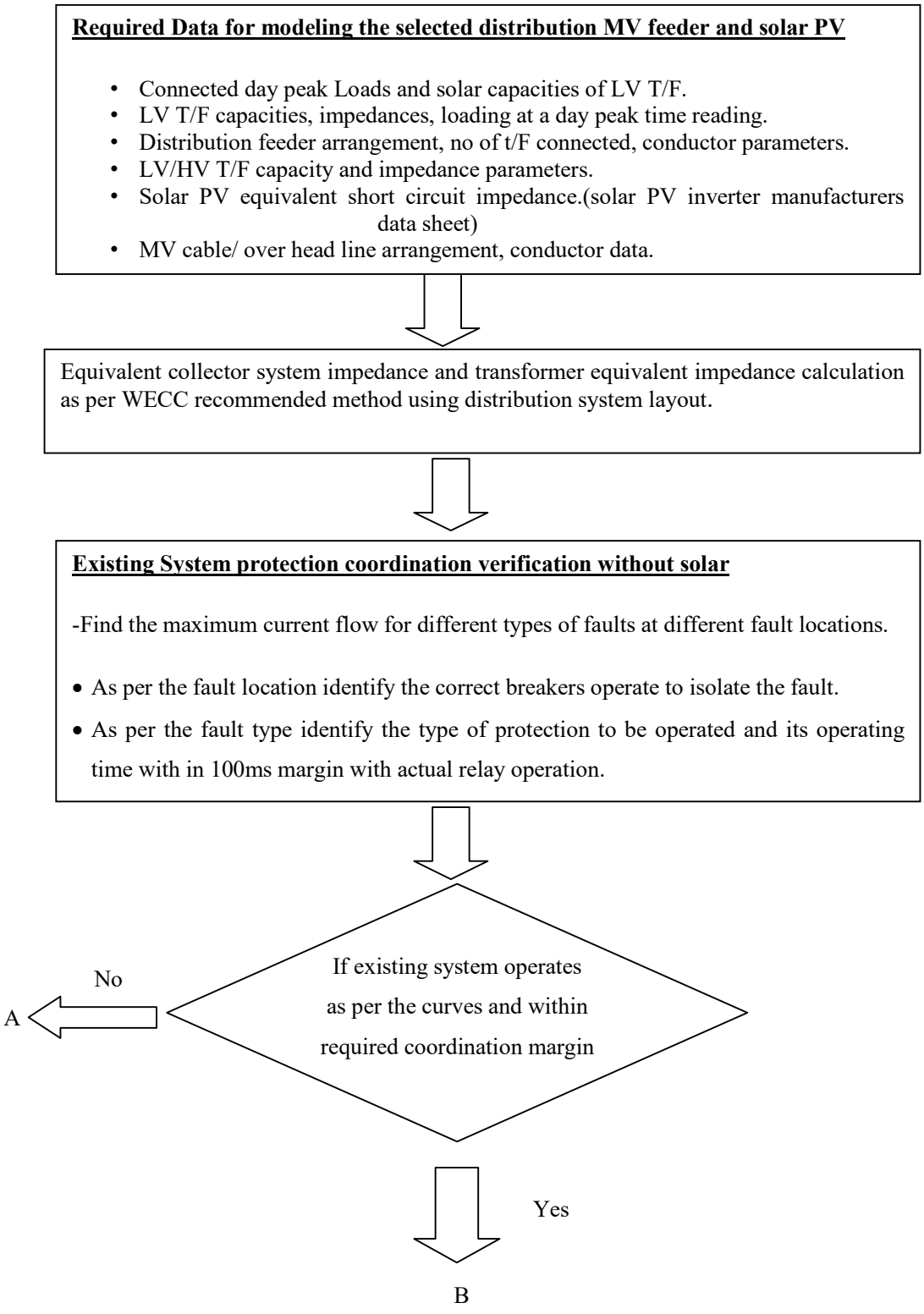
Required Data for modeling the selected distribution MV feeder and solar PV
• Connected day peak Loads and solar capacities of LV T/F.
• LV T/F capacities, impedances, loading at a day peak time reading.
• Distribution feeder arrangement, no of t/F connected, conductor parameters.
• LV/HV T/F capacity and impedance parameters.
• Solar PV equivalent short circuit impedance.(solar PV inverter manufacturers data sheet)
• MV cable/ over head line arrangement, conductor data.
Equivalent collector system impedance and transformer equivalent impedance calculation as per WECC recommended method using distribution system layout.
Existing System protection coordination verification without solar
-Find the maximum current flow for different types of faults at different fault locations.
• As per the fault location identify the correct breakers operate to isolate the fault.
• As per the fault type identify the type of protection to be operated and its operating time with in 100ms margin with actual relay operation.
If existing system operates as per the curves and within required coordination margin
No
A
Yes
B

"If No" (A)- Reviewing the Existing philosophy

MV level Protection Philosophy Need to be reviewed. The provided table illustrates the basic concept to obtain each setting, as per the existing setting parameter calculation philosophy of the utility.

Bay	Protection Function	Protection Theory	Setting Parameters	Setting Principle	Calculation
33kV feeder	OC Protection (51)	To operate as back Up protection for the Transformer 33/11kV. For a down steam ph-ph fault to have a discriminating time (0.30s) with 33/11 kV TF LV O/C protection	Pick Up Current	1.1* Current Carrying Capacity of Cu 240mm2 Cable	$= 1.1 \times 380$
			TMS	Operate 0.6s For three phase fault	$0.6s = \frac{TMS \times 0.14}{(\frac{I\,f,\,3\emptyset\ at\ 33kV\ Level}{PS})^{0.02} - 1}$
	EF Protection(51N)	To operate as back Up protection for the Transformer. For a down steam ph-earth fault to have a discriminating time (0.30s) with 132/33kV TF LV E/F protection	Pick Up Current	From failure analysis data CEB theory consider the minimum earth fault current higher than 40A for 33kV level Feeder	=80A
			TMS	Operate 0.6s For single phase fault	$0.6s = \frac{TMS \times 0.14}{(\frac{I\,f,\,1\emptyset}{PS})^{0.02} - 1}$
	OC Protection- 50	Current setting base on minimum of 33kV Fault current level in to safety factor and 10 times if T/F HV rated current)	Pick Up Current	10 times of Downstream T/F HV rated current	1600A
			Delay	Instantaneous	0.4 ms
	EF Protection(50N)	Current setting base on the fault current data of the previous records.	Pick Up Current	From failure analysis data CEB theory	320A
			Delay	Instantaneous	0.4 ms

Figure 5-0-1: Protection Philosophy for 33kV Feeder protection Setting Parameter Determination

The below table 5-2 provides the setting philosophy for the transformer LV and HV side. The selected example is for a 33/11 kV transformer.

Bay	Protection Function	Protection Theory	Setting Parameters	Setting Principle
11 /33kV T/F feeder HV side	OC Protection (51)	To operate as back Up protection for the Transformer. For a down steam ph-ph fault to have an adequate discriminating time) with LV side TMS will be determined.	Pick Up Current	$1.1 \times \frac{tr.f\ Capacity}{\sqrt{3} * V_{LL-HV}}$
			TMS	$t\ down\ stream\ LV + margin = \frac{TMS \times 0.14}{(\frac{I\,f,\,3\emptyset\ at\ 11kV\ Level}{PS})^{0.02} - 1}$

Figure 5-0-2: Protection Philosophy for 11/33kV Transformer HV side protection Setting Parameter Determination

Bay	Protection Function	Protection Theory	Setting Parameters	Setting Principle	Calculation
33kV /11kV T/F feeder LV side	OC Protection (51)	To operate as back Up protection for 11kV Feeder. For a downstream ph-ph fault to have an adequate discriminating time TMS will be determined.	Pick Up Current	$= 1.1 \times \frac{tr.f\ Capacity}{\sqrt{3} * V_{LL-LV}}$	$= 1.1 \times \frac{10 \times 10^3}{\sqrt{3} * 11}$
			TMS	Operate adequate coordination margin for three phase fault	$t\ 11kV\ feeder\ operate + margin = \frac{TMS \times 0.14}{(\frac{I\ f, 3\emptyset\ at\ 11kV\ Level}{PS})^{0.02} - 1}$
	EF Protection(51N)	To operate as back Up protection for 11kV Feeder. For a downstream ph-earth fault to have an adequate discriminating time TMS will be determined.	Pick Up Current	From failure analysis data CEB	=160A
			TMS	Operate adequate coordination margin for single phase fault	$t\ 11kV\ feeder\ operate + margin = \frac{TMS \times 0.14}{(\frac{I\ f, 1\emptyset}{PS})^{0.02} - 1}$

Figure 5-0-3: Protection Philosophy for 11/33kV Transformer LV side protection Setting Parameter Determination

Bay	Protection Function	Protection Theory	Setting Parameters	Setting Principle	Calculation
11kV feeder	OC Protection (51)	To operate as back Up protection for any downstream AR for a three phase faults after AR location with an adequate clearance margin.(coordination margin will be based on number of Protective devices for coordination)	Pick Up Current	1.1* Current Carrying Capacity of 11kV Conductor	$= 1.1 \times conductor\ current\ carring\ capacity$
			TMS	Operate adequate coordination margin for three phase fault	$t\ down\ stream\ AR + margin = \frac{TMS \times 0.14}{(\frac{I\ f, 3\emptyset\ at\ 11kV\ Level}{PS})^{0.02} - 1}$
	EF Protection(51N)	To operate as back Up protection for any downstream AR for a single phase faults after AR location with an adequate clearance margin.(clearing margin will be based on number of Protective devices for coordination)	Pick Up Current	From failure analysis data CEB consider the minimum earth fault current higher than 40A for 11kV level Feeder	=40A
			TMS	Operate adequate coordination margin for single phase fault	$t\ down\ stream\ AR + margin = \frac{TMS \times 0.14}{(\frac{I\ f, 1\emptyset}{PS})^{0.02} - 1}$
	OC Protection-50	This pick up shall be higher than the maximum three phase fault current for a fault near downstream AR.	Pick Up Current	From failure analysis data CEB	1000A
			Delay	Instantaneous	0.01 s
	EF Protection(50N)	This pick up shall be higher than the maximum single phase fault current for a fault near downstream AR.	Pick Up Current	From failure analysis data CEB	160A
			Delay	Instantaneous	0.01 s

Figure 5-0-4: Protection Philosophy for 11kV Feeder protection Setting Parameter Determination

Without violating the setting principle the setting shall be slightly adjusted and process can be carried out until the protection system operates with in the acceptable fault clearing margin. When the allowable margin obtained with particular set of settings, need to be moved to step B.

"If Yes" (B)- With Solar PV-Protection System performance evaluate.

The flow chart can be continuing as given steps to evaluate the system performance with solar penetration.

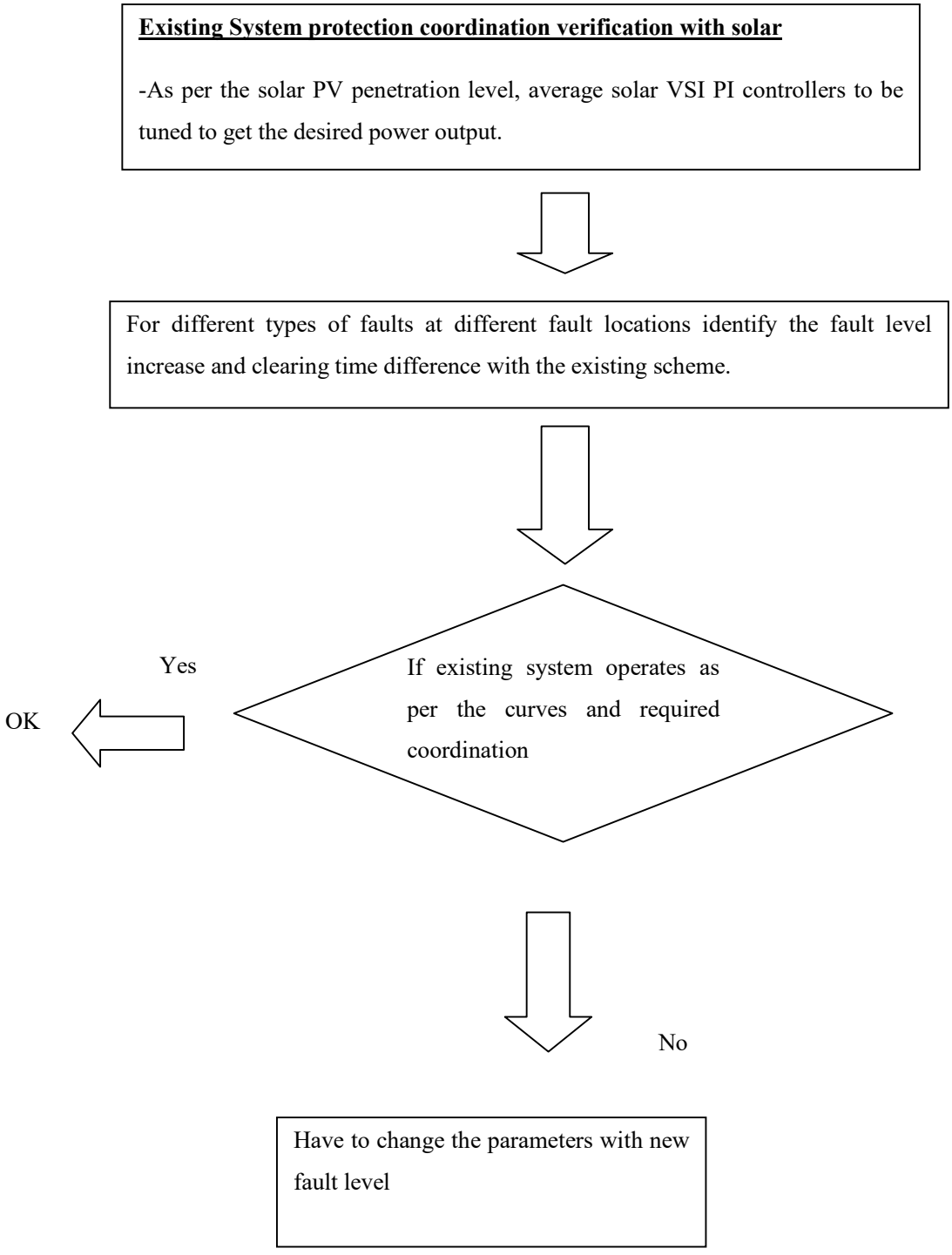

It can be concluded that the research objectives has been fulfilled and very useful method has been proposed to evaluate the accurate protection performance at MV level and suggesting new setting parameter process adopting all the existing protection philosophies.

CHAPTER 5

5. Conclusions

The level of PV penetration has been increased in the LV distribution system. Hence it is a vital factor to evaluate the impact to the MV level fault current when the PV penetration level increases in the distribution system. But many challengers have to be overcome in order to analyze the impact from solar PV to the MV protection level coordination.

As the LV distribution widely dispersed in a large geographical area, it is difficult to simulate each and every component. In Sri Lankan contest, presently simulated LV system for the analysis is not available. As the research scope extends to the MV level protection, it is really difficult to model in micro level considering each customer individually. Even when single transformer is considered, there may be hundreds of connected consumers with rooftop solar PV and loads. When one MV feeder is considered, it might be comprised with hundreds of that type of transformers. It is not realistic to simulate all the consumers with solar PV`s in the simulation.

On the other hand in research, main focus is on the MV level protection system and impact from the solar PV penetration. Thus it is not required to model the entire complex switching power electronic devices of a solar PV in detailed manner. Hence average equivalent voltage source inverter model has been developed which can be used to represent the equivalent impact of the large number of solar PV at the MV level. The behaviour of the average voltage source inverter for both steady state and transient performance, have been verified with the detailed model which had been already verified and developed on PSCAD/EMTDC platform. An idea about the aggregated fault current contribution from large number of photovoltaic sources has been obtained using the experimental data from the published papers. [17]

Furthermore, this research describes in detail how the equivalent collector system parameters can be obtained for any research as per the WECC recommendations.

From the simulation results, it has been observed that the existing solar PV penetration has no considerable impact on the MV level protection coordination for the considered Ethul-Kotte Grid substation. But it can be assumed that if the PV penetration level is increased (up to 80%), the fault current level also gets increased. Similarly the equipment can be difficult to withstand the fault current due to inadequate fault current withstanding capability. In order to evaluate the impact to the fault current level and, same simulation has been done for 80% PV penetration level.

Fault current level is increased (maximum up to 1%) due to the added parallel impedance path through PV. The PV fault current contribution is less than 150% of the rated current during fault. But that fault current is comparatively small compared to the grid fault current (When the fault current contribution from the grid is kA range PV fault current contribution at 33kV level is only at 110A range). Therefore with the existing penetration level, the protection system can perform within the expected limits (Tripping time has reduced due to rise of fault current contribution, in the 100ms range).

The PV penetration level is increased up to 80% of the total capacity, and then the protection system performance is observed. It is identified that both the fault level has been increased. The fault level has increased up to 4% compared with “without solar scenario”. When the grid side fault current is vary in the kA range, PV side fault current contribution is vary only in 130A range. Hence it can be concluded that with the rise of penetration level, the fault current level gets increased. But the existing relay protection can operate reliably within limits to fully isolate the faults for the feeders (Kotikawaththa, Welikada, Kalubowila, and Parliament) connected to the Ethul-Kotte grid substation. But this scenario may be not applicable to another feeder. Most of the time 33/11kV protection equipments are selected based on the nominal values. Place specific fault current calculation is not carried out most of the time. In such cases, it is very important to evaluate the impact on fault current level due to PV penetration. On the other hand, the equipment coordination has also been done using the expected fault current from the grid side only. Due to PV penetration if the fault current gets increased, the expected coordination might not be available.

Hence it is important to carryout detailed simulation as discussed in this research if the PV penetration level exceeds 50% of the system capacity. Under section 4.6, a generalized methodology has been suggested which can be used to analyze the fault current contribution increase due to solar PV. Furthermore, the proposed generalized method can be used to propose more accurate settings for the MV protection relay settings if any miss coordination occurred.

The presented methodology under section 4-6 is so important in evaluating and finding accurate and most suitable MV protection level setting parameters calculation because, the existing generalized protection setting philosophy for 33kV level has been represented very clearly.

Thus it can be concluded that in this research a simplified, yet accurate methodology has been suggested to evaluate the impact form heavy solar PV penetration in distribution system fault level. It can be clearly identified that the fault level increases with solar penetration due to the added parallel path. When the fault is closer to the PV side, fault current increase due to PV penetration is more significant. Rise of fault current level may be different from feeder to feeder because the equivalent impedance is different as per location of the network. So it is important to analyze the impact accurately if the PV penetration level increases more than 50% of the system capacity as presented in the section 4-6.

As described under section 4.3 in homogenous system, as per the super position theorem the fault current contribution from the source is independent from the other source. In homogenous system when other source connected parallel, each source provides fault current as per the equivalent impedance seen by each source. Hence fault current contribution from grid side will not vary, but the fault level of the particular faulted bus can vary due the added fault current contribution from the PV contribution. But if the system is non-homogenous the fault current contribution can vary. Mainly this depends upon the solar PV source impedances. As per the ref.[18] if the sequence components considered, positive sequence of the solar PV source is considerable value compared to the negative sequence impedance and there is no zero sequence value. If the solar PV controllers can fully filter the waveforms it causes to

negligible negative sequence impedance. Hence only positive sequence impedance added as parallel to the 33kV source impedance. When a parallel path is added the equivalent positive sequence impedance gets smaller than the smallest impedance of parallely connected impedances. Then the voltage across the positive sequence impedance gets smaller and thus the positive sequence fault current contribution reduced compared with the without solar PV scenario.

But if the solar source has negative sequence impedance value that causes the equivalent negative sequence impedance to reduce and that will reduce the voltage across negative sequence loop. That scenario can lead to increase voltage across positive sequence loop and that can lead to increase the positive sequence fault current contribution increase.

But in this simulation (which is done on PSCAD platform) as the voltage source with The PLL in the control scheme is locked onto the A phase of the inverter voltage and as such there is some positive and negative sequence injected during an unbalanced fault. Finally, the grid side source has the option of entering various positive sequence and zero sequence impedances.

But in impedance based RMS fault calculation it is very important to estimate the sequential impedance of the PV which is used for simulation. It if an experimental values of the fault current contribution available easily it can be identified each sequential component and can correctly identify the fault current contribution variations of the both grid and PV side.

But in this simulation as the voltage source with The PLL in the control scheme is locked onto the A phase of the inverter voltage and as such there will be some positive and negative sequence injected during an unbalanced fault. Finally, the grid side source has the option of entering various positive sequence and zero sequence impedances.

References

[1] Yun Tiam Tan, Impact on the power system with large penetration of Photovoltaic generation, February 2004

[2] Sachin Soni,Solar PV Plant Model Validation for Grid Integration Studies,Approved April 2014.

[3] WECC, Western Electricity Coordination Council Modelling and Validation Work Group, WECC Guide for Representation of Photovoltaic Systems In Large –Scale Load Flow Simulations, August 2010

[4] Xiang Choo, John Mansour,Andrew Halley , Modeling od Emnedded PV Generation indistribution Networks, *IEEE transaction paper, 12 November 2015*

[5] Mesult E. Baran,Hossein Hooshein Hooshyer,Zhan Shen, Alex Hung, "Accommodating High PV penetration on Distribution Feeders" ,*IEE Transactions in Smart Grid, Vo 2, No 2, June 2012*

[6] Liwanga Namangolwa, Elizabath Begumsa, "Imoacts if Solar Photovoltic on the Protection System of Distribution Networks,University of Chalmers, Department od Energy and Environment, Seeden 2016

[7] Ahmed Kamel, M.A Alam, Ahmed Azmy and A.Y Abdekaziz" Peotection Coordination of Distribution systems equipped with distributed generation, Electrical ans Electronic :An international Journal Vol 2, No2, May 2013.

[8] Adly Girgis,Sukumar Nrahma, "Effect of Distributed Generation on Protective device Coordination in Distribution System", Clemson University.

[9] Subahashich Bhattacharya, "Power system protection problems caused by grid connected PV systems", University of Queesland in 2014

[10] S.N Affifi, M. Darwish,Gareth Anthony Tylor,"Imapact of Photovoltic Penetration on Shortcircuit levels in Distribution Networks", 02 February 2016.

[11] Sumei Lu, Tianshu Bi, Yanlin Liu, “Theoritical Analysis on the Short circuit of Inverter-Interfaced Renewable Energy Generators with fault ride through Capability,MDPI article 25 December 2017.

[12] Umid Mamadaminov,”Impacts od Increased Distributed Solar Penentration on Distribution Network Review”,March 2014

[13] Jamie Keller, Benamin Kroposki,Richard Bravo and Steven Robeles” Fault current contributio form singe phase PV invterters, 11 January 2015

[14] E.Muljadi, M. Singh and V.Geveorgian, “PSCAD Modlues Rpresenting PV generator” Augest 2013, Technical Report.

[15] KEMA Limited, The contribution to distribution Network Fault levels from the connection of distribution Generation,

[16] Farid Katirael, Juergen Holdbach, Tim Chang, Wesley John,” nvestigation of Solar PV Inverters Current Contributions during Faults on Distribution and Transmission Systems Interruption Capacity”Quontra Technology 2011

[17] E.Muljadi, M. Singh and V.Geveorgian,”User Guide for PV Dynamic Model Simulation Writtem in PSCAD Platform”

[18] E.Muljadi, M. Singh and V.Geveorgian,” Dynamic Model Validation of PV Inverters under Short Circuit Condition”